

**ASSESSMENT OF CHEMICAL MARKERS AS SURROGATES FOR EFFICACY  
AND SAFETY OF ROOIBOS EXTRACTS**



**UNIVERSITY OF  
ZULULAND**

A thesis submitted in fulfilment of the academic requirements for the degree of  
Master of Science in Biochemistry, Faculty of Science and Agriculture, University of  
Zululand (Kwa-Dlangezwa), Kwa-Zulu Natal, South Africa

BY

AMSHA VIRARAGAVAN

Student number: 201160287

Supervisors: Prof CJF Muller and Prof AK Basson

Co-Supervisor: Dr S Riedel

March 2017

# DECLARATION

I, Amsha Viraragavan declare that the entirety of the work contained therein is my own, original work, (except where acknowledgements indicate otherwise), and that neither the whole work or part of it has been, is being, or is to be submitted for another qualification in this or any other University. I hereby permit the University of Zululand to reproduce for the purpose of research, either the whole or any portion of the contents thereof.

Amsha Viraragavan (Student Number: 201160287)

Signature: .....

Date: .....

# ABSTRACT

## BACKGROUND

Research interest in the bioactive polyphenols of rooibos, to which its health-promoting properties are attributed, has escalated. Defining the quality attributes for assessing the efficacy of rooibos health products forms part of a quality control system. The aim of this study was to identify chemical markers in green rooibos extract (GRE) that could predict bioactivity in cell-based assays, with particular focus drawn to the dihydrochalcone C-glucoside, aspalathin, which has displayed antidiabetic effects *in vitro* and *in vivo*.

## METHODS

Two ethanol-based (80% and 60% ethanol) and aqueous extracts were prepared from ten randomly selected plant batches of green rooibos. HPLC-DAD analysis was performed to quantify aspalathin and other major flavonoids present in the extracts. A radioimmunoassay was used to measure 2-deoxy- $^3\text{H}$ -D-glucose absorption in C2C12 murine skeletal muscle and C3A human liver cells, exposed to 10  $\mu\text{g}/\text{mL}$  of the extracts. The effect of the green rooibos extracts (GRE's) and reference extracts ARC 2 and GRT on glucose uptake and lipid accumulation was also tested in 3T3-L1 adipocytes. GRE's were also tested at concentrations ranging from 1 and 100  $\mu\text{g}/\text{mL}$  for inhibitory activity against the protein tyrosine phosphatase 1B (PTP1B) enzyme. To investigate the possible mechanism of action of glucose uptake in C2C12 cells, protein expression studies were conducted. Multivariate statistical analysis was performed using principle component analysis (PCA), to elucidate the relationship of extract type, plant batch variation and bioactivity.

## RESULTS

HPLC-DAD analysis of the different GRE's demonstrated that extraction with 80% ethanol yielded the highest average phenolic compound enrichment (17.09  $\pm$  2.66% aspalathin), compared to the 60% ethanol and aqueous GRE (12.54  $\pm$  2.51% and 9.52  $\pm$  1.85% aspalathin, respectively). In C2C12 cells glucose uptake was related to the phenolic content, as activity increased in the 80 and 60% ethanol extracts (by up to 182% and 142%, respectively). The glucose uptake was comparable to ARC 2 the reference extract. While in C3A cells the aqueous extract appeared to be more effective. Lipid accumulation was greatly enhanced in 3T3-L1 adipocytes by the

ethanolic GRE's. Furthermore, all extracts showed potent inhibitory activity on PTP1B with  $IC_{50}$  values  $\leq 20 \mu\text{g/mL}$ . Principle component analysis demonstrated clustering between the 80% ethanol-based extracts and the reference extracts. For C2C12 glucose uptake and 3T3-L1 lipid accumulation, a positive correlation was demonstrated with aspalathin and nothofagin, isoorientin and orientin as well as isovitexin and vitexin.

## **CONCLUSION**

The chemical complexity of these different extracts make it difficult to identify single active pharmaceutical ingredients, however activity was associated with aspalathin and the 3-deoxy-dihydrochalcone, nothofagin, and their flavone derivatives.

# ACKNOWLEDGEMENTS

I give gratitude to God for granting me life and good health to see the end of this programme successfully.

To my Supervisor, Prof CJF Muller, no amount of words can express how grateful I am to you for your undivided hours spent in grooming me into the scientist I am today. Your guidance, encouragement and belief in me has tremendously contributed to this dissertation. Dr Muller, you have been a pillar of strength to me and together with your patience and knowledge I would like to acknowledge you. You are the best!

I wish to thank Prof AK Basson for this opportunity and for his continued support and motivation throughout this journey.

I am also grateful to Dr S Riedel for her efforts in perfecting my laboratory skills and for her supervision throughout this study.

To Dr R Johnson, I would like to thank you for your expertise and assistance with the molecular work in this study.

A special acknowledgement goes to Prof J Louw and the staff at the Biomedical Research and Innovation Platform (BRIP). Thank you all for affording me this opportunity and for your immense contribution in this dissertation.

To my parents, Mr and Mrs ML Viraragavan, a very big thank you for granting me quality education and for your unconditional love and support in my academic career.

I would like to appreciate and thank Prof E Joubert and her entire team at the Agricultural Research Council for all the extracts, characterisation and statistical analysis and for the support in this study.

I would also like to thank Afriplex, for the 60% ethanol aspalathin-enriched green rooibos extract (GRT).

Last but not least, I thank the University of Zululand, the South African Medical Research Council, the Agricultural Research Council and the National Research Foundation for their funding and support.

# TABLE OF CONTENTS

DECLARATION.....	i
ABSTRACT .....	ii
ACKNOWLEDGEMENTS .....	iv
ABBREVIATIONS .....	xii
CHAPTER 1 .....	1
INTRODUCTION TO THIS STUDY .....	1
Chapter 2 .....	3
LITERATURE REVIEW .....	3
2.0. Diabetes mellitus.....	3
2.1. Factors causing Type 2 Diabetes.....	4
2.2. Insulin and glucose regulation.....	4
2.4. Protein Tyrosine Phosphatase 1B (PTP1B) .....	7
2.5. Insulin resistance .....	9
2.6. AMPK in glucose regulation .....	9
2.7. Energy metabolism .....	11
2.8. Transport of glucose .....	11
2.9. Glycolysis .....	13
2.10. Fatty acid oxidation .....	14
2.11. Lipids and lipid metabolism .....	14
2.12. Cell models used in this project.....	17
2.13. Indigenous medicinal plants .....	20
2.14. Phenolic compounds as phytomedicines .....	21
2.15. Polyphenols.....	22
2.16. Bioactivity of polyphenols.....	22
2.17. Flavonoids.....	25
2.18. Bioavailability vs bioactivity .....	26

2.19. <i>Aspalathus linearis</i> (Rooibos).....	27
2.20. Quality control .....	30
2.21. Principle components which can be used as predictors of bioactivity .....	30
2.22. Chemical markers .....	31
Aim:.....	31
Objectives: .....	31
CHAPTER 3 .....	32
EXPERIMENTAL PROCEDURES.....	32
3.1. Materials.....	32
3.2. Extract and control preparation .....	34
3.3. Cell lines.....	34
3.4. Cell culture .....	35
3.5. Sub-culture of cells.....	37
3.6. Cell Seeding for experiments .....	38
3.7. Cell treatment with GRE and controls .....	39
3.8. Experimental outline for C2C12 and C3A cells .....	41
3.9. Induction process for adipocyte differentiation and experimental design for 3T3-L1 cells .....	42
3.10. Bioactivity assays.....	43
3.11. Protein Tyrosine Phosphatase 1B (PTP1B) Enzyme assay .....	46
3.12. Protein expression studies .....	47
3.13. Statistical Analysis .....	51
CHAPTER 4 .....	52
RESULTS .....	52
4.2. <i>In vitro</i> results.....	56
4.3. Protein Tyrosine Phosphatase 1B (PTP1B) enzyme inhibition.....	67
4.4. Western blot analysis .....	69
4.5. Statistical analysis.....	74

4.6. Principle Component Analysis (PCA) of all three GRE's compared to bioactivity .....	75
Chapter 5 .....	77
DISCUSSION AND CONCLUSION .....	77
5.1. Rooibos as a health product.....	78
5.2. Phenolic composition of three different types of GRE .....	79
5.3. Bioactivity of GRE .....	79
5.4. PTP1B inhibition studies .....	83
5.5. Molecular effects of selected GRE in C2C12 muscle cells.....	83
5.6. Multivariate statistical analysis .....	84
5.7. Summary.....	85
5.8. Conclusion .....	86
5.9. Limitations of this study.....	86
5.10. Future work .....	87
Bibliography .....	88
Appendix 1 .....	112
Chemicals and reagents used in this study.....	112
Appendix 2 .....	117
Krebs Ringer Bicarbonate HEPES (KRBH) buffer.....	117
Sorenson's buffer .....	117
Protein Tyrosine Phosphatase 1B (PTP1B) .....	118
3T3-L1 adipocyte differentiation medium .....	121

## LIST OF FIGURES

Figure 1. Molecular mechanisms involved in the insulin signalling pathway that regulates glucose transporter 4 (GLUT4) translocation to cell membrane.	6
Figure 2. Insulin and leptin signalling pathways by PTP1B.	8
Figure 3. A schematic diagram of the glycolytic pathway.	13
Figure 4. Malonyl-CoA and CPT-I regulation in fatty acid metabolism.	16
Figure 5. Beneficial effects of polyphenols in the management of blood glucose in diabetes.	24
Figure 6. Structure of the dihydrochalcones aspalathin and nothofagin and the flavones isoorientin and orientin in <i>Aspalathus linearis</i> .	29
Figure 7. HPLC chromatogram of an aspalathin-enriched green rooibos extract. (c) ARC at 288 nm; (d) ARC at 350 nm.	31
Figure 8. Representation of the reference extracts (ARC 2 and GRT) and three different types of green rooibos extracts (80% and 60% EtOH and Aq GRE) used in this study (as described by Walters 2016).	33
Figure 9. An illustration of the haemocytometer used to count the number of cells/mL.	36
Figure 10. Experimental outline for C2C12 and C3A cells.	41
Figure 11. Experimental design for the 3T3-L1 adipocytes.	42
Figure 12. Diagram illustrating the cassette used to transfer proteins onto a LF PVDF membrane with the Trans-Blot™ Turbo Transfer system	49

Figure 13. A typical HPLC chromatogram of a hot water green rooibos extract at 288 and 350 nm depicting the presence of the major phenolic compounds:	54
Figure 14. Cellular ATP quantification of C2C12 cells treated with ethanol and aqueous green rooibos extracts from ten different plant batches.	57
Figure 15. Glucose uptake in differentiated C2C12 myocytes after treatment with green rooibos extracts (GRE) produced from 10 different plant batches by 80% ethanol extraction (a), 60% ethanol (b) and hot water extraction (c). (d) represents the combined glucose uptake of all three extracts.	59
Figure 16. Glucose uptake in C3A hepatocytes after treatment with green rooibos extracts (GRE) produced from 10 different plant batches by 80% ethanol extraction (a), 60% ethanol (b) and hot water extract (c), and combined are presented (d).	61
Figure 17. Glucose uptake in 3T3-L1 adipocytes after treatment with green rooibos extracts (GRE) produced from 10 different plant batches by 80% ethanol extraction (a), 60% ethanol (b) and hot water extraction (c), and combined are presented (d).	63
Figure 18. Oil Red O stained 3T3-L1 adipocytes demonstrating lipid accumulation.	64
Figure 19. Quantification of lipid accumulation in 3T3-L1 adipocytes.	66
Figure 20. <i>In vitro</i> PTP1B enzyme inhibition studies with 80% and a 60% ethanol extract, and aqueous extracts of ten different plant batches.	67
Figure 21. Effect of green rooibos extract on AMPK activation.	70
Figure 22. Effect of green rooibos extract on AKT activation.	71
Figure 23. Effect of green rooibos extract on ACC activation.	72
Figure 24. Effect of green rooibos extract on MLYCD activation.	73

Figure 25. Principal component analysis loadings (a) and scores (b) plots showing association between bioactivity, phenolic composition and extract samples. 75

## LIST OF TABLES

Table 1. Growth medium used to culture the three different cell lines used in this study.	35
Table 2. Cell densities used for seeding different plate types.	39
Table 3. Preparation of standards for the standard curve.	45
Table 4. Protein and gel concentrations used for Western blot analysis.	48
Table 5. Source, catalogue numbers, size and dilutions of antibodies used.	50
Table 6. Chemical characterisation of three GRE's by HPLC -DAD analysis.	55
Table 7. IC <sub>50</sub> values of enzyme inhibition against the PTP1B enzyme using three different types of GRE's.	68
Table 8. Comparative table of bioactivity and chemical composition.	74

# ABBREVIATIONS

ACC	Acetyl-CoA
ACC 1	Acetyl-CoA 1
ACC 2	Acetyl-CoA 2
ADA	American Diabetes Association
ADP	Adenosine-5-diphosphate
AICAR	5-Aminoimidazole-4-carboxamide-1- $\beta$ -D-ribofuranoside
Akt	Threonine kinase B
AMP	Adenosine monophosphate
AMPK	Adenosine monophosphate-activated protein kinase
ANOVA	Analysis of variance
ASP	Aspalathin
ATCC	American type culture collection
ATP	Adenosine-5-triphosphate
BSA	Bovine serum albumin
Ca <sup>2+</sup>	Calcium dichloride
CO <sub>2</sub>	Carbon dioxide
CPM	Counts per minute
CPT-I	Carnitine palmitoyltransferase one
CBS	Crystathionine- $\beta$ -synthase
CTRL	Control
CVD	Cardiovascular disease
DMEM	Dulbecco's modified eagle's medium
DMSO	Dimethyl sulfoxide
DOG	2-Deoxy-[ <sup>3</sup> H]-D-glucose
DPBS	Dulbecco's phosphate buffered saline
DPM	Disintegrations per minute
ECACC	European Collection of Authenticated Cell Cultures
EFFAs	Essential free fatty acids
EMEM	Eagle's minimum essential medium
EtOH	Ethanol
F6P	Fructose-6-phosphate

FADH <sub>2</sub>	Flavin adenine dinucleotide
FBP	Fructose-1,6-biphosphate
FBS	Foetal bovine serum
FFA	Free fatty acid
G3PDH	Glyceraldehyde 3-phosphate dehydrogenase
G6P	Glucose-6-phosphate
G6Pase	Glucose-6-phosphatase
G6PD	Glucose-6-phosphate dehydrogenase
GAPDH	Glyceraldehyde-3-phosphate dehydrogenase
GLUT	Glucose transporter
GLUT 1	Glucose transporter 1
GLUT 2	Glucose transporter 2
GLUT 3	Glucose transporter 3
GLUT 4	Glucose transporter 4
GRE	Aspalathin-enriched green rooibos extract
GRT	Green rooibos tea (aspalathin-enriched) extract
GSK3	Glycogen-synthase kinase 3
h	Hour
HPLC-DAD	High-performance liquid chromatography with diode-array detection
HRP	Horseradish peroxidase
HS	Horse serum
HYP	Hyperoside
IBMX	3-Isobutyl-1-methylxanthine
IDDM	Insulin-dependent diabetes mellitus
IDF	International Diabetes Federation
INS	Insulin
IR	Insulin receptor
IRK	Insulin receptor kinase
IRS	Insulin receptor substrate
IRS1	Insulin receptor substrate1
IRS2	Insulin receptor substrate 2
ISOO	Isoorientin

ISOVIT	Isovitexin
ISOQ	Isoquercetrin
JAK2	Janus kinase
LCFA	Long chain fatty acids
LKB 1	Liver kinase B1
LUT7GLC	Luteolin-7-O-glucoside
MLYCD	Malonyl-CoA decarboxylase
MAPK	Mitogen-activated protein kinase
MTT	3-(4,5-dimethylthiazol-2-yl)-2,5-diphenyltetrazolium bromide
Na <sub>3</sub> VO <sub>4</sub>	Sodium orthovanadate
NADH	Nicotinamide adenine dinucleotide
NaHCO <sub>3</sub>	Sodium bicarbonate
NaOH	Sodium hydroxide
NEFA	Non-esterified fatty acids
NF-κB	Nuclear factor kappa β
NIDDM	Noninsulin-dependent diabetes mellitus
NOT	Nothofagin
OAA	Oxaloacetate
OD	Optical density
ORI	Orientin
pAKT	Phosphorylated AKT
pAMPK	Phosphorylated AMPK
PBS	Phosphate buffered saline
PCA	Principle Component Analysis
PDH	Pyruvate dehydrogenase
PDK 1	Phosphatidylinositol-dependent kinase 1
PEP	Phosphoenolpyruvate
PFK	Phosphofructokinase
PI3K	Phosphatidylinositol 3-kinase
PIP3	Phosphatidylinositol (3, 4, 5)-triphosphate
PKC	Protein kinase C
PKC-ζ	Protein kinase C theta

PPAG	Enolic phenylpyruvic acid glucoside
PTP1B	Protein tyrosine phosphatase 1B
PTPs	Protein tyrosine phosphatases
PVDF	Polyvinylidene difluoride
Q3ROB	Quercetin-3-O-robinobioside
RIA	Radioimmunoassay
RUT	Rutin
SDS	Sodium dodecyl sulphate
STAT	Signal transducer and activator of transcription
STZ	Streptozotocin
T1D	Type 1 diabetes
T2D	Type 2 diabetes
TBST	Tris-buffered saline and Tween 20
TCA	Tricarboxylic citric acid
TG	Triglycerides
VIT	Vitexin
WHO	World Health Organisation

# CHAPTER 1

## INTRODUCTION TO THIS STUDY

Diabetes mellitus is defined as a metabolic disease which is caused by derangements in the metabolism of carbohydrate, fat and protein. This results from defective insulin secretion, insulin action or both, with characteristic hyperglycaemia (ADA, 2008; Wagman and Nuss, 2001; WHO, 1999). With a global increase in diabetes, the International Diabetes Federation (IDF) estimated that 415 million people were diabetic in 2015 and this figure is predicted to escalate to 642 million in 2040 (<http://www.idf.org/sites/default/files/Atlas7e-poster.pdf>). Three quarters of diabetics live in low and middle-income countries (Levitt, 2008). Currently an estimated 14.2 million Africans are living with diabetes, which is predicted to rise to 34.2 million by 2040. In sub-Saharan Africa, over 90% of diabetics are diagnosed with type 2 diabetes (T2D), owing to the changes in lifestyle (Levitt, 2008). These modifications include changes in diet, in particular high calorific diets rich in carbohydrates and sugar, lack of physical activity, smoking and an increased alcohol intake (Gill *et al.*, 2009). South Africa is estimated to have the highest prevalence of type 2 diabetes with 2.28 million recorded in 2015 (IDF Africa).

Apart from healthy lifestyle interventions, the majority of diabetic patients require pharmacological intervention which consists of one or more oral antidiabetic drug. Of these drugs, metformin, sulfonylureas or thiazolidinediones (TZD's) are most commonly prescribed (Bodmer *et al.*, 2008; Luna and Feinglos, 2001). Current therapeutics in the treatment of diabetes is aimed at maintaining normoglycaemia and median HbA1c levels at  $\leq 7\%$  (Bennett *et al.*, 2011, He *et al.*, 2011, Inzucchi *et al.*, 2015). In most cases, despite the medication, the diabetic condition worsens over time, necessitating combination therapies including the use of insulin to control glycaemia (Hemmingsen *et al.*, 2012; Zonszein and Groop, 2016). Some adverse side-effects associated with these treatments include hypoglycaemia, weight gain, peripheral oedema, gastrointestinal disturbances and potential cardiovascular diseases (Inzucchi *et al.*, 2015, Tahrani *et al.*, 2011). Hence, the search for safer and more effective long-term therapeutics, able to sustain glycaemic levels and prevent disease progression,

is becoming a priority. Ideally, such a therapeutic agent should improve insulin action, reverse or hinder diminished  $\beta$ -cell function, reduce excess weight-loss, prevent hypoglycaemia and reduce the risk for cardiovascular disease (Tahrani *et al.*, 2011; Qiu *et al.*, 2014).

As potential antidiabetic remedies, the effectiveness and safety of natural products have attracted much attention as alternative or adjunct therapies. *Aspalathus linearis*, commonly known as rooibos, a popular South African tea consumed as a hot or cold beverage, was shown to improve infantile colic, allergies, asthma and dermatological problems (Joubert *et al.*, 2008; Morton, 1983). Recently, research into the health properties of rooibos has also focussed on its antidiabetic, anti-inflammatory and anti-obesity properties (Ajuwon *et al.*, 2013; Kamakura *et al.*, 2015; Mazibuko *et al.*, 2013; Muller *et al.*, 2012; Son *et al.*, 2013).

Studies conducted on aspalathin-enriched unfermented (green) rooibos extracts were demonstrated to have antihyperglycaemic properties and ameliorate insulin resistance *in vitro* and *in vivo* (Ajuwon *et al.*, 2013; Kamakura *et al.*, 2015; Mazibuko *et al.*, 2013; Muller *et al.*, 2012; Son *et al.*, 2013). Its potential as a nutraceutical in the management of diabetes still requires further research, in terms of developing a standardised extract with predictable potency. In addition, for commercialisation of such a nutraceutical, it should have minimal or no side-effects and be cost-effective. To ensure the quality of such a nutraceutical, it is imperative that the active pharmaceutical ingredients (API's) are defined as components of the quality control system (Preethi *et al.*, 2014).

The unique flavonoid, aspalathin and its flavone derivatives, orientin and isoorientin, have been identified as bioactive constituents of rooibos (Joubert and de Beer 2011). However, their usefulness as predictive surrogate markers for antidiabetic efficacy still need to be assessed. The current study is designed to link the phenolic composition of green rooibos extract and its bioactivity *in vitro*, as well as investigate whether single chemical entities such as aspalathin can be used to predict bioactivity. The study hypothesized that the chemical marker content correlates with the bioactivity of green rooibos extracts. Thus, investigating the relationship between green rooibos phenolic compounds and bioactivity through advanced statistical methodology (Principle Component Analysis), quality control parameters were simplified for bioactivity assurance.

# CHAPTER 2

## LITERATURE REVIEW

### 2.0. Diabetes mellitus

Diabetes mellitus, often referred to as “diabetes”, is defined as a group of metabolic diseases, that is caused by defaults in the secretion of insulin, insulin action or both (American Diabetes Association 2014). Increased blood glucose levels (hyperglycaemia) are a primary feature on which the diagnoses of diabetes is based (American Diabetes Association 2014; Schulze and Hu 2005). Chronic complications in the eyes, kidneys, heart, nerves and vascular system are common in all cases of hyperglycaemia-related diabetes (American Diabetes Association 2014; Brownlee 2001). A deficiency in the action of insulin on target tissues (skeletal muscle, liver and adipose) is the foundation of defective carbohydrate, protein and fat metabolism (American Diabetes Association 2014). Based on these chronic complications, the disease can be grouped into Type 1 diabetes (T1D) sometimes referred to as insulin-dependent diabetes mellitus (IDDM) or Type 2 diabetes (T2D) also known as non-insulin dependent diabetes (NIDDM) (El-Abhar and Schaalan 2014). T1D is prevalent in 5-10% of diabetics and is caused by autoimmune destruction of the pancreatic  $\beta$ -cells resulting in insulin deficiency (American Diabetes Association 2014; Daneman 2006). On the other hand, T2D is described as a metabolic disease characterised by insulin resistance and pancreatic  $\beta$ -cell dysfunction (DeFronzo 2004). Type 2 diabetes is thought to be triggered by environmental and behavioural factors and also through a genetic predisposition (DeFronzo 2004; Tuomilehto *et al.* 2001). These patients may present with little or no symptoms for years (National Diabetes Data Group, 1979), presenting an opportunity for interventions through healthy living, which includes exercise and the consumption of fruit and vegetables. thought to delay or possibly prevent the clinical onset of T2D (Eyre *et al.*, 2004; Schulze and Hu 2005; Zimmet *et al.*, 2003). Current management of diabetes recommends, together with dietary and lifestyle changes, regular monitoring of glucose levels and frequent medical assessments to optimize medication (Al-Arouj *et al.*, 2010). In developing countries, including South Africa, proper management of diabetes, especially in rural

communities, is poor and contributes to the severity of diabetic complications (Azevedo and Alla 2008).

### **2.1. Factors causing Type 2 Diabetes**

Genetics plays an important role in the pre-disposition of individuals for T2D. Apart from environmental factors, epigenetics also contributes to the development of diabetes (Ali 2013; Kanherkar *et al.*, 2014; Sousa *et al.*, 2011). Genetics, sedentary lifestyle and a hypercaloric diet perpetuate conditions such as insulin-resistance, glucose-intolerance, dyslipidaemia and hypertension, collectively known as the metabolic syndrome, which is strongly associated with obesity and T2D (Cohen 1999; Leclercq *et al.*, 2007; Roberts *et al.*, 2013).

### **2.2. Insulin and glucose regulation**

Wilcox (2005) defines insulin as a dipeptide hormone secreted by pancreatic  $\beta$  cells in the islets of Langerhans, whose function is to maintain normoglycaemic levels through cellular glucose uptake, carbohydrate regulation, lipid and protein metabolism as well as cell proliferation. In the fed state, insulin is responsible for the regulation of cellular energy supply, macronutrient balance and anabolic pathways (Burks and White 2001). Muscle and adipose tissue are the major tissues modulating the metabolism of glucose, which depend on insulin for the intracellular transport of glucose (Guilherme *et al.*, 2008; Wilcox 2005).

### **2.3. Insulin signalling**

Insulin has been the sole pharmacological treatment for diabetic patients who have been diagnosed with type 1 diabetes and a vital therapeutic for type 2 diabetic patients suffering with insulin-deficiency (Zhang *et al.*, 2015). In response to increased glucose levels, insulin is secreted by the pancreatic  $\beta$  cells to stimulate glucose uptake in the liver, muscle and fat cells, thereby maintaining normoglycaemia (Wilcox 2005). For insulin to exert its effects, it binds to the insulin receptor (IR) on target tissues such as muscle, liver and adipose. After binding to the extracellular  $\alpha$ -subunits, a conformational change is triggered by the IR, which subsequently activates intrinsic tyrosine kinases in the intracellular  $\beta$ -subunit (Lee *et al.*, 2014; Maruyama 2014). Once phosphorylated, the cytoplasmic and membrane portion of the IR subunit initiates a phosphorylation cascade of signalling proteins. The insulin signalling cascade commences with phosphorylation of insulin receptor substrates (IRS) at their tyrosine residues. IRS1 and 2 are the predominant effector IRS's for muscle and liver,

respectively (Chang *et al.*, 2004). Key to effective perpetuation of the insulin cascade is the activation and membrane docking of phosphatidylinositol-3 kinase (PI3K) with the phosphorylated IRS. The activated PI3K complex in turn phosphorylates a cascade of kinases including phosphatidylinositol-(4,5)-biphosphate (PI-4,5-P2) to form phosphatidylinositol -3,4,5-triphosphate (PIP3) (Gruzman *et al.*, 2009) (Figure 1). Phosphorylation of PIP3 activates phosphosinositide-dependent kinase 1 (PDK1) which in turn activates protein kinase B (PKB) also known as AKT and protein kinase C- $\zeta$  (PKC- $\zeta$ ). In muscle, activation of Akt and PKC- $\zeta$  promote the translocation of cytoplasmic glucose transporter GLUT-4 vesicles into the cell membrane, which substantially increases glucose uptake into muscle tissues (Giri *et al.*, 2004). Dysregulation of Akt signalling is directly implicated in diabetes, cardiovascular and neurological diseases (Hers *et al.*, 2011).

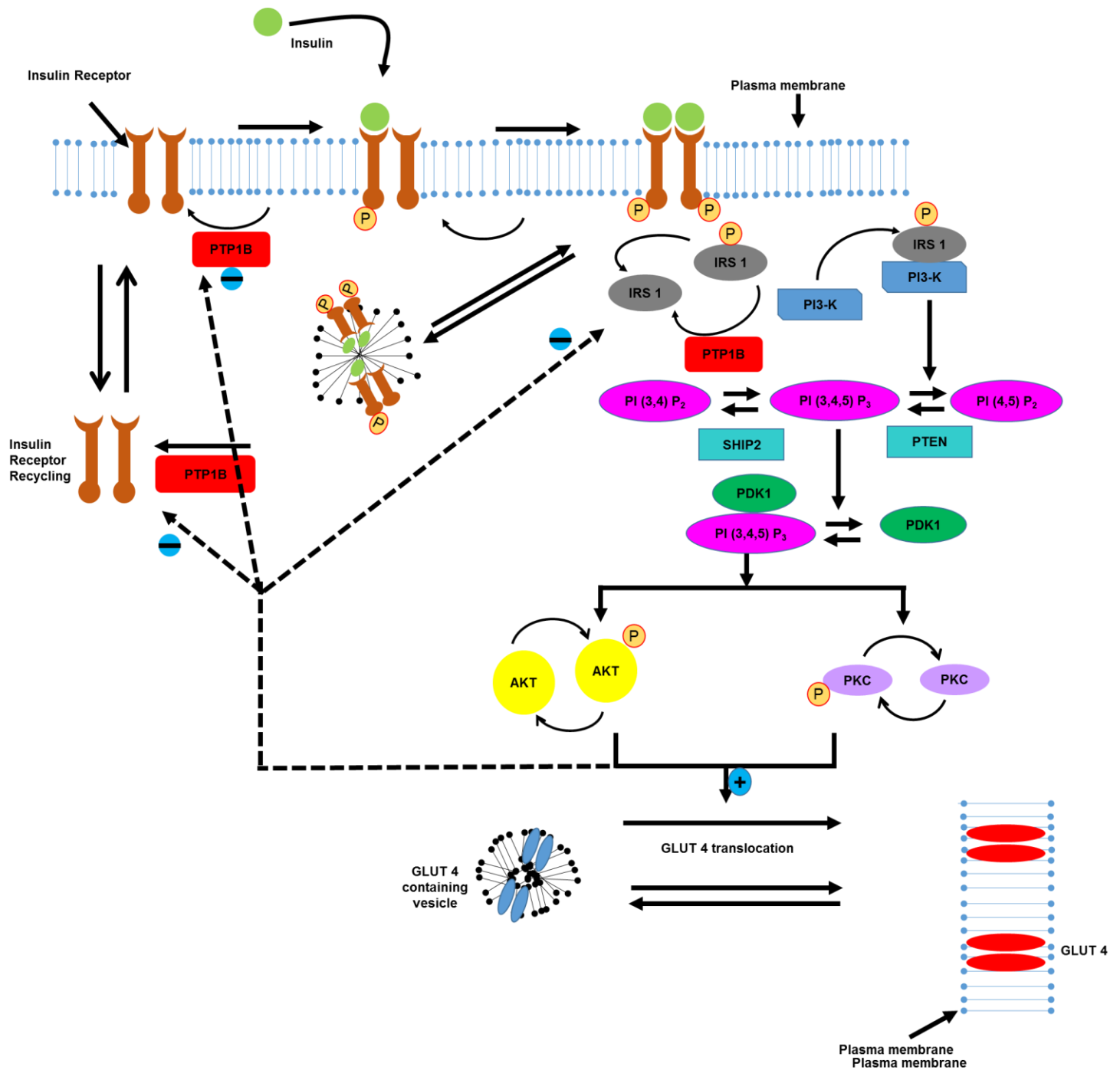


**Figure 1. Molecular mechanisms involved in the insulin signalling pathway that regulates glucose transporter 4 (GLUT4) translocation to cell membrane.** [PTP1B – Protein tyrosine phosphatase 1B. IRS 1 – Insulin receptor 1. PI3K - (PI-4,5-P2) - Phosphatidylinositol-3 kinase. phosphatidylinositol-(4,5)-biphosphate. PIP3 - Phosphatidylinositol -3,4,5-triphosphate. PDK1 - Phosphosinositide-dependent kinase 1. AKT - Protein kinase b. PKC-ζ Protein kinase C-ζ. GLUT 4 – Glucose transporter 4] (Giri *et al.*, 2004).

#### **2.4. Protein Tyrosine Phosphatase 1B (PTP1B)**

The global rise in the prevalence of T2D and obesity-related metabolic diseases has inspired the search for new drug targets. In T2D, drug targets will include effectors that modulate insulin action and ameliorate insulin resistance. Protein tyrosine phosphatases (PTPs) dephosphorylate the insulin receptor (IR) as well as other proteins and thus play a critical role in the signalling of insulin and metabolism (Kang *et al.*, 2015; Tiganis and Bennett 2007). PTPs, such as protein tyrosine phosphatase 1B (PTP1B), emerge as potential target proteins which negatively regulate insulin signalling and ultimately attenuate insulin action by translocation of glucose transporter 4 (GLUT 4) (Goldstein 2001; Oh and Jun 2014). Overexpression of PTP1B has been shown to inhibit the insulin receptor signalling cascade (Asante-Appiah and Kennedy 2003; Cook and Unger 2002) shown in Figure 2. The enzyme also negatively regulates the leptin signalling pathway and the GLUT 4 transporter, which is implicated in peripheral energy expenditure and glucose uptake, respectively (Kang *et al.*, 2015). Therefore, inhibition of PTP1B presents itself as a suitable antidiabetic drug target (Kang *et al.*, 2015).

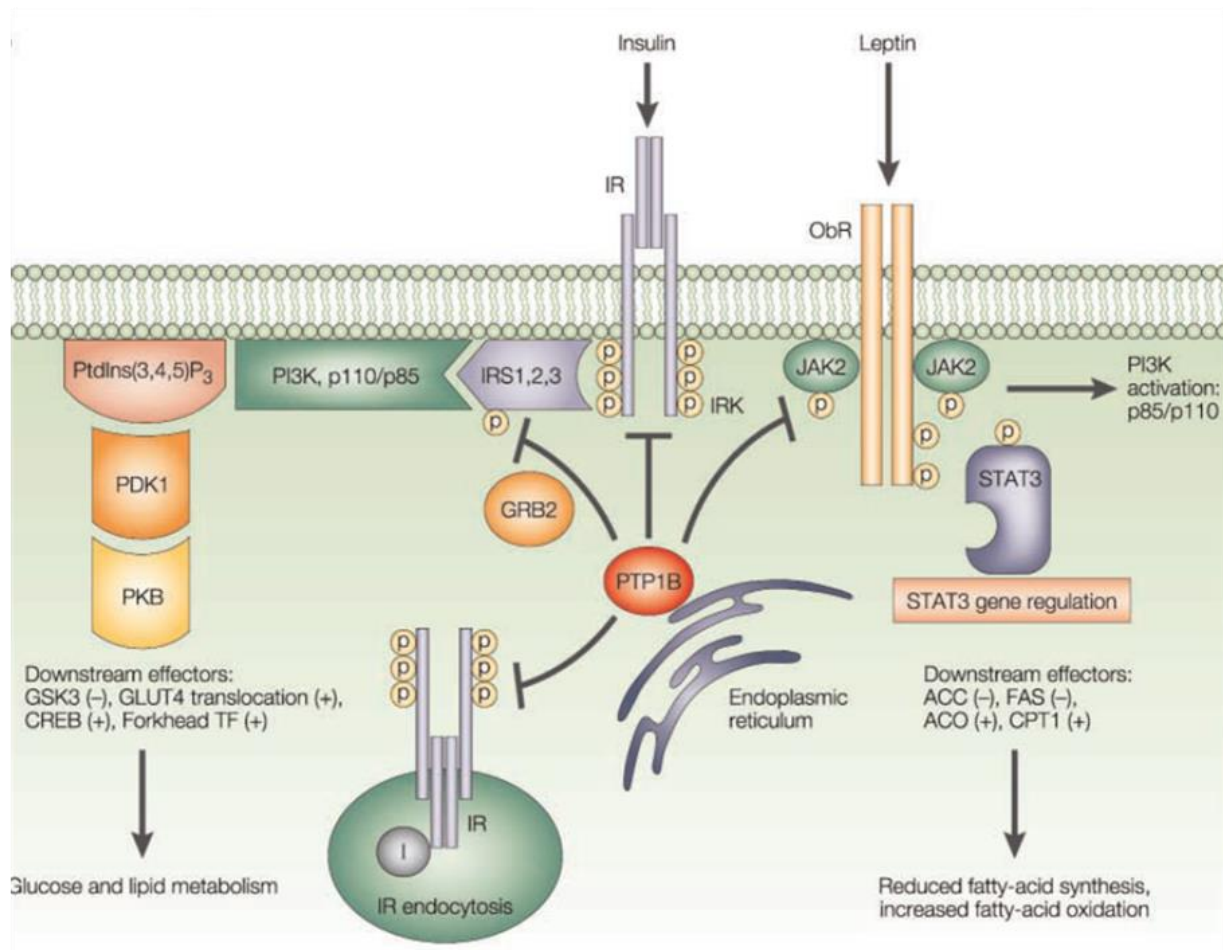


**Figure 2. Insulin and leptin signalling pathways by PTP1B.** Negative regulation of the insulin metabolic signal transduction pathways by PTP1B. Insulin binds to its receptor and activates the insulin receptor kinase (IRK) through autophosphorylation. Insulin receptor substrate (IRS) proteins are recruiting thereby activating phosphatidylinositol-3-kinase (PI3K) through binding the p58 subunit and activating the catalytic p110 subunit. The activation of PI3K induces downstream effectors such as phosphatidylinositol-dependent kinase 1 (PDK 1) and protein kinase B (PKB, known as AKT), which results in the translocation of GLUT 4 and glucose uptake in muscle and inactivation of glycogen-synthase kinase 3 (GSK3). Leptin binds to its receptor ObR, phosphorylating janus kinase (JAK2), and activates the JAK/signal transducer and activator of transcription (STAT) pathway as well as the PI3K pathway. Once activated by JAK2 phosphorylation, STAT3 is translocated to the nucleus, whereby STAT3 induces gene responses that reduce acetyl-coenzyme A carboxylase (ACC) in turn reducing malonyl-CoA and fatty acid biosynthesis while increasing fatty acid oxidation. Cytoplasmic PTP1B dephosphorylates membrane-bound insulin and leptin receptors which leads to their deactivation. Other PTP1B substrates such as IRS1 and PTP1B can downregulate IRK activity through complex formed with growth-factor-receptor-bound protein 2 (GRB2) (Johnson *et al.*, 2002)

## 2.5. Insulin resistance

Insulin resistance, impaired  $\beta$ -cell function and increased reactive oxygen species (ROS) are major causal factors for the onset of T2D (Wang *et al.*, 2013). Most of the peripheral insulin-mediated glucose uptake occurs in the skeletal muscle and adipose tissue which are both largely responsible for maintaining glucose homeostasis. Insulin resistance or failure of insulin to elicit its metabolic effects in insulin sensitive tissues such as the liver, skeletal muscle and adipose tissue, results in inadequate glucose disposal from the circulatory system into these tissues (Roberts *et al.*, 2013). Non-esterified fatty acids (NEFA's) are largely responsible for inducing insulin resistance and impairing the function of  $\beta$ -cells. In humans, insulin resistance occurs within hours after an increase in the level of NEFA's (Kahn *et al.*, 2006). The pancreatic  $\beta$ -cells compensate for insulin resistance by hypersecreting insulin (Kasuga, 2006). However, increasing insulin levels has a hyperbolic effect, whereby the initial effect is to increase glucose uptake but persistent hyperinsulinaemia further perpetuates insulin non-responsiveness or insulin resistance in these insulin sensitive tissues (DeFronzo and Tripathy 2009; Roberts *et al.*, 2013).

## 2.6. AMPK in glucose regulation

The energy sensing molecule AMP-activated protein kinase (AMPK) is a serine/threonine (Ser/Thr) protein kinase (Jørgensen *et al.*, 2004) that senses changes in cellular energy and regulates energy metabolism in the cell (Hardie *et al.*, 2012; Harada *et al.*, 2016). AMPK is a heterodimeric kinase consisting of a catalytic  $\alpha$  subunit and two regulatory ( $\beta$  and  $\gamma$ ) subunits (Gwinn *et al.*, 2008). AMPK is also a GLUT4 translocation promoter, primarily activated by changes in the AMP:ADP/ATP ratio (Hardie *et al.*, 2012), temporary increases in intracellular calcium ( $\text{Ca}^{2+}$ ) concentration or through an AMPK-dependent pathway, mediated by liver kinase B1 (LKB1) which results in contraction-induced glucose uptake (Son *et al.*, 2013).

AMPK can be activated through canonical or non-canonical mechanisms with the former implicating cellular increases in AMP, ADP or  $\text{Ca}^{2+}$  and the latter caused by other stimuli that do not involve increases in the level of AMP, ADP or  $\text{Ca}^{2+}$  (Hardie *et al.*, 2016). Hypoxia and nutrient deficiency result in an increase of AMP and a decrease in ATP, thus activating AMPK. AMP binds directly to tandem repeats of cystathionine-

$\beta$ -synthase (CBS) domains in the  $\gamma$  subunit of AMPK during energy stress. Upon binding, the phosphorylation of the activation threonine loop in the  $\alpha$  subunit is essential for the activation of AMPK (Gwinn *et al.*, 2008).

Mammalian activation of AMPK through canonical mechanisms include glucose or oxygen starvation, metabolic poison and muscle contraction. Xenobiotics, antidiabetic drugs, plant products with health-beneficial properties and traditional Chinese medicinal products also play a role in the activation of AMPK (Hardie *et al.*, 2012). Hawley *et al.*, (2010) demonstrated, using a cell line that expresses an AMP and ADP-insensitive AMPK mutant, that metformin and resveratrol (from grapes and red wine) indirectly activate AMPK through the inhibition of mitochondrial ATP synthesis, resulting in increased levels of cellular AMP. The non-canonical mechanisms involve reactive oxygen species (ROS), such as hydrogen peroxide ( $H_2O_2$ ), which activate AMPK in culture (Hardie *et al.*, 2012). AMPK is also activated by  $H_2O_2$  through a mechanism involving ataxia telangiectasia mutated (ATM), which is a cytoplasmic form of phosphoinositide 3-kinase-like kinase (PIKK). In the nucleus, genotoxic-DNA damaging-treatments including doxorubicin, etoposide and ionizing radiation, also activate AMPK (Hardie *et al.*, 2012).

Downstream targets at Ser/Thr residues are phosphorylated by AMPK and its orthologues within a sequence motif containing hydrophobic residues at the -5 and +4 positions and basic residues at -4 and -3 or both (Gwinn *et al.*, 2008). Once AMPK is activated, catabolic processes that generate ATP are switched on while anabolic processes that consume ATP are turned off. Translocation of GLUT 4 from intracellular storage vesicles to the plasma membrane enhance glucose uptake in resting and contracting muscle (Hardie *et al.*, 2016). Treatment with 5-aminoimidazole-4-carboxamide-1- $\beta$ -D-ribofuranoside (AICAR) may also activate AMPK in human, mouse and rat skeletal muscle cells and in conscious rats *in vivo*. AICAR treatment increases glucose uptake through an insulin-dependent mechanism which depends on GLUT 4 translocation to the surface of the muscle membrane (Jørgensen *et al.*, 2004).

## **2.7. Energy metabolism**

Cells require the use of energy to live, grow and reproduce (Boundless 2016 b). The oxidation of nutrients and formation of high-energy molecules, especially adenosine triphosphate (ATP), is the principle energy vehicle in cells. ATP is synthesized by two mechanisms: 1. Oxidative phosphorylation, which takes place in the mitochondrion, and involves the production of ATP from adenosine diphosphate (ADP) and inorganic phosphate (Pi). 2. Substrate level phosphorylation which takes place in the mitochondrion (during the tricarboxylic citric acid (TCA) cycle) and cytoplasm (during glycolysis), where ATP is synthesized through the transfer of high-energy phosphoryl groups from high-energy compounds to ADP (Lodish *et al.*, 2000).

## **2.8. Transport of glucose**

Glucose uptake in the skeletal muscle cell comprises a series of steps which include the movement of glucose from the blood to the interstitial space, following transmembrane transport inside the muscle cell, which then undergoes intracellular glucose metabolism. Physical exercise enhances the capacity of muscle membrane glucose transport, which simultaneously increases blood flow in the muscle. This then results in increased glucose delivery and enzymatic activity during glucose metabolism (Richter *et al.*, 2001).

### **2.8.1. Glucose transporter 1 (GLUT 1)**

The glucose transporter 1 (GLUT 1) is made up of 492 amino acids with a single N-linked glycosylation at N<sup>45</sup> (Mueckler *et al.*, 1985). Glucose is the main substrate transported by GLUT 1 but mannose, galactose, glucosamine and reduced ascorbate can also be transported by this transporter. However, cytochalasin B and phloretin inhibit the activity of this transporter (Carruthers *et al.*, 2009). GLUT 1 is highly expressed in the membrane of human erythrocytes, where glucose is freely exchanged between the plasma and cytoplasm of these cells. The expression of GLUT 1 in the red blood cells is upregulated, to enhance the capacity of the blood to effectively transport glucose. The brain relies on glucose as a major source of energy under normal physiological conditions and the transport of glucose across the blood-brain barrier is rate limiting (Mergenthaler *et al.*, 2013). In humans, the GLUT 1 transporter mediates materno-placental transfer of glucose and GLUT 1 placental levels fluctuate, affecting the foetus under certain pathological conditions (Mueckler and Thorens

2013). GLUT 1 is crucial in pre-implantation embryo survival and foetal development (Heilig *et al.*, 2003).

### **2.8.2. Glucose transporter 2 (GLUT 2)**

This glucose transporter is characterised as a low affinity glucose transporter synthesized in pancreatic  $\beta$ -cells, intestinal epithelium, kidney and in the adult liver (Gorovits and Charron 2003). During the fed and fasted state, GLUT 2 is responsible for glucose uptake and release respectively, in the liver. However, hepatic glucose expenditure works in the absence of GLUT 2 transporters via a membrane-traffic based system which releases glucose once glucose production from the liver is stimulated (Mueckler and Thorens 2013).

### **2.8.3 Glucose transporter 3 (GLUT 3)**

A high affinity glucose transporter primarily designated as a brain and neuronal glucose transporter, GLUT 3 is also detected in minor levels in the placenta, liver and human myocardium (Gorovits and Charron 2003; Mueckler and Thorens 2013). Immunofluorescence and immunohistochemical localization of GLUT 3 proved this transporter to be located across the human skeletal muscle. Glucose transporters 1, 3 and 4 promote basal glucose uptake at the plasma membrane (Gorovits and Charron 2003).

### **2.8.4. Glucose transporter 4 (GLUT 4)**

Adipocytes, cardiomyocytes and skeletal muscle cells express glucose transporter 4 (GLUT 4) which functions as an insulin-responsive glucose transporter (Huang and Czech 2007). GLUT 4 is found intracellularly in membrane compartments during an insulin-depleted state. Following the ingestion of carbohydrates, the level of insulin rises, mobilising intracellular glucose transporters to the plasma membrane which intensifies glucose uptake and metabolism, thereby lowering blood glucose concentrations. However, peripheral insulin resistance results when there is a deficiency of this insulin-stimulated translocation of GLUT 4 to the plasma membrane which, together with defective insulin secretion from pancreatic  $\beta$ -cells and hepatic insulin resistance, leads to the onset of type 2 diabetes mellitus (Wilcox 2005; Mueckler and Thorens 2013).

## 2.9. Glycolysis

The process by which a single molecule of glucose is phosphorylated and degraded into two pyruvate molecules is known as glycolysis (Guo *et al.*, 2012; Lodish *et al.*, 2000). This pathway also generates substrates for energy production in the form of ATP and for glycogenesis and lipogenesis (Guo *et al.*, 2012). In the first steps of this pathway, two ATP molecules are consumed to activate glucose and fructose-6-phosphate. Most of the free energy obtained from the breakdown of glyceraldehyde 3-phosphate (G3P) in the latter part of glycolysis is conserved in the acyl phosphate group of 1,3-bisphosphoglycerate (1,3-BPG) which is high in free energy. Energy released from the conversion of 1,3-BPG to 3-phosphoglycerate is coupled to ADP resulting in ATP production. Another molecule of ATP is synthesized when phosphoenolpyruvate (PEP) is converted to pyruvate (Figure 3). The phosphate-ester bond in PEP deems it as a high energy biomolecule and thus its conversion is coupled with the phosphorylation of ADP. The reactions leading to the formation of ATP is known as substrate level phosphorylation (Boundless 2016 a; Poian and Castanho 2015)

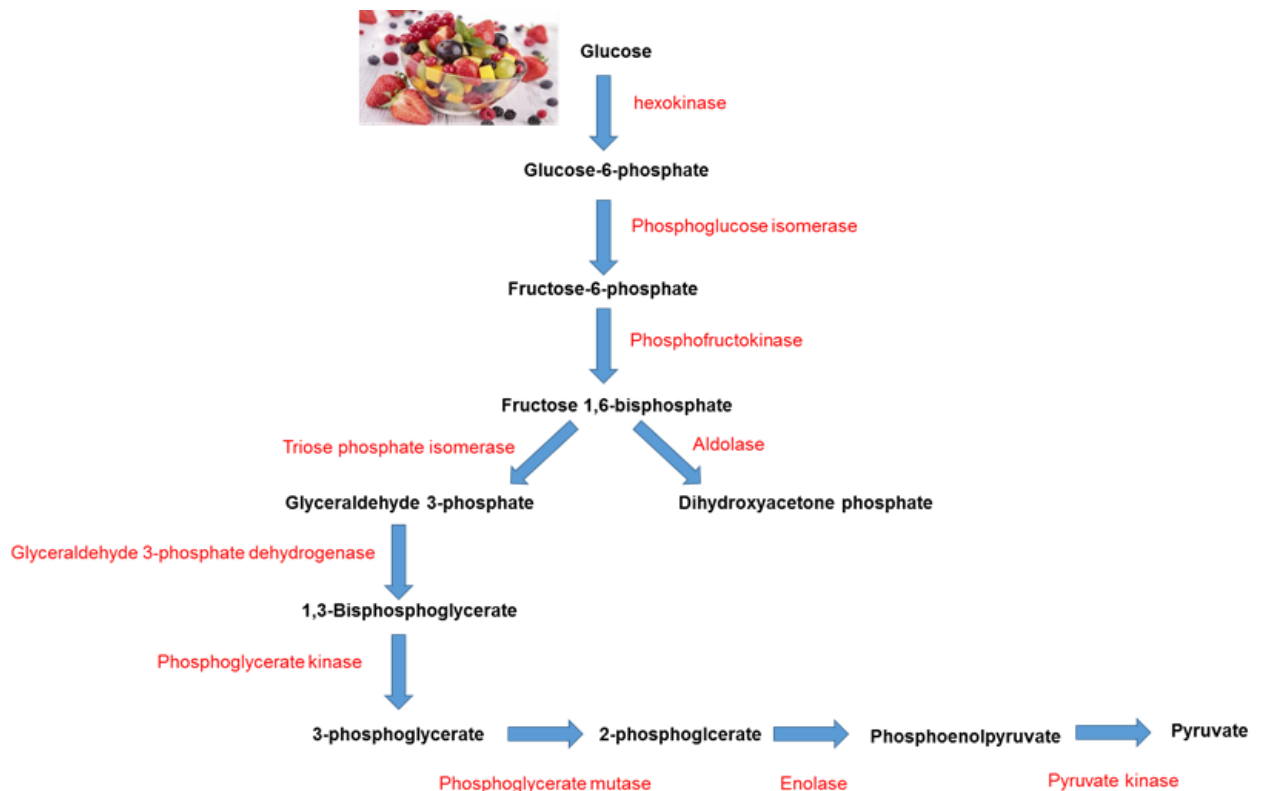


**Figure 3. A schematic diagram of the glycolytic pathway.** In glycolysis, glucose from food sources such as fruit and vegetables is metabolized into high energy biomolecules (e.g. pyruvate) which can enter the tricarboxylic acid cycle (TCA cycle) and then further broken down to release energy (Aryal, 2015).

## 2.10. Fatty acid oxidation

The four reaction pathway of fatty acid oxidation generates acetyl-CoA and an acyl-CoA. These two biomolecules are shortened by two carbons with the reduction of flavin adenine dinucleotide (FAD) by acyl-CoA dehydrogenase, and nicotinamide adenine dinucleotide (NAD<sup>+</sup>) by  $\beta$ -hydroxyacyl-CoA dehydrogenase. This process is often referred to as  $\beta$ -oxidation, because the  $\beta$ -carbon atom is metabolized before the bond between the  $\beta$  and  $\alpha$  carbon is cleaved. The process of  $\beta$ -oxidation continues until acyl-CoA is completely oxidized to acetyl-CoA, which re-enters the TCA cycle (Berg *et al.*, 2002).

## 2.11. Lipids and lipid metabolism

Free fatty acids are important constituents of membrane lipids which serve as a major energy reserve and also act as cellular signalling molecules in the metabolic syndrome. Acetyl-CoA carboxylases 1 and 2 (ACC1 and ACC2) play a role in the catalysis of the formation of malonyl-CoA, a substrate for fatty acid synthesis and a regulator of fatty acid oxidation. They play pivotal roles in energy metabolism of fatty acids in animals and are highly regulated. These key regulators are seen as targets in the regulation of obesity, hyperglycaemia, cancer and cardiovascular diseases (Wakil and Abu-Elheiga 2009).

Long chain fatty acids (LCFA's) are major sources of energy and vital components of lipids situated in the cellular membrane. They are either food derived or synthesized from acetyl-CoA through the glycolytic pathway and the TCA cycle, which form the backbone carbons of fatty acids and glycerols in fat synthesis.  $\beta$ -oxidation of fatty acids results in the production of acetyl-CoA, which is therefore recognized as a key intermediate in the metabolism of carbohydrates, lipids and amino acids (Wakil and Abu-Elheiga, 2009).

Fatty acid synthase (FAS) is a complex used in the synthesis of fatty acids which requires acetyl-CoA, malonyl-CoA and NADPH as substrates and cofactors, respectively. Malonyl-CoA donates the C<sub>2</sub> *de novo* in the synthesis of fatty acids and inhibits the carnitine/palmitoyl shuttle systems for the breakdown of fatty acids. ACC1 and ACC2 have both evolved to facilitate the different roles of fatty acid synthesis and oxidation (Wakil and Abu-Elheiga, 2009). In the absence of food, stored glycogen, muscle proteins and fats are broken-down and consumed. In order for animals to

survive long periods of starvation, the synthesis and storage of fat utilizes special mechanisms involving ACC1, ACC2 and carnitine palmitoyl transferase 1 (CPT-1) (Wakil and Abu-Elheiga, 2009).

The TCA cycle shows that acetyl-CoA, generated in the mitochondria by pyruvate dehydrogenase (PDH), condenses with oxaloacetate (OAA) to form citrate, which in turn undergoes oxidation to produce energy or is transferred to the cytosol to generate acetyl-CoA through ATP citrate lyase (ACLY) (Pietrocola *et al.*, 2015). Acetyl-CoA is carboxylated to malonyl-CoA by ACC 2, inhibiting the action of CPT-1 and limits the entry of acyl-CoA into the inner mitochondria for  $\beta$ -oxidation (Su and Abumrad 2009). Thus, the overall effect is decreased fatty acid oxidation and increased synthesis of fatty acids and triglycerides (TG) (Skorve *et al.*, 1990).

The formation of malonyl-CoA from acetyl-CoA is catalysed through the ATP-dependent carboxylation of acetyl-CoA carboxylase (ACC) (Figure 4). This rate limiting reaction initiates fatty acid synthesis. Apart from its role in fatty acid biosynthesis, malonyl-CoA also regulates mitochondrial fatty acid uptake through allosterically inhibiting CPT-1, which catalyzes the first step in mitochondrial fatty acid oxidation (Cheng *et al.*, 2006). Hence, malonyl-CoA controls the switch between carbohydrate and fatty acid metabolism in skeletal muscle and in the liver (Tong and Harwood, 2006).

The conversion of malonyl-CoA to acetyl-CoA is catalyzed by the enzyme malonyl-CoA decarboxylase (MLYCD), thereby regulating the levels of malonyl-CoA. This enzyme is expressed in muscle and heart tissue, liver, kidney and pancreas. This enzyme also exists in the cytosol, mitochondria and peroxisomes (Dyck *et al.*, 1998; Joly *et al.*, 2005; Rodriguez *et al.*, 2014). CPT-1 is an important enzyme in the mitochondrial metabolism of long-chain fatty acids. In fatty acid oxidation, CPT-1 is the rate-limiting enzyme which catalyzes the formation of acylcarnitine which is mobilized across the mitochondrial membrane by acylcarnitine transferase (Zammit, 1999).

In the mitochondria, CPT-II converts long-chain fatty acids back to their coenzyme-A parts, and acyl-CoA enters  $\beta$ -oxidation resulting in the production of acetyl-CoA. Fatty acid synthesis in the liver is promoted through elevated levels of acetyl-CoA, which leads to an increase in malonyl-CoA, thereby inhibiting CPT-1. Low concentrations of malonyl-CoA favour  $\beta$ -oxidation, thereby transporting long-chain fatty acids into the

mitochondria. Hence, malonyl-CoA is a pivotal metabolite which maintains the balance between the synthesis and breakdown of fatty acids (Joly *et al.* 2005; Tong and Harwood 2006). The role of malonyl-CoA and malonyl-CoA decarboxylase in skeletal and cardiac muscle is to maintain the metabolism of fatty acids through inhibiting muscle CPT-1 (Young *et al.*, 2001). Cardiac and skeletal muscle CPT-1 is more sensitive to malonyl-CoA than the liver form, thus decreasing fatty acid synthesis in these muscle tissues (Cheng *et al.*, 2006; Ronnett *et al.*, 2006).

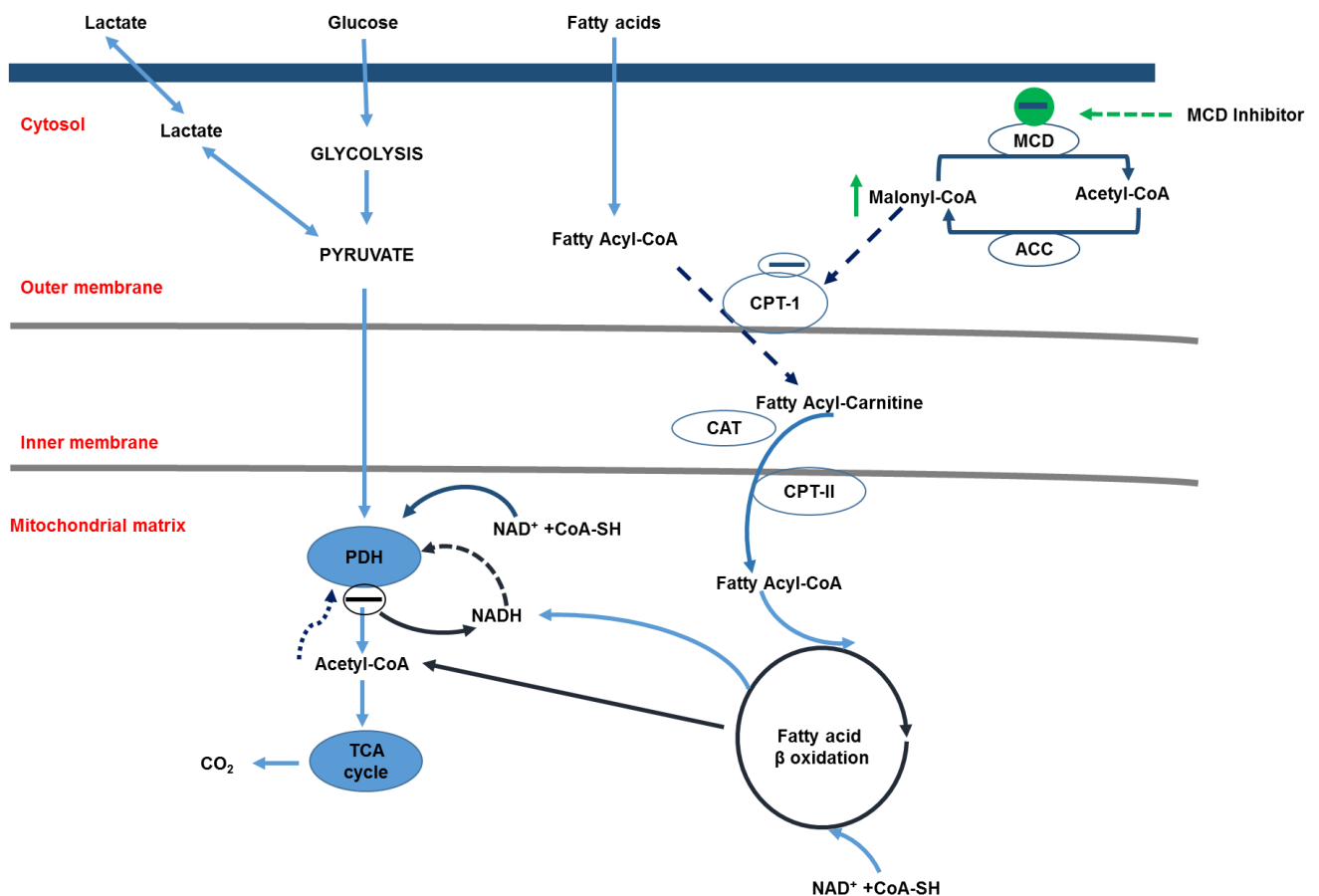


**Figure 4. Malonyl-CoA and CPT-I regulation in fatty acid metabolism.** PDH – pyruvate dehydrogenase, TCA – tricarboxylic citric acid, NAD<sup>+</sup> - nicotinamide adenine dinucleotide, CoA-SH – Co-enzyme A, CAT - Carnitine acyl transferase, CPT-1 - carnitine palmitoyltransferase 1, CPT-II – carnitine palmitoyl transferase II, ACC – acetyl-CoA carboxylase, MCD – malonyl-CoA decarboxylase (adapted from Cheng *et al.*, 2006).

## **2.12. Cell models used in this project**

### **2.12.1. C2C12 murine skeletal muscle cells**

Skeletal muscle regulates glucose homeostasis by disposing of approximately 70-80% glucose in an insulin-dependent pathway. In a resting state, the muscle needs insulin in order for excess nutrients to be stored (Conejo and Lorenzo 2001). Insulin action may be directly affected once there are alterations in blood glucose which is evident in chronic hyperglycaemia. Insulin and exercise have important roles in the modulation of glucose transport and its metabolism (Jensen *et al.*, 2011). Skeletal muscle and adipocytes display insulin-stimulated GLUT 4 translocation and glucose uptake which is dependent on phosphatidylinositol 3-kinase (PI3K) activity. The transport of glucose in skeletal muscle is enhanced by an insulin-independent pathway through the activation of 5' AMP-activated protein kinase (AMPK). Muscle contraction and hypoxia have been speculated to activate this mechanism (Jørgensen *et al.*, 2004).

The transport of glucose in skeletal muscle is controlled by two glucose transporters, namely GLUT 1 and GLUT 4. Insulin stimulation, hypoxia and muscle contraction stimulate GLUT 4 translocation from intracellular storage reserves to the cell surface, thereby enhancing glucose transport (Bryant *et al.*, 2002). Thus, a defect in this type of insulin action in skeletal muscle could be responsible for the insulin-resistant characteristics in T2D. Research, using whole animal experiments, has been extensively used to understand the mechanisms of insulin and exercise-induced glucose uptake in skeletal muscle. However, the precise mechanism of GLUT 4 translocation in response to insulin and exercise, using skeletal muscle cells, would provide a better understanding at a molecular level (Lauritzen 2013).

Studies on insulin action, glucose metabolism and GLUT 4 translocation have employed various cell lines derived from skeletal muscle (L6, C2C12 and BC<sub>3</sub>H1). The most frequently used cell line, as a model for investigating the insulin-stimulated glucose transport system, is the L6 line from rat skeletal muscle (Nedachi and Kanzaki, 2006). The overexpression of GLUT 4 leads to an increase in insulin-induced glucose, in both differentiated or undifferentiated cells (Ariga *et al.*, 2008).

Mouse derived C2C12 skeletal muscle cells are often used in the investigation of muscle cell differentiation and development, myofibrillogenesis, sarcomere development and myotube contractions. C2C12 cells are murine myoblasts which are

derived from satellite cells and they behave similar to progenitor cells. Progenitor cells arise from stem cells which develop into specialized cells (Hill and Olson, 2012). Myoblasts are the pre-cursors of muscle cell, which fuse to form myotubes that can be differentiated further into myocytes. They display the fully matured features of functional muscle cells (Burattini *et al.*, 2004). After muscle differentiation, the remaining myoblasts develop in adult muscles as satellite cells which are located between the sarcolemma and the basal membrane of muscle fibers (Cooper *et al.*, 1999). The C2C12 cell line are a subclone of C2 myoblasts (Yaffe and Saxel 1977) and differentiate spontaneously after serum removal (Blau *et al.*, 1983). In terms of sarcomere formation, which is necessary for muscle contractility, C2C12 cells differentiate more efficiently than when compared to the L6 cells (Nedachi and Kanzaki, 2006).

### **2.12.2. C3A human liver cells**

A major target tissue involved in metabolism is the liver and it performs a number of functions, some of which include the storage of glucose in the form of glycogen, detoxification and the synthesis of proteins in plasma. In addition, the liver also secretes bile, which plays a role in digestion and it also regulates specific substances at accurate concentrations in the body. Above all, the main function of this tissue is to modulate the biotransformation and excretion of toxins from the body (Baudoin *et al.*, 2011). *In vitro* or *in vivo* experimental models are used to study the metabolic pathways such as metabolizing enzymes involved in the degradation of xenobiotics, chemicals, drugs and molecules (Jia and Liu 2007). The liver metabolizes glucose into substrates such as acetyl-coA for the synthesis of fatty acids (Do *et al.*, 2013). HepG2 cells are cancer derived cells of the liver which are characteristic of both hepatocyte and tumour cells. The primary metabolism of the flow of carbon into or out of hepatocytes begins with glycolysis or gluconeogenesis and as such, directly influences the modulation of metabolic pathways which include urea production, lipid and glutamine metabolism (Rui 2014). The HepG2 cell line was established by Aden *et al.* (1979) and exhibits characteristics of normal hepatocytes which include synthesis of serum proteins and binding of asialoglycoproteins (Kelly and Darlington 1989). The C3A cell line is a clone derivative of the hepatoblastoma-based HepG2 lineage which is an excellent choice employed in the bioartificial liver support system (BALSS) trials as it is selected for its well differentiated hepatic phenotype (Filippi *et al.*, 2004). Hence, these cells are used as a model for studying the cellular physiology of hepatocytes such as response to

inflammatory stimuli and *in vitro* toxicology studies (Plant 2004). The HepG2/C3A lineage has also been used as a source for studying bioartificial livers (Filippi *et al.*, 2004; Iyer *et al.*, 2010; Mavri-Damelin *et al.*, 2008). In a study aimed at establishing a method for hepatic differentiation *in vitro* by Kelly and Darlington, 1989, they demonstrated that as the HepG2 cells reach high density, they display foetal to adult features seen in the liver. Thus, the C3A liver cells do not need to be differentiated as they maintain normal liver biological activities once confluent (Kelly, 1994).

### **2.12.3. 3T3-L1 murine preadipocytes**

3T3-L1 preadipocytes are a subclone of murine Swiss 3T3 fibroblasts, cloned by Green and colleagues (1974). The preadipocytes are differentiated in culture to resemble morphological and biochemical characteristics of adipocytes. This is because synthesis and accumulation of fat is switched on, as well as the enzymes involved in the lipogenic pathway. The activity of acetyl-CoA carboxylase is increased in this pathway due to increased enzyme activity (Reed *et al.*, 1977).

Under standard culture conditions, adipocyte formation in the 3T3-L1 cells only begins once cells are confluent and cell division halted. Chronically exposing the cells to insulin accelerates the expression and may further be enhanced by treating the confluent cells with prostaglandin F<sub>2a</sub> or methylisobutylxanthine. Differentiation of preadipocytes results in changes in the reaction of the 3T3-L1 cells to adipocyte regulatory hormones. Only differentiated 3T3-L1 cells are able to stimulate glucose oxidation. Thus, the 3T3-L1 preadipocyte is a unique model in understanding the mechanisms by which differentiating cells respond to specific hormones (Reed *et al.*, 1977).

After growth arrest, the fibroblastic phenotype of this cell line is treated with prodifferentiative agents which enable the conversion to adipocytes. These agents include 1 µg/mL insulin, 0.25 µM dexamethasone and 0.5 mM 3-isobutyl-1-methylxanthine (IBMX). About four days after treatment, the cells start accumulating lipids in the form of fat droplets which, over a cultivation period, grow in size and number (Zebisch *et al.*, 2012).

Obesity is increasing globally and it plays a role in predisposing a variety of other illnesses, such as type 2 diabetes, hypertension and coronary heart disease (Hurt *et al.*, 2010). Adipose tissue is a major storage site for fat. This tissue depot is responsible for balancing the energy homeostasis in the body (MacDougald and Lane 1995; Saltiel and Kahn 2001). Important processes performed by adipocytes include satiety, reproduction and bone function which are elicited through the proteins secreted by adipocytes (Spiegelman and Flier 2001). Leptin, secreted by adipocyte tissue is an example which acts on the hypothalamus to regulate the ingestion of food (Baskin *et al.*, 1999; Havel 2000; Woods *et al.*, 1998).

### **2.13. Indigenous medicinal plants**

South Africa is blessed with a diversity of plants, of which the Cape Floral Region has been identified as an UNESCO biodiversity hotspot due to its diversity, density and endemism of its plant species which are among the highest in the world (Wilgen *et al.*, 2016). Unique to this area are the fynbos species. These plants are limited to the coastal and mountainous areas within 200 kilometres from the coast. Fynbos has an exceptional biodiversity with approximately 8500 different species, of which approximately 6000 are endemic to the Cape floral region (Wilgen *et al.*, 2016).

Included in these endemic fynbos species is the leguminous plant, *Aspalathus linearis* (Brum.f) Dahlg. (family Fabaceae; tribe Crotalarieae), indigenously known as “rooibos” which is endemic to the Cederberg Mountain area of the Western Cape (Joubert *et al.*, 2008). Rooibos tea production has a major impact on economy of this arid region. Based on anecdotal evidence, rooibos tea has traditionally been used for treating infantile colic, allergies, asthma and dermatological matters (Joubert *et al.*, 2008; Morton 1983). This unique plant, apart from its pleasant taste and soothing effects is attracting more and more interest from the cosmeceutical and pharmaceutical industry, mainly due to its unique polyphenol constituents (Joubert and de Beer 2011). The rooibos plant is bright green with needle-like leaves on slender branches. Once bruised, the oxidation process begins turning the leaves into a reddish-brown colour (Morton 1983). The oxidized (fermented) type of rooibos is often consumed as an infusion (Joubert and de Beer 2011; von Gadow *et al.*, 1997). But of great interest is the green (unfermented) rooibos, which has displayed antidiabetic properties and

protective effects on insulin resistance *in vitro* and *in vivo* (Kamakura *et al.*, 2015; Mazibuko *et al.*, 2013; Muller *et al.*, 2012; Son *et al.*, 2013).

#### **2.14. Phenolic compounds as phytomedicines**

Phenolic compounds have become the centre of extensive research efforts directed at elucidating antidiabetic and other health properties of secondary plant metabolites (Babu *et al.*, 2013). They are targeted for their beneficial health-supporting effects which correlate to their anti-oxidant, anti-inflammatory, cardio-protective, anticancer and neuro-protective abilities (Del Rio *et al.*, 2013). In terms of the health attributes of rooibos, research interest has shifted towards green (unfermented) rooibos since it has higher polyphenol concentrations compared to the fermented rooibos (Joubert and de Beer 2011).

The use of phytomedicines in the form of capsules, extract, powders, fresh or dried plants and tablets are consumed to better one's health and well-being (Preethi *et al.*, 2014). These medicines are perceived to be safe and countless number of people often purchase them off-the-counter, without medical oversight. To ensure the efficacy and safety of these products, regulation and standardisation of the active ingredients found within these medicinal plants are essential (Barnes 2003; Kunle *et al.*, 2012). Therefore, chemical and bioactive profiling of these health products should be performed (Bahadoran *et al.*, 2013; Das *et al.*, 2012; Preethi *et al.*, 2014).

In the search for novel, rooibos-based therapeutics, the effectiveness and safety of these products will depend on its chemical composition. Scientifically rooibos has been shown to have antidiabetic, anti-inflammatory and anti-obesity activity amongst other benefits (Kamakura *et al.*, 2014; Mazibuko *et al.*, 2013, 2014; Muller *et al.*, 2012; Son *et al.*, 2013). Due to these beneficial health properties, public and commercial interest has escalated, with rooibos nutraceuticals and cosmeceuticals appearing on the market. However, these products have not been validated for efficacy and safety (Veronin *et al.*, 2014) as no standards for dosage or chemical content have been established (Brin *et al.*, 2014). The popular belief that natural medicines are safer than conventional pharmaceuticals contributes to the demand of such products. Hence, in the absence of effective regulatory control in health products, the need for quality attributes such as the quantity of active pharmaceutical ingredients (API's) exists, so

that they can be used by the research and pharmaceutical industry as a pharmaceutical guideline.

### **2.15. Polyphenols**

Plants produce primary and secondary metabolites with the former responsible for essential metabolic roles such as growth, development and reproduction (Croteau *et al.*, 2000; Hussain *et al.*, 2012). The secondary metabolites aid in the protection against biotic and abiotic stress (Anhê *et al.*, 2013) and has shown to play a role in the defence against several diseases in humans (Kennedy and Wightman 2011; Korkina 2007). The beneficial health-properties of plant polyphenols are demonstrated in Figure 5. Polyphenols usually possess antioxidants (Han *et al.*, 2007) richly sourced in fruits, vegetables and beverages (Del Rio *et al.*, 2013). Produced as secondary metabolites of plants, polyphenols aid in the defence against ultraviolet radiation, attack by pathogens and other stressors (Ramakrishna and Ravishankar 2011). They contribute toward factors such as astringency, bitterness, flavour, colour, odour and stability in food (Oliveira *et al.*, 2014). Polyphenols are classed into 4 major groups based on the number of functional phenol rings and the structural elements that bind these rings to one another. These groups include phenolic acids, flavonoids, stilbenes and lignins. Of particular interest to this study are the flavonoids, which are the most studied group of polyphenols (Babu *et al.*, 2013; Manach *et al.*, 2004; Pandey and Rizvi 2009).

### **2.16. Bioactivity of polyphenols**

Polyphenols are natural antioxidants that have the ability to slow or prevent other molecules from undergoing oxidation, thus making them suitable reducing agents. Chain oxidation reactions can be disrupted in cellular components through the phenolic groups in polyphenols which form stable phenoxyl radicals by accepting an electron (Balasaheb Nimse and Pal 2015). Bioactive polyphenols from olives, wine and berries have protective antimicrobial effects, however the chemical structure of the compound and bacterial species determines the degree of microbial inhibition (Del Rio *et al.*, 2013). Research on the anti-inflammatory activity of phenolic compounds have been documented *in vitro* and *in vivo* (Ambriz-Pérez *et al.*, 2016; Ferrándiz and Alcaraz 1991). Anti-inflammatory effects are expressed through the regulation of pro-

inflammatory gene expression, chiefly utilizing nuclear factor-kappa B (NF- $\kappa$ B) and mitogen-activated protein kinase signalling (MAPK) (Santangelo *et al.*, 2007). Some polyphenols interfere with nutrient absorption by chelating metals like iron and zinc, thereby reducing their absorption, inhibiting digestive enzymes and precipitating proteins (Etcheverry *et al.*, 2012). In the plant kingdom, there are a variety of polyphenolic antinutrients which form insoluble complexes with mono, di- and tri-valent cations at physiological pH, thereby prohibiting absorption and decreasing bioavailability (Agbaire 2011). Among other health benefits linked to polyphenols, some phenolic compounds are said to have prebiotic effects since they are poorly digested, these attractive compounds stimulate the proliferation of gastrointestinal bacteria leading to a balance in colonic flora (Del Rio *et al.*, 2013).

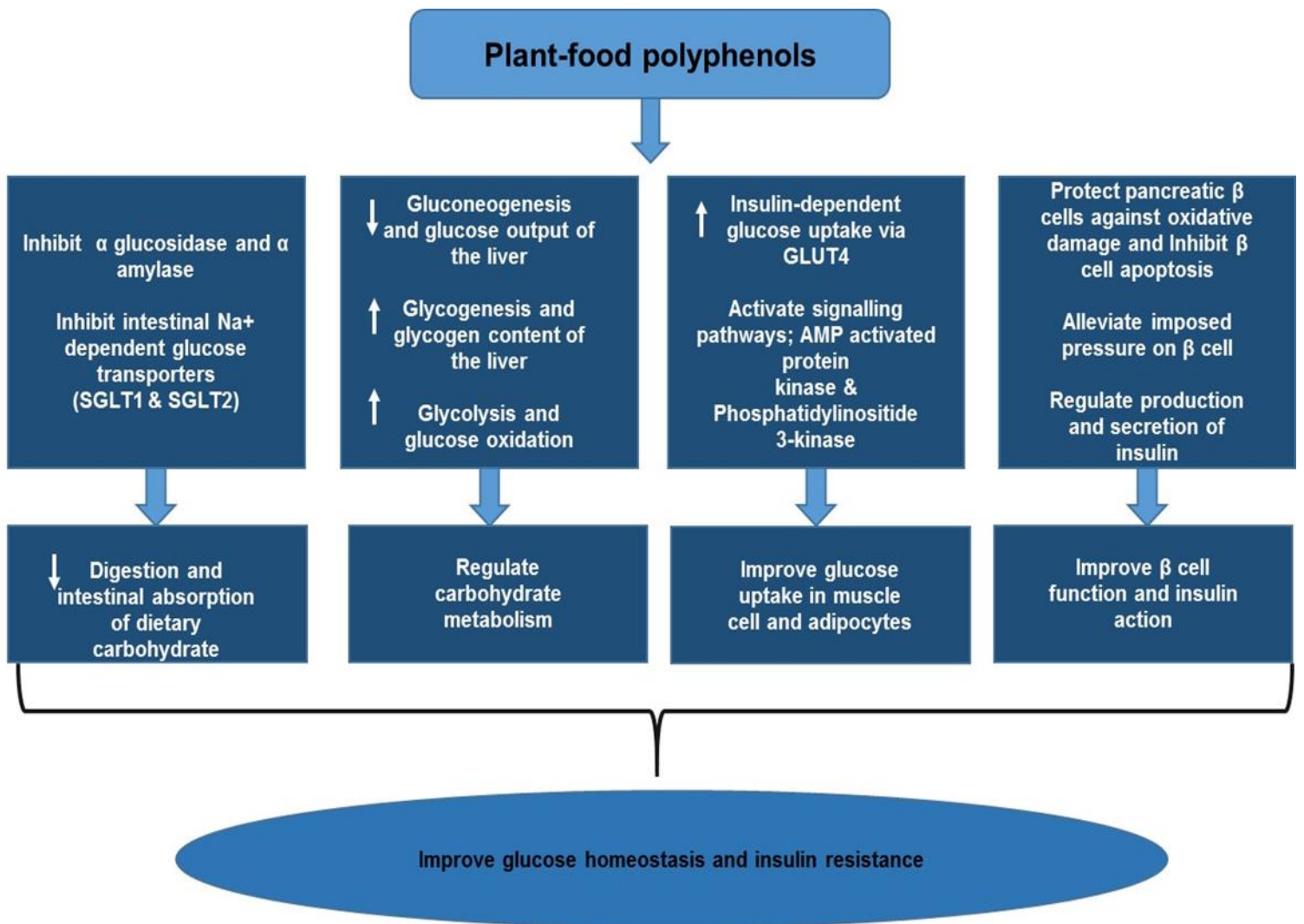


**Figure 5. Beneficial effects of polyphenols in the management of blood glucose in diabetes.** The hypoglycemic effects of polyphenols are mainly attributed to reduce intestinal absorption of dietary carbohydrate, modulation of the enzymes involved in glucose metabolism, improvement of  $\beta$ -cell function and insulin action, and stimulation of insulin secretion. (Adapted from Bahadoran *et al.*, 2013).

## 2.17. Flavonoids

Flavonoids are a sub-group of polyphenols which occur as glycosides, aglycones or methylated derivatives. The glucose moiety is unattached to the structure of flavonoids (aglycones) in plants (Tapas *et al.*, 2008). The structure of a flavonoid comprises two aromatic rings, A and B, which are connected by a 3-carbon chain that forms an oxygenated heterocyclic ring (C ring). Major classes of flavonoids are flavan-3-ols, flavanones, flavonols, anthocyanidins and isoflavones. Flavonoids are classed into different groups based on the saturation of the C ring, functional groups on the rings and the position at which the B ring is attached to the C ring. Some of the beneficial characteristics of flavonoids include (a) the enhancement of insulin secretion, diminished apoptosis and promotion of the proliferation of pancreatic  $\beta$ -cells; (b) improvement of hyperglycaemia by regulating glucose metabolism in hepatocytes; (c) diminishing insulin resistance, inflammation and oxidative stress in fat and muscle and (d) increasing uptake of glucose in skeletal muscle and white adipose tissue (Babu *et al.*, 2013; Vinayagam and Xu 2015). The digestion of carbohydrates, secretion and signalling of insulin, in insulin-sensitive tissues, is controlled by flavonoids (Babu *et al.*, 2013). The most abundant flavonoid found in rooibos is aspalathin (2',3,4,4',6'-pentahydroxy-3'-C- $\beta$ -D-glucopyranosyl), a dihydrochalcone unique to rooibos (Chen *et al.*, 2013). A range of 4 – 12% of aspalathin is contained in unfermented rooibos plant material (Kreuz *et al.*, 2008).

## 2.18. Bioavailability vs bioactivity

Bioavailability, defined by Massimo *et al.*, (2007), is the amount of nutrient that is digested, absorbed and metabolised through normal pathways. Polyphenols are further modified during absorption where they are conjugated in the cells of the intestine and then in the liver through methylation, sulfation and/or glucuronidation (Cardona *et al.*, 2013; Manach *et al.*, 2004; Pandey and Rizvi 2009). Thus, resulting in different forms which reach the blood and tissues as those found in food. The key factor determining the rate and magnitude of the absorption of polyphenols is dependent upon its chemical structure and not its concentration (Pandey and Rizvi 2009). The absorption and metabolism of polyphenols are determined by the physicochemical properties which are the sole chemical structures (Bravo 1998). Generally, low molecular weight phenolic acids which include gallic acid and isoflavones are readily absorbed by the gastrointestinal tract. However, large-sized polyphenols are less easily absorbed; some of these include proanthocyanidins, galloylated tea catechins as well as anthocyanidins (Manach *et al.*, 2004). The degree of bioavailability varies from one polyphenol to another and the most abundant polyphenol is not likely the one resulting in increased active metabolites in the plasma. Recent studies performed in humans have shown that fasting enhances bioavailability of epigallocatechin gallate (EGCG) (Rein *et al.*, 2013). Based on their ability of absorption, polyphenols can be categorized as easily or uneasily absorbed. They can be extractable polyphenols or nonextractable. Whereby extractable polyphenols are low to medium molecular sized phenolics that can be extracted with different solvents such as water or methanol. Nonextractable polyphenols can be defined as high molecular weight compounds which bind dietary fiber/protein and become insoluble in water and methanol. This is why they develop resistance to intestinal digestion and absorption and are excreted in the faeces (Martin and Appel 2010).

## **2.19. *Aspalathus linearis* (Rooibos)**

Rooibos is accredited for numerous health benefits mentioned in section 2.6. in addition to its low tannin and caffeine-free status. Rooibos contributes toward a wide variety of herbal products currently available as herbal supplements or cosmetic products. Research is now being aimed at characterising the phenolic composition of rooibos extracts and identifying marker compounds for extract standardisation and quality control (Joubert *et al.*, 2008). Rooibos is a rich source of bioactive phenolic compounds, of which the most abundant is the dihydrochalcone C-glucoside aspalathin (Joubert *et al.*, 2012), unique to rooibos, and its oxidative products, the flavones orientin and isoorientin (Joubert *et al.*, 2008). It's large-scale production is used in the beverage industry and sold to consumers who drink it as a herbal tea, but extracts are also commercially available (Canda *et al.*, 2014). An unfermented (green) rooibos extract previously displayed antidiabetic properties as well as protective effects on insulin resistance in cell cultures and animal models (Kamakura *et al.*, 2015; Mazibuko *et al.*, 2013; Muller *et al.*, 2012; Son *et al.*, 2013). The phenolic compounds in unfermented (green) rooibos extract have been found to be in much higher concentrations than the fermented rooibos, as they are diminished in the fermentation process. (Joubert and de Beer, 2011).

### **2.19.1. Fermented vs. Unfermented rooibos**

Factors that play a role in grading rooibos include; colour, flavour and cut length with the highest grade named "super grade" (Erickson 2003). Commercial production of rooibos entails harvesting the needle-like leaves in the summer to late spring (Joubert and de Beer 2011). The rooibos plant (both leaves and stems) is grown 30 cm above the ground and harvested during the summer months (Standley *et al.*, 2001; de Beer *et al.*, 2016). Rooibos is processed in two different ways yielding two kinds of tea. The leaves and stems of the rooibos plant can be bruised and fermented or instantly dried to prevent oxidation (Joubert and de Beer 2011). Fermentation leads to a colour change in the green leaves to orange/red which designated the name "rooibos" to the fermented type, which in Afrikaans means "red bush". During the fermentation process, the fermented rooibos loses some polyphenols hence, the unfermented type typically known as "green rooibos" contains a higher polyphenol content. Unfermented rooibos

tea appears tan/yellow in colour compared to the rich reddish colour seen in fermented rooibos tea (Erickson 2003).

### **2.19.2. Agro-processing and seasonal variation**

The method of production, annual climate variations, post-harvest processing and storage are key factors that determine polyphenol concentrations (Jassey *et al.*, 2011) of rooibos. Regardless of the production method, climate can significantly affect the annual amount of polyphenols produced by the plant (Ahmed *et al.*, 2014; Bitu and Gerats 2013). In general, high stress conditions i.e. drought and other extreme weather conditions, forces the plant to produce more secondary metabolites (Jassey *et al.*, 2011). In addition, there is significant plant-to-plant variation between plants within a single plantation. Furthermore, in rooibos, most of the polyphenols including aspalathin are found in the leaves of the plant (Joubert *et al.*, 2008). The ratio of leaves to stems is related to the time of harvest, age of the plants, soil conditions and climate. Post-harvesting practices can also severely impact on the phenolic composition between different batches (Martin and Appel 2010). By far the most common agro-processing of rooibos is intended for tea production in which harvested rooibos plants are bruised and allowed to oxidize by different producers. Although this enhances the taste, it reduces the polyphenolic content dramatically (Standley *et al.*, 2001).

### **2.19.3. Biologically active compounds found in rooibos**

Aspalathin, the dihydrochalcone C-glucoside (Johnson *et al.*, 2016; Joubert 1996), is a unique polyphenol abundant in rooibos which contributes toward the antioxidant characteristics of the plant (Breiter *et al.*, 2011). The second most abundant dihydrochalcone, nothofagin, is a 3-deoxyderivative of aspalathin which is similar in structure to aspalathin (Beelders *et al.*, 2012). This compound displays antioxidant and anti-mutagenic activity while aspalathin contains hypoglycaemic activity (Kawano *et al.*, 2009; Muller *et al.*, 2012; Son *et al.*, 2013). Nothofagin (phloretin-3-C-glucoside) has been suggested to have therapeutic potential in treating diabetes due to its similarity in structure to aspalathin (3-hydroxyphloretin-3-C-glucoside) and the sodium glucose co-transporter inhibitor phloridzin (phloretin-2-O-glucoside). Although their bioactivity has not yet been completely elucidated, aspalathin and nothofagin

represent valuable bioactive compounds (de Beer *et al.*, 2015). The dihydrochalcones, aspalathin and nothofagin, as well as the flavone derivatives of aspalathin, isoorientin and orientin, have been illustrated in Figure 6. Quercetin and luteolin are two flavonoids present in rooibos tea which are potent antioxidants shown to cause apoptosis in cancer cells *in vitro* (Lee *et al.*, 2002; Mouria *et al.*, 2002). In a pancreatic model, Srivastava and co-workers (2014) demonstrated that quercetin decreased primary tumour growth and prevented metastasis. Luteolin is a naturally occurring flavonoid in rooibos with anti-oxidant, anti-inflammatory and anti-cancer properties (Lin *et al.*, 2008).

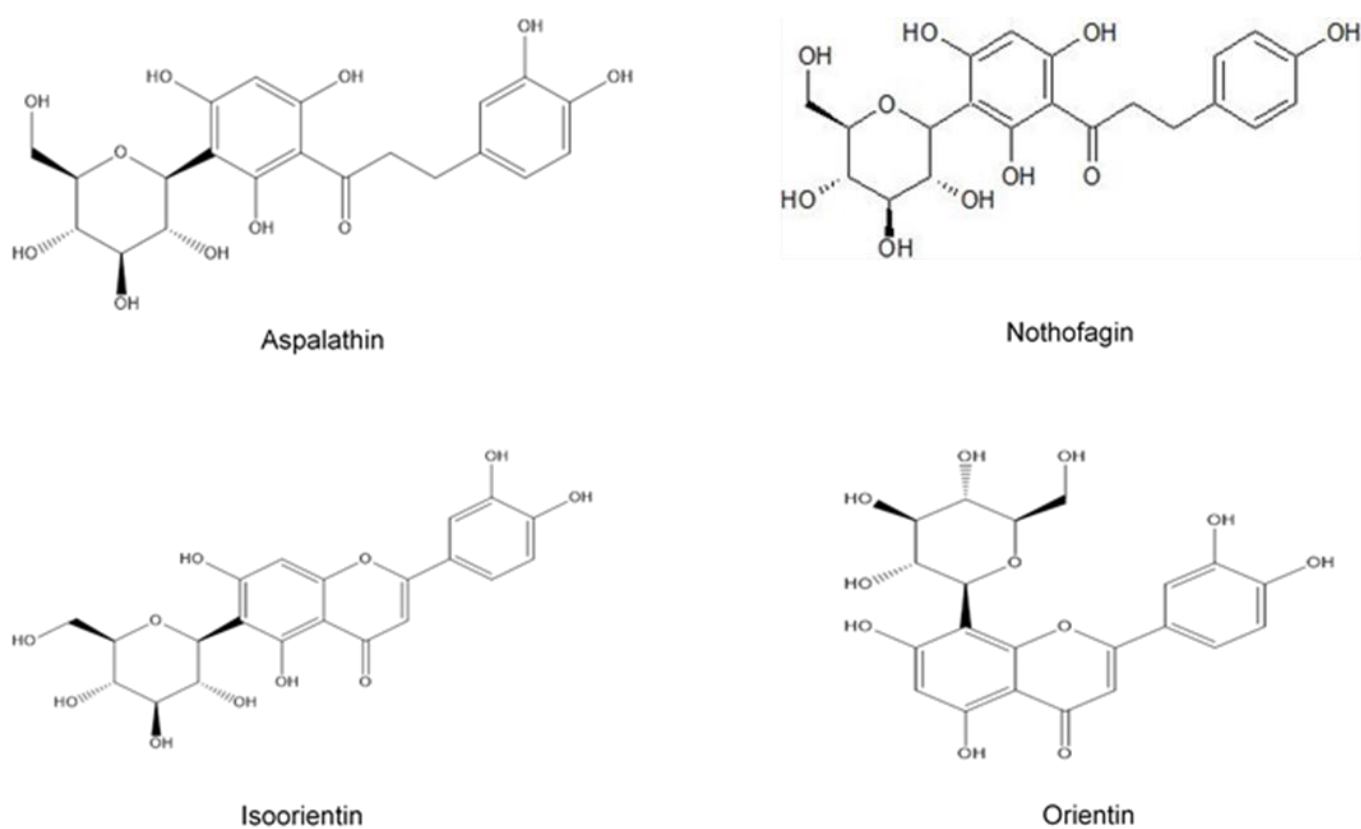


**Figure 6. Structure of the dihydrochalcones aspalathin and nothofagin and the flavones isoorientin and orientin in *Aspalathus linearis*.**

#### **2.19.4. Ratio of the major constituents of rooibos**

As explained by Beelders (2012), HPLC-DAD analysis confirmed the presence of aspalathin, nothofagin, and PPAG at 288 nm, while orientin, isoorientin, vitexin, isovitexin, hyperoside, isoquercetin, rutin and quercetin-3-O-robinobioside were quantified at 350 nm (Muller *et al.*, 2012; Joubert *et al.*, 2008). In all extracts, the major compounds were the dihydrochalcones, aspalathin (9-18 g/100 g) and nothofagin, the flavone analogues of aspalathin, orientin and isoorientin and quercetin-3-O-robinobioside (>0.5 g/100 g). The flavone derivatives of nothofagin, vitexin and isovitexin, the flavonol glycosides rutin (RUT), hyperoside (HYP), isoquercetin (ISOQ) and phenylpropanoic acid glucoside (PPAG) were present in minute concentrations below 0.5 g/100 g (Muller *et al.*, 2012). Rutin was collected at an average concentration of 0.544 g/100 g in the solvent-based extracts (Joubert and de Beer 2011; Joubert *et al.*, 2008; Muller *et al.*, 2012).

#### **2.20. Quality control**

The safety and efficacy of a natural or pharmaceutical product depends on its composition (Kunle *et al.*, 2012). Quality control is a measure used to ensure each dosage unit of the product carries the same amount of active ingredients and is free of toxic substances and impurities (Hasani-Ranjbar *et al.*, 2010). In herbal medicine, extracts are products of complex mixtures derived from biological sources and it is a challenging process to guarantee constant and adequate quality. Choosing a suitable chemical marker(s) is necessary for the quality control and development of herbal therapeutics (Sahoo and Manchikanti 2013).

#### **2.21. Principle components which can be used as predictors of bioactivity**

One of the most widely used multivariate statistical techniques used by most scientific disciplines (Abdi and Williams 2010), to simplify and analyse a set of data, is principle component analysis (PCA) (Hotelling 1933; Jolliffe 2002). The aim of this statistical technique is to use a set of tabulated data and extract important information which is expressed as orthogonal variables, referred to as principle components. PCA plots/maps can be used to illustrate the pattern of similarity of the data and the variables (Abdi and Williams, 2010).

## 2.22. Chemical markers

Active pharmaceutical ingredients (API's), serving as chemical markers, can be used to predict the biological effects and attributes of complex mixtures such as plant extracts. Chemical markers are used for quality management purposes, irrespective if they possess any therapeutic activity. The measure of a chemical marker indicates the quality of an herbal medicine (Li *et al.*, 2008). In this study emphasis was drawn to the chemical markers measured against known biological parameters which are predictive of bioactivity of the rooibos extract *in vitro*. An HPLC chemical fingerprint of green rooibos extracts prepared by different extraction methods was used to identify API's specific to each extract (Figure 7).

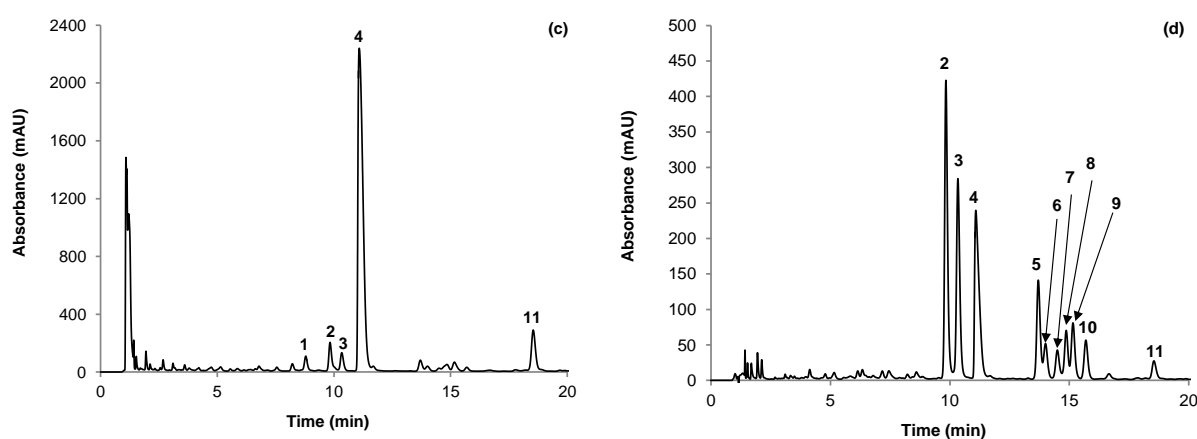


**Figure 7. HPLC chromatogram of an aspalathin-enriched green rooibos extract. (c) ARC at 288 nm; (d) ARC at 350 nm.** [1, enolic phenylpyruvic acid-2-O-glucoside; 2, isoorientin; 3, orientin; 4, aspalathin; 5, quercetin-3-O-robinobioside; 6, vitexin; 7, hyperoside; 8, rutin; 9, isovitexin; 10, isoquercitrin; 11, nothofagin] (Muller *et al.*, 2012).

### Aim

To identify chemical markers that could predict bioactivity in cell based assays.

### Objectives

1. To evaluate bioactivity of different types of green rooibos extracts in C2C12 muscle, C3A liver and 3T3-L1 adipocyte cell models.
2. To establish the relationship between composition and activity using advanced statistical analysis methodology (Principal Component Analysis).
3. To determine the effect of the most effective extract on protein expression of relevant signalling targets in cells demonstrating the highest bioactivity.

# CHAPTER 3

## EXPERIMENTAL PROCEDURES

### 3.1. Materials

The chemicals and reagents used in this project, together with their catalogue numbers and suppliers, has been tabulated in Appendix 1. Reference extract ARC 2 (80% ethanol green rooibos extract) as well as the three different types of green rooibos extracts (80 and 60% ethanol and aqueous) were characterised and supplied by Professor E. Joubert, Post-Harvest and Wine Technology Division, Agricultural Research Council (ARC), Infruitec-Nietvoorbij, Stellenbosch, South Africa. An aspalathin-enriched pharmaceutical grade 60% ethanol (EtOH) green rooibos extract (GRT) was supplied by Afriplex, Paarl, Cape Town, South Africa and included as a potential rooibos nutraceutical. Ten plant batches were randomly selected as described by Walters (2016) and three different types of extract was prepared by either ethanol (EtOH) or water extraction, yielding an 80% EtOH, 60% EtOH and aqueous green rooibos extracts (GRE). Figure 8 illustrates the three different types of extracts and reference extracts used in this study. The phenolic composition of all extracts including reference extracts were characterised by Walters (2016) at the ARC. Principle component analysis (PCA) was conducted by Marieta van der Rijst, the ARC statistician, (Statistics Unit) to assess the effect of extract preparation on the *in vitro* bioactivity testing in C2C12 muscle cells, C3A liver cells and 3T3-L1 adipocytes.

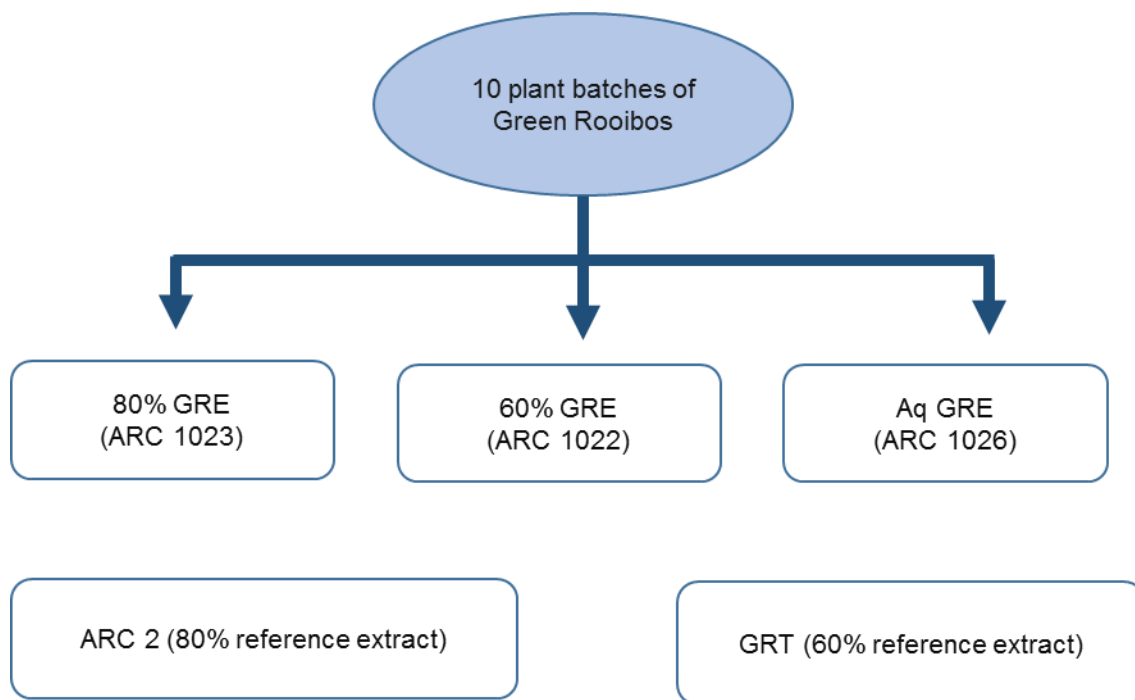


**Figure 8. Representation of the reference extracts (ARC 2 and GRT) and three different types of green rooibos extracts (80% and 60% EtOH and Aq GRE) used in this study (as described by Walters 2016). The green rooibos extracts were tested at an optimum dose of 10  $\mu\text{g}/\text{mL}$  (Muller et al., 2012; Mazibuko et al., 2013). ARC 2 – aspalathin-enriched 80% ethanol green rooibos extract. GRT – aspalathin-enriched pharmaceutical grade 60% ethanol green rooibos extract. EtOH – ethanol. Aq – aqueous.**

### **3.2. Extract and control preparation**

For the *in vitro* studies, stock solutions of all extracts (80% and 60% ethanol and aqueous GRE) and reference extracts (ARC 2 and GRT) were prepared by dissolving them in DMSO to a final concentration of 100 mg/ mL and stored in aliquots at -20°C. On the day of the assay, for the C2C12 and C3A cells, the extracts were thawed at room temperature and then fresh stock solutions prepared by a 1:100 dilution of the DMSO aliquots, yielding a stock concentration of 1 mg/mL. A final working solution was prepared by further diluting the stock concentration 1:100 to yield a final concentration of 10 µg/mL in Krebs Ringer Bicarbonate Hepes (KRBH) buffer pH 7.4, with a final concentration of 0.01% DMSO. The extracts were then filtered using 0.22 µm pore sized syringe filters into new tubes. For the vehicle control, 2 µL of 100% DMSO was dissolved with 19 998 µL KRBH (8mM glucose in KRBH) to yield a final concentration of 0.01% DMSO. A 1 µM insulin solution was prepared by diluting 2.03 µL of 10 mg/mL insulin stock in 3997.97 µL normal control.

The selected concentrations of 10 µg/mL for the experimental extracts was based on published data for ARC 2 also known as SB1 (Muller *et al.*, 2012; Mazibuko *et al.*, 2013). At this concentration, ARC 2, an 80% aspalathin-enriched green rooibos extract with an aspalathin content of 18%, has proven *in vitro* and *in vivo* antidiabetic activity to which the other extracts could be compared.

### **3.3. Cell lines**

#### **3.3.1. Source of cells**

Murine skeletal muscle cells (C2C12, ECACC catalogue number 91031101), human hepatocellular carcinoma cells (HepG2/C3A, ATCC catalogue number CRL-10741) and murine pre-adipocytes/fibroblasts (3T3-L1, ATCC catalogue number CL-173) were purchased from the European Collection of Authenticated Cell Cultures (ECACC, Salisbury, UK) and American Type Culture Collection (ATCC, Manassas, USA), respectively.

#### **3.3.2. Culture (growth) medium**

The cell lines were cultured in either Dulbecco's Modified Eagle's Medium (DMEM) or Eagle's Minimum Essential Medium (EMEM) and maintained at standard cell culture conditions (37°C, 5% CO<sub>2</sub> in humidified air). Growth medium with supplements, either

foetal bovine serum (FBS) or new-born calf serum (NCS), and specific culture components are tabulated below in Table 1.

**Table 1. Growth medium used to culture the three different cell lines used in this study.**

Cell Line	Media	Supplement
C2C12 murine skeletal muscle cells	DMEM containing 4.5 g/L glucose and L-glutamine	10% (FBS)
C3A human liver cells	EMEM containing Earle's balanced salt solution, non-essential amino acids and 1 mM pyruvate	10% FBS 2 mM L-glutamine
3T3-L1 murine preadipocytes	DMEM containing 4.5 g/L glucose and L-glutamine	10% NCS

### 3.4. Cell culture

#### 3.4.1. Cryopreservation of cells

To limit contamination, maintain consistency and store cells for long periods, cells are preserved in cryo-protectant medium containing dimethyl sulfoxide (DMSO) in liquid nitrogen at  $-196^{\circ}\text{C}$ . Cryopreservation also prevents changes in phenotypic and genotypic variation and permits easy transfer of cells between different laboratories (Yokoyama *et al.*, 2012). C2C12, C3A and 3T3-L1 cells were cryo-preserved in freshly prepared cryo-preservation (freezing) medium containing cryo-protectant [7.5% DMSO and 20% FBS/NCS (for 3T3-L1 preadipocytes) in DMEM/EMEM (for C3A cells)] at a concentration of  $1 \times 10^{-6}$  cells/mL in cryo vials at  $-80^{\circ}\text{C}$  in a freezing box overnight. The next day the cells were transferred to a liquid nitrogen tank for long-term storage at a temperature of  $-196^{\circ}\text{C}$ .

#### 3.4.2. Thawing of cells

Cryopreserved cells, taken from the nitrogen tank, were thawed in a water bath set at  $37^{\circ}\text{C}$  until just before all the ice was melted. Growth medium (Table 1.) was pre-

warmed at 37°C and 9 mL was transferred to a 50 mL centrifuge tube. Thereafter, the thawed cell suspension (1 mL) was slowly added to the 9 mL pre-warmed growth medium and centrifuged at 200 x g for 5 minutes. The supernatant was aspirated to remove the DMSO in the medium and the cell pellet was re-suspended in 3 mL fresh growth medium. A sample was taken for counting and viability assessment. Cells were seeded in 75 cm<sup>2</sup> flasks at a density of 1.8 x 10<sup>5</sup> cells/flask for C2C12 cells, 1.0 x 10<sup>6</sup> for C3A cells and 2.0 x 10<sup>5</sup> cells/flask for 3T3-L1 cells in a total volume of 18 mL/flask. The newly seeded flasks were returned to the incubator and allowed to grow at standard cell culture conditions (37°C, 5% CO<sub>2</sub> and humidified air).

### **3.4.3. Determination of cell concentration and viability**

Viability, as described by Browne and Al-Rubeai (2011), is defined as an intact plasma membrane which is quantified through dye-exclusion or the release of intracellular enzymes such as lactate dehydrogenase (Browne and Al-Rubeai 2011). In order to determine cell count and viability, 20 µL of the thawed cell suspension was mixed with 20 µL of 0.4% trypan blue in phosphate buffered saline (PBS). To determine the concentration and viability of cells, 10 µL of this cell suspension was loaded into a haemocytometer (Figure 9 a). The cells were counted using the 10x magnification lens on an inverted light microscope (Olympus CK x31, Tokyo, Japan) using phase contrast. Cells in each of the nine squares (Figure 9 b) of the haemocytometer were used to calculate cell viability. Cell viability percentage (unstained cells vs. stained dead cells) was calculated and a cell viability of ≥ 90% was required for culture (Promega Corporation, 2015).

The number of cells were calculated using the following equation:

$$\text{Cells/mL} = \frac{\text{Average count per mm}^2 \times 2 \text{ (1:1 cell suspension and trypan blue solution)}}{\text{Volume counted (1x1x0.1 mm=0.1 } \mu\text{L)}}$$

where Average of cells/1mm<sup>2</sup> multiplied by 2 (1:1 trypan blue dilution) divided by the volume (0.1mm<sup>3</sup> = 0.1 µL).

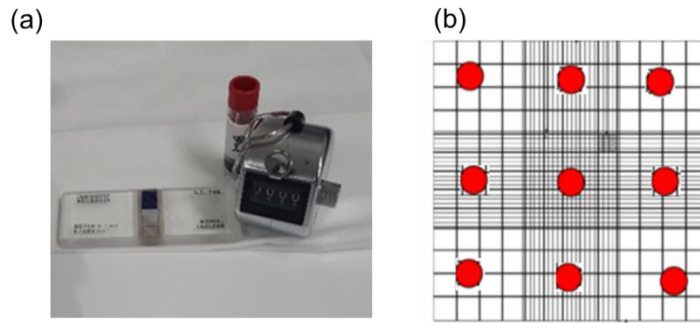


**Figure 9. An illustration of the haemocytometer used to count the number of cells per mL.**

(a). The two counting chambers on the haemocytometer. (b). The number of cells in nine squares were counted in each counting chamber (indicated by red dots) and averaged to obtain number of cells/mL (Adapted from Mazibuko, 2014).

### **3.5. Sub-culture of cells**

#### **3.5.1. C2C12 cells**

Cells were sub-cultured into 75 cm<sup>2</sup> flasks once 60-80% confluent to prevent over-growth and depletion of the myocytic population. Briefly, the media was aspirated, cells washed with 12 mL warm Dulbecco's phosphate saline buffer (DPBS) and incubated for 7 minutes with 2 mL 0.25% Trypsin-versene (Lonza, Walkersville, USA) at standard cell culture conditions (37°C in humidified air with 5% CO<sub>2</sub>). Thereafter, 8 mL fresh growth medium was added to stop trypsinisation. The detached cells were mixed into suspension as single cells by gently pipetting up and down. Afterwards, the cell suspension was transferred into a centrifuge tube and centrifuged at 200 x g for 5 minutes at room temperature. Thereafter, the supernatant was aspirated, the pellet re-suspended in 3 mL DMEM and cells counted (Figure 9 b). Cells were seeded into new flasks (180 000 cells/75 cm<sup>2</sup> flask).

#### **3.5.2. C3A cells**

C3A cells were sub-cultured into 75 cm<sup>2</sup> flasks using EMEM supplemented with 10% FBS and L-glutamine. The EMEM culture medium was aspirated from the flask and the cells washed with 12 mL DPBS. Thereafter, the cells were trypsinized for 12 minutes in 2 mL trypsin-versene at standard cell culture conditions. The loosened cells were re-suspended in 6 mL culture medium and pipetted up and down the bottom of the flask, to disaggregate cell clumps and obtain a single cell suspension. The newly passaged cells were seeded at a density of 1 000 000 cells/flask.

### **3.5.3. 3T3 -L1 cells**

Once 70-80% confluent, the 3T3-L1 preadipocytes were sub-cultured into 75 cm<sup>2</sup> flasks as described in section 3.5.1, using DMEM supplemented with 10% new-born calf serum (NCS). The cells were seeded into new 75 cm<sup>2</sup> flasks at a density of 200 000 cells/flask.

## **3.6. Cell Seeding for experiments**

### **3.6.1. C2C12 cells**

For glucose uptake and adenosine triphosphate (ATP) experiments, C2C12 cells were seeded into 24-well and 96-well plates, respectively as depicted in Table 2. For protein studies, cells were grown into 25 cm<sup>2</sup> flasks at a density of 80 000 cells/flask and cultured to 100% confluency in DMEM supplemented with 10% FBS. After 3 days culture, the cells reached confluency and were differentiated by replacing the medium with DMEM supplemented with 2% horse-serum for a further 2 days. Differentiated C2C12 cells are characterised by a distinct change in morphology; from single, polyglonal shaped cells to long-spindle shaped multi-nucleate myocytes. Assays were performed on the fifth day after seeding.

### **3.6.2. C3A cells**

C3A cells were seeded into 24-well plates and cultured in EMEM supplemented with 10% FBS and L-glutamine. They were refreshed two days after seeding and assays performed on the 4<sup>th</sup> day. These cells do not require any form of induction as they maintain normal liver biological activities once confluent (Kelly, 1994).

### **3.6.3. 3T3-L1 cells**

3T3-L1 fibroblasts were seeded into 96-well plates (Table 2) and grown for 3 days in DMEM supplemented with 10% NCS. To initiate adipocytic differentiation, the growth medium was replaced with adipocyte differentiation media (ADM) consisting of DMEM supplemented with 10% FBS, 1 µM dexamethasone (dex), 0.5 mM 3-isobuty-1-methylxanthine (IBMX) and 1 µg/mL insulin. The cells were incubated at standard cell culture conditions for 3 days. On day 3, once adipocyte formation was induced, the medium was replaced with adipocyte maintenance medium (AMM), comprised of DMEM with 10% FBS and 1 µg/mL insulin, for a further two days. Thereafter, on day 5, adipocytes were maintained in DMEM supplemented with 10% FBS until fully differentiated (day 8) for glucose uptake and lipid accumulation studies.

**Table 2. Cell densities used for seeding different plate types.**

Cell type	Plate type	Cell concentration	Volume ( $\mu\text{L}$ )	Cell density
C2C12	96 well	$5 \times 10^4$ cells/mL	100 $\mu\text{L}$	$5 \times 10^3$ cells/well
	24 well	$2.5 \times 10^4$ cells/mL	1000 $\mu\text{L}$	$2.5 \times 10^4$ cells/well
C3A	24 well	$1.1 \times 10^5$ cells/mL	1000 $\mu\text{L}$	$1.1 \times 10^5$ cells/well
3T3-L1	96 well	$2.0 \times 10^4$ cells/mL	200 $\mu\text{L}$	$4.0 \times 10^3$ cells/well

The 96 well plates were used for cell viability assays (C2C12 cells), colorimetric glucose uptake and lipid accumulation assays (3T3-L1 cells).

### 3.7. Cell treatment with GRE and controls

#### 3.7.1. C2C12 and C3A cells

On the day of the experiment, differentiated C2C12 myocytes and C3A hepatocytes were glucose and serum starved for 1 hour in 1 mL pre-warmed DPBS under standard cell culture conditions (37°C, 5% CO<sub>2</sub>, humidified air). Extracts and controls were prepared in Krebs Ringer Bicarbonate Hepes (KRBH) buffer (see Appendix 1) with 8 mM glucose. As described in section 3.2, the cells were incubated for 4 hours at standard cell culture conditions with GRE (80 and 60% ethanol and aqueous GRE), reference extracts (ARC 2 and GRT) or normal control (0.01% DMSO) prepared in KRBH buffer containing 8 mM glucose (illustrated in Figure 10). For C2C12 and C3A glucose uptake determination, 2.9  $\mu\text{L}$  of medium in the positive control wells was replaced with the same amount of 1  $\mu\text{M}$  insulin, for the last 15 and 60 minutes of the 4 hour assay, respectively. The insulin was mixed into the medium by gentle pipetting. Thereafter, C2C12 cells and C3A cells were subjected to bioactivity assays.

#### 3.7.2. 3T3-L1 adipocytes

On day 8, the adipocyte maintenance medium (AMM) was aspirated from the mature adipocytes and the cells washed in 100  $\mu\text{L}$  warm (37°C) DPBS. The cells were then serum and glucose-deprived by incubating with 100  $\mu\text{L}$  DPBS at standard cell culture conditions for 1 hour. The DPBS was removed and the starved cells were treated for 4 hours with green rooibos extracts and controls (Figure 11) at standard cell culture conditions. The extracts (80 and 60% EtOH and Aq GRE), reference extracts (ARC 2

and GRT) and controls (DMSO and insulin) were prepared in phenol red free DMEM containing 25 mM glucose.

### 3.8. Experimental outline for C2C12 and C3A cells

Differentiated, serum and glucose starved C2C12 cells were used to test controls and extracts at concentrations of 1 and 10  $\mu\text{g}/\text{mL}$  for cell viability and at 10  $\mu\text{g}/\text{mL}$  for glucose uptake assays. Serum and glucose starved C3A cells were used to conduct glucose uptake assays as described in section 3.7.1. Represented below is an experimental outline for the C2C12 and C3A cell lines.

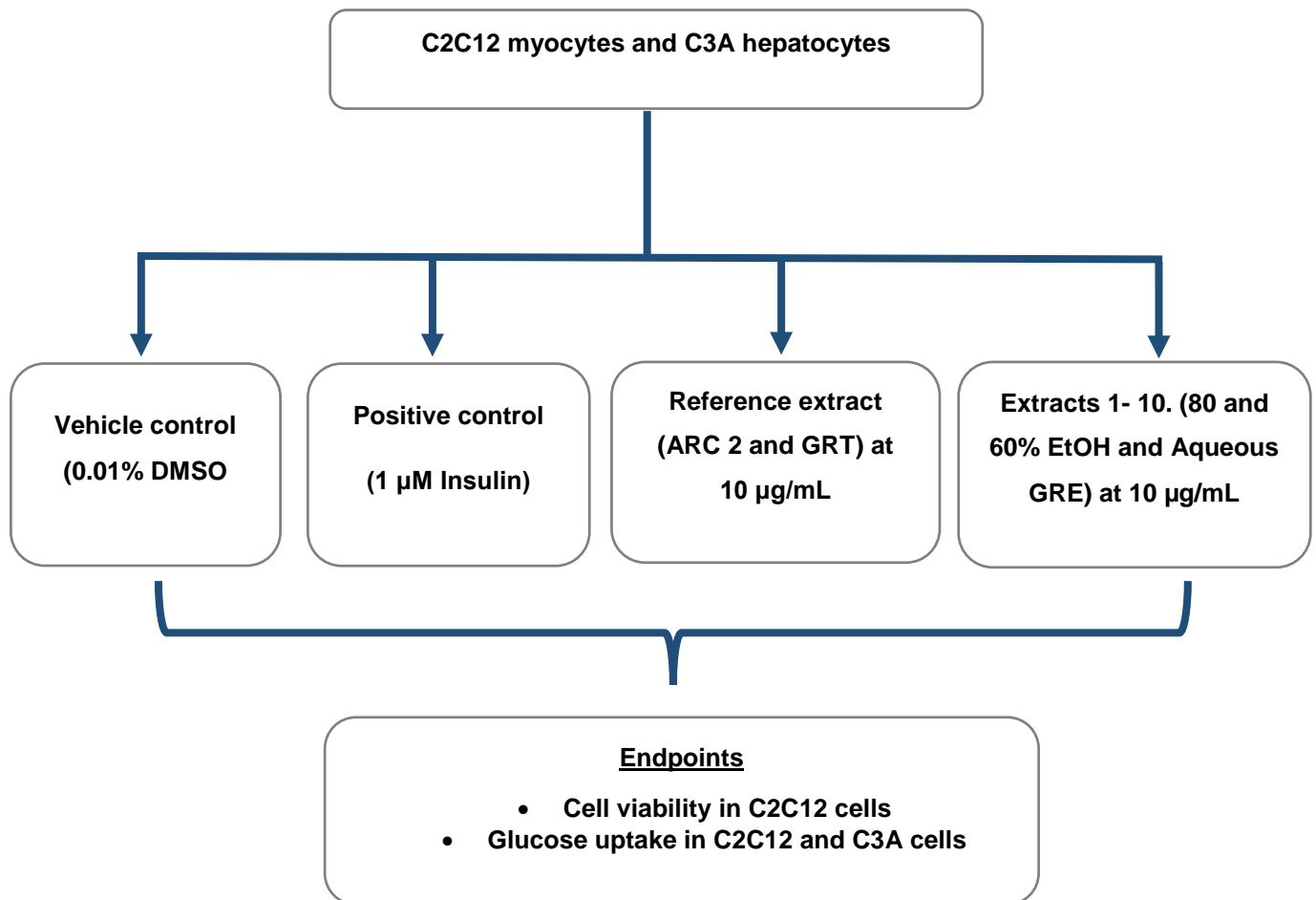


Figure 10. Experimental outline for C2C12 and C3A cells.

### 3.9. Induction process for adipocyte differentiation and experimental design for 3T3-L1 cells

Once fully (100%) confluent, 3T3-L1 preadipocytes were differentiated as described in section 3.6.3 and on day 8, the mature adipocytes were treated for 4 hours with controls and extracts (10 µg/mL) described in section 3.7.2. Figure 11 below demonstrates the process of 3T3-L1 preadipocyte differentiation and the experimental design for this cell line.

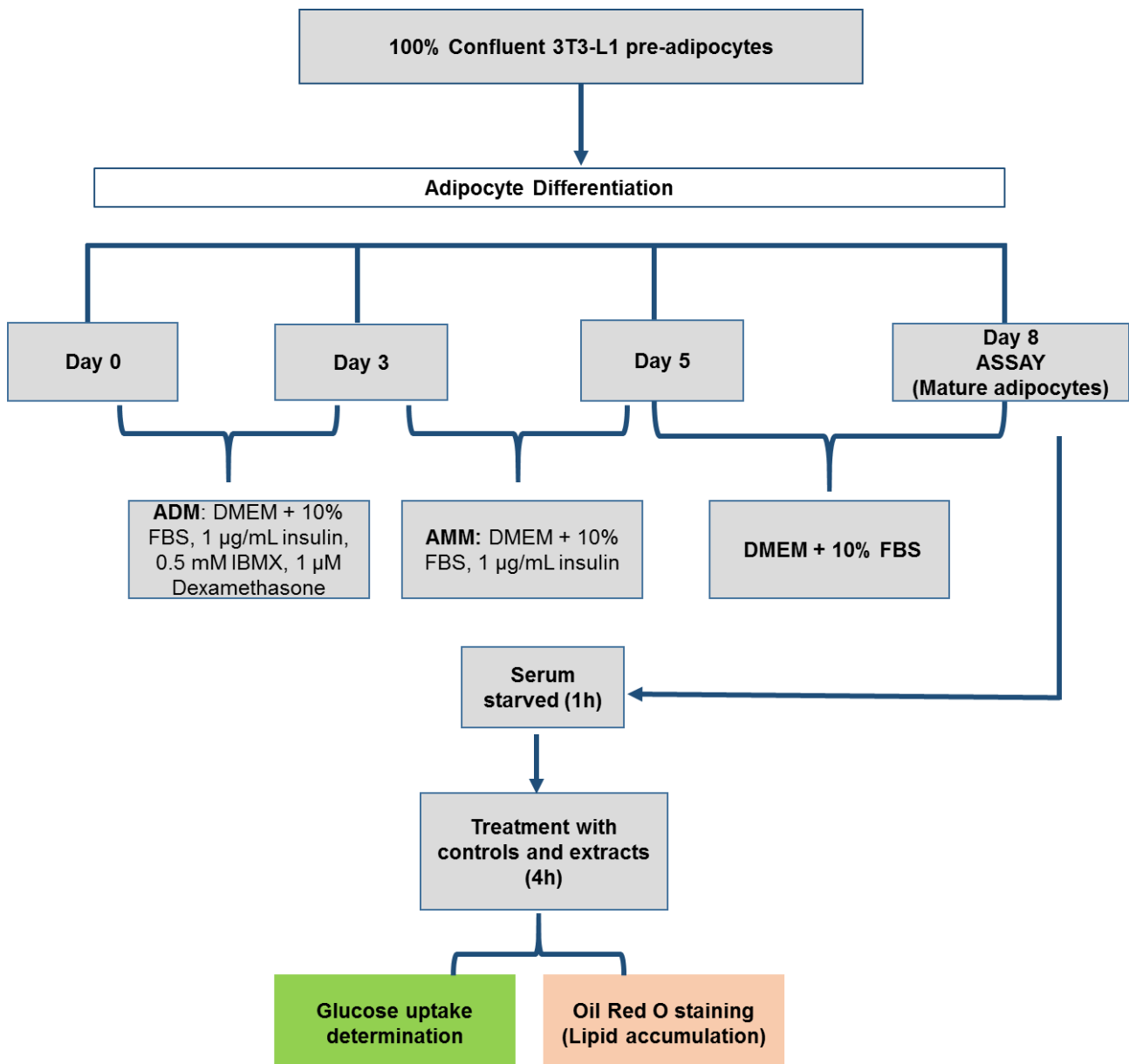
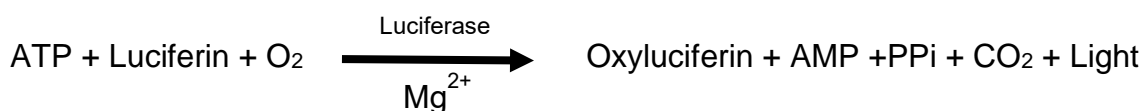


Figure 11. Experimental design for the 3T3-L1 adipocytes.

### 3.10. Bioactivity assays

#### 3.10.1. Cell viability studies

To assess the effect of the extracts on cell viability *in vitro*, the ATP assay was performed on C2C12 skeletal muscle cells. Measurement of cellular ATP is the most accurate and effective technique used to determine the number of viable cells in culture (Riss *et al.*, 2004). C2C12 cells, seeded and differentiated in 96-well plates (see Table 2 for seeding density), were treated with 0.01% DMSO (normal control), 1  $\mu$ M insulin and 1  $\mu$ M metformin (positive controls) and green rooibos extracts (1 and 10  $\mu$ g/mL). After a 4 hour incubation at standard cell culture conditions, an ATP (Coombes *et al.*, 2002; Crouch *et al.*, 1993) assay was conducted using the ViaLight™ plus ATP kit (ViaLight, Lonza, Basel, Switzerland). The kit enables the bioluminescent quantification of ATP which is the energy generating molecule found in metabolically active cells. This method utilizes luciferase which is an enzyme that catalyses the formation of light from ATP and luciferin according to the following reaction:



The emitted light intensity is linearly related to the ATP concentration and is measured using a luminometer.

After treatment, the media was aspirated and to extract ATP from the cells, 50  $\mu$ L ATP lysis reagent was added to all wells and incubated for 10 minutes at 37°C. After extraction, 100  $\mu$ L lysate was transferred to a white assay plate, mixed with 100  $\mu$ L ATP reagent and incubated for a further 2 minutes. Luminescence was quantified on a BioTek® FLX 800 plate reader using Gen5™ software.

##### 3.10.2.1. The 2-deoxy-[<sup>3</sup>H]-D-glucose (<sup>3</sup>H-2-DOG) uptake method

To quantify glucose uptake in C2C12 and C3A cells, a radioimmunoassay (RIA) adapted from Mazibuko (2013) was used. This method involves labelling the cells with <sup>3</sup>H-2-DOG for 15 minutes and measuring the accumulation of <sup>3</sup>H-2-DOG using a liquid scintillation counter (Perkin Elmer, Tricarb 2810TR, USA). The cells were treated for 4 hours as described in section 3.7.1 and the media aspirated. Afterwards, the cells were further incubated for 15 minutes with 500  $\mu$ L KRBH buffer containing 0.5  $\mu$ Ci/mL <sup>3</sup>H-2-DOG and either GRE (10  $\mu$ g/mL), insulin (1  $\mu$ M) or a DMSO control (see Figure 10)

without glucose. The KRBH buffer contained a final concentration of 0.01% DMSO. Following incubation, the treatments were aspirated and the cells washed twice with 500  $\mu$ L ice-cold DPBS. Thereafter, cells were lysed with 500  $\mu$ L 0.1 M NaOH and 1% SDS lysis buffer for 1.5 hours on a shaker at 37°C. To ensure proper lysing of the cells, the cell lysates were mixed by pipetting up and down. Thereafter, 5  $\mu$ L cell lysate was transferred into a 96-well microtiter plate for the determination of protein content.

For scintillation analysis, the remaining 495  $\mu$ L cell lysate was added to a scintillation cocktail, which was prepared by mixing 2.5 mL Ready Gel Ultima Gold (Perkin Elmer, Waltham, USA) with 500  $\mu$ L distilled water. The scintillation vials were vigorously mixed by shaking until a gel-like liquid was formed. The samples were subjected to liquid scintillation and the QuantaSmart program was used to quantify the  $^3\text{H}$ -isotope. The results obtained from the scintillation counter were calculated using the counts per minute (CPM) to determine  $^3\text{H}$ -2-DOG concentration and disintegrations per minute (DPM) to determine counter efficiency using the following formula:

$$\text{Counter efficiency \%} = \frac{\text{CPM}}{\text{DPM}} \times 100$$

The specific radioactivity (cpm/fmol) was calculated from the counter efficiency using GraphPad radioactivity calculator ([www.graphpad.com/quickcalcs/radcalcform.cfm](http://www.graphpad.com/quickcalcs/radcalcform.cfm)). The formula below was used to calculate  $^3\text{H}$ -2-DOG activity/mg protein in the lysates:

$$^3\text{H-2-DOG accumulation (Fmol/mg)} = \text{CPM/Specific activity/mg protein}$$

### **3.10.2.2. Protein content determination**

To determine the protein content of the cell lysates, the Bradford reagent was used according to the manufacturer's instructions (Bio-Rad, Berkeley, CA). A protein standard curve was prepared in a 96-well plate by pipetting 5  $\mu$ L bovine serum albumin (BSA) standards in duplicate with concentrations ranging from 0.03125 to 2.0 mg/ mL. Thereafter, 5  $\mu$ L of each sample lysate (as described in section 3.12.2) was added in duplicate to the remaining wells. Based on the manufacturer's instructions, 250  $\mu$ L Quickstart™ Bradford Reagent was added to each well and incubated at room temperature for 10 minutes and the absorbance measured at 570<sub>nm</sub> in a BioTek®

ELX800 (BioTek Instruments Inc., Winooski, USA) plate reader. The concentration of protein in the samples (mg/mL) were used to normalise the cell count for the 2-deoxy-<sup>3</sup>H]-D-glucose uptake assay.

### 3.10.3. Colorimetric glucose uptake assay in adipocytes

The LabAssay™ Glucose kit (WAKO Chemicals, Osaka, Japan) was used to determine the remaining glucose concentration in the medium of the 3T3-L1 adipocytes. This reagent converts  $\alpha$ -glucose to  $\beta$ -glucose by mutarotase, which then oxidizes  $\beta$ -D-glucose yielding hydrogen peroxide. In the presence of peroxidase, a red pigment is produced from the hydrogen peroxide during quantitative oxidation with phenol and 4-aminoantipyrine (Miwa *et al.*, 1972). Following 4 hour treatment, a standard curve was prepared in a new 96-well plate as shown in Table 3. Thereafter, 2  $\mu$ L media from each of the treatments in section 3.7.2 was pipetted in the remaining wells for glucose determination. Afterwards, 300  $\mu$ L of LabAssay Glucose Chromogen Reagent was added to all wells to start the reaction. The plate was then incubated at 37°C for 5 minutes, after which the absorbance was measured at 490 nm in a BioTek® plate reader ELX 800 using Gen5® software.

**Table 3. Preparation of standards for the standard curve.**

Tube	Glucose standard 1 [11.11 mmol/L] ( $\mu$ L)	Glucose standard 2 [27.78 mmol/L] ( $\mu$ L)	Distilled/Deionized water ( $\mu$ L)	Sample volume ( $\mu$ L)	Concentration (mmol/L)
1	50	-	150	2	2.78
2	100	-	100	2	5.56
3	20 (undiluted)	-	-	2	11.11
4	-	150	100	2	16.67
5	-	200	50	2	22.22
6	-	20 (undiluted)	-	2	27.78

#### **3.10.4. Lipid content determination using Oil Red O**

To determine lipid accumulation in the 3T3-L1 cells, following a 4-hour treatment incubation period (as described in section 3.10), the treatment medium was collected for glucose determination and the cells rinsed with 100  $\mu$ L DPBS. The cells were fixed with the addition of 50  $\mu$ L neutral buffered formalin (10% w/v) in DPBS for 15 minutes. The formalin was aspirated and the cells washed twice with 100  $\mu$ L DPBS. Lipid was stained using 50  $\mu$ L 0.7% (v/v) Oil Red O (Sigma-Aldrich, Saint Louis, USA) solution dissolved in 100% isopropanol for 30 minutes at room temperature. The Oil Red O stain was removed and the cells washed thrice with 100  $\mu$ L distilled water after which the excess water was aspirated. Thereafter, 50  $\mu$ L isopropanol was used to extract the Oil Red O stain with gentle swirling. The extracted stain was transferred into a microassay plate and the absorbance measured at 490 nm. To quantify the cell numbers, the cells were washed with 50  $\mu$ L of 70% ethanol and aspirated to near dryness. Cell nuclei were stained with 80  $\mu$ L 0.5% (v/v) crystal violet in distilled water for 5 minutes at room temperature. The crystal violet was completely aspirated and the cells washed thrice with 80  $\mu$ L DPBS. The DPBS was aspirated to near dryness for the last wash. Thereafter, 50  $\mu$ L of 70% ethanol was added to extract the crystal violet stain, and the extracted dye was transferred into a microassay plate and the absorbance measured at 570 nm.

#### **3.11. Protein Tyrosine Phosphatase 1B (PTP1B) Enzyme assay**

PTP1B inhibitory activity was assessed *in vitro* as described by Li (2015). Briefly, 30  $\mu$ L of a 50 mM citrate buffer (pH 6.0) containing 0.1 M sodium chloride (NaCl) and 1 mM ethylenediaminetetraacetic acid (EDTA) was added to a 96-well microtiter plate. Fresh stock solutions of 10 mM dithiothreitol (DTT) and 10 mM *p*-nitrophenol phosphate (pNPP) substrate was prepared and 10  $\mu$ L of each was pipetted into each well, with a final concentration of 1 mM for both DTT and pNPP. A 25  $\mu$ L aliquot of sample prepared from the frozen GRE stock solutions, including ARC 2 and GRT (100  $\mu$ g/mL) in DMSO, consisting of a range of serial dilutions (100 – 0.00001  $\mu$ g/mL) in 50 mM citrate buffer (pH 6.0) or 0.2% DMSO was added in duplicate to the respective wells as seen in the plate layout (Appendix 2). Lastly, 25  $\mu$ L of 0.05  $\mu$ g PTP1B enzyme (Abcam, UK) was added and the plates gently tapped to start the reaction. The plates were then incubated for 30 minutes at 37°C and the reaction quenched with the addition of 50  $\mu$ L of 1 M NaOH. The amount of pNPP produced was quantified by

measuring the absorbance at 490 nm. The non-enzymatic hydrolysis of pNPP was corrected by measuring the increase in absorbance at 490 nm obtained in the absence of the PTP1B enzyme. The inhibitory effects of the extracts on the enzyme were determined as 50% inhibitory concentration (IC<sub>50</sub>) using GraphPad Prism 6 program (GraphPad Software Inc., La Jolla, USA).

### **3.12. Protein expression studies**

To assess the molecular mechanism (s) of action of GRE on selected signalling and effector proteins, Western blot analysis was performed using the C2C12 skeletal muscle cells. These proteins include specific markers of insulin signalling (protein kinase B (PKB)) which will be referred to as AKT, 5' adenosine monophosphate-activated protein kinase (AMPK) and lipid metabolism effectors, such as acetyl-CoA carboxylase (ACC) and malonyl-CoA decarboxylase. The housekeeping protein  $\beta$ -actin, was used to normalise the data.

#### **3.12.1. Western blotting**

C2C12 muscle cells were cultured in 25 cm<sup>2</sup> flasks and treated accordingly as depicted in Figure 8. After treatment, cells were washed in 5 mL DPBS and the cells frozen at -20°C until lysed. Western blot analysis was performed using a standardised protocol from Johnson *et al.*, 2016. The frozen cells were thawed on ice and the cells scraped into 350  $\mu$ L commercially available tissue lysis buffer (Invitrogen, Carlsbad, CA) supplemented with protease inhibitor tablets (Roche, Basel, Switzerland) using a rubber cell scraper. The cell lysates were then transferred into a microcentrifuge tube and stored at -20°C for protein detection.

#### **3.12.2. Protein Isolation from cells**

Cell lysates were thawed on ice and a stainless-steel ball added into each Eppendorf tube (2 mL). The tubes were then placed into a pre-cooled tissue lyser block (Qiagen, Hilden, Germany) and the samples homogenized at 25 Hertz for 60 seconds, after which the tubes were cooled on ice for another 60 seconds. This step was repeated 5 times. The homogenized cell lysates were centrifuged for 15 minutes at 13 000 x g at 4°C using a microcentrifuge (Whitehead Scientific, Stikland, SA). The supernatant containing protein lysates was carefully transferred into fresh 1.5 mL tubes and placed on ice for protein content determination.

### 3.12.3. Protein concentration determination

The protein content was determined using the reducing agent and detergent compatible (RA/DC) method as per the manufacturer's (Bio-Rad, Berkeley, CA) instructions. A standard curve was prepared in a 96-well plate, using 5  $\mu$ L BSA standards (0.125, 0.25, 0.5, 0.75, 1, 1.5 and 2 mg/mL) in duplicate. Thereafter, 5  $\mu$ L of each protein lysate (section 3.12.2) was added in duplicate to the remaining wells. Afterwards, 25  $\mu$ L of reagent A' (prepared by mixing 1 mL of DC reagent A with 20  $\mu$ L of reagent S) was added to each well followed by the addition of 200  $\mu$ L Protein Assay Reagent B. The plate was placed on a shaker set at 500 rpm for 15 minutes and the absorbance measured at 630 nm using a BioTek® ELX 800 plate reader.

### 3.12.4. Gel electrophoresis

Protein samples were diluted 1:1 with a 2x Laemmli sample buffer (see Appendix 2), followed by heating on a heating block for 5 minutes at 95°C. They were then immediately placed on ice. A 12  $\mu$ L Precision Protein Western C standard (Bio-Rad) was pipetted into the first lane of a precast gel followed by loading of protein samples into the remaining 9 lanes. The respective concentrations of protein that were loaded on to the differently sized gels are shown in Table 4. The gel was electrophoresed using a Power Pac High Current (Bio-Rad, California, USA) for ~80 minutes at 150 V until the Laemmli sample buffer dye had run off the gel.

**Table 4. Protein and gel concentrations used for Western blot analysis.**

Protein	Protein concentration ( $\mu$ g)	% Gel
AMPK	30	10
AKT	30	10
ACC	60	12
MLYCD	20	12

### 3.12.5. Preparation and Transfer of proteins onto a LF-PVDF membrane

A low fluorescence polyvinylidene difluoride (LF PVDF) membrane was immersed in 100% methanol for 2 minutes and then transferred to a gel tray containing 30 mL 1x transfer buffer (Appendix 2) and equilibrated for 3 minutes. In addition, two sets of transfer stacks were immersed in 50 mL 1x transfer buffer for 3 minutes. After equilibration, one wet transfer stack was placed on to the bottom of the cassette

(bottom ion reservoir stack). The wet LF PVDF membrane was then placed on top of the stack and the gel was then sized to fit directly over the membrane and air bubbles were removed by gently rolling with a blot roller. The second wet transfer stack was placed on to the gel (top ion reservoir stack). The cassette was closed, the lid locked and the cassette inserted into the Trans-Blot Turbo Transfer System (Bio-Rad, Munich, Germany) and allowed to transfer for 8 minutes at 25 volts and 2.5 constant Amps (see Figure 12).

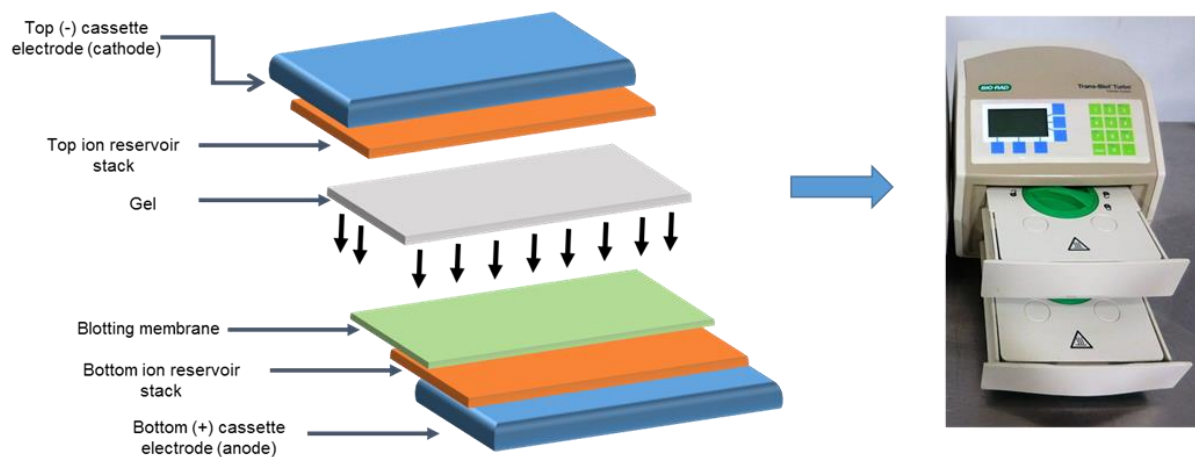


**Figure 12. Diagram illustrating the cassette used to transfer proteins onto a LF PVDF membrane with the Trans-Blot™ Turbo Transfer system (Bio-Rad, Berkeley, CA).**

### **3.12.6. Protein detection**

To determine how well the proteins were transferred, the LF PVDF membrane was removed from the transfer cassette and submerged into a container with Ponceau S stain (Sigma-Aldrich, St Louis, USA) and then incubated for 5 minutes on an orbital shaker. The membrane was rinsed with distilled water until the background turned clear and then washed in 1x Tris Buffered Saline 0.1% Tween-20 (1x TBST-20) to reverse the Ponceau stain.

### **3.12.7. Western blot analysis**

To detect the protein of interest, the membrane was incubated in 5% (w/v) fat-free milk powder prepared in 1x TBST-20 to block non-specific binding of proteins. To detect the protein of interest, the membranes were incubated overnight with the relevant primary antibody (Ab) in 1x TBST-20 on a shaker at 4°C. The primary (1°) and

secondary (2°) antibodies used in this study are tabulated in Table 5. The morning after, the membrane was washed three times in 1x TBST-20 for 10 minutes at room temperature and labelled with the secondary antibody in 2.5% fat-free milk together with 2 µL StrepTactin horseradish peroxidase (HRP) on a shaker for 90 minutes at room temperature. The protein marker used in this study was not visible, therefore to address this issue StrepTactin (HRP) was added together with the secondary antibody. The labelled proteins were detected by chemiluminescence using the Chemidoc-XRS imager and quantified with the use of Quantity One software (Bio-Rad).

**Table 5. Source, catalogue numbers, size and dilutions of antibodies used.**

Anti-body (Ab)	Company	Catalogue number	Mw (KDa)	1° Ab dilution	2° Ab dilution
<b>pAKT</b>	Cell Signalling Technology (CST)	4060	60	1:1000	1:4000
<b>AKT</b>	CST	9272S	60	1:1000	1:4000
<b>pAMPK</b>	CST	2535S	62	1:800	1:4000
<b>AMPK<math>\alpha</math></b>	CST	2532S	62	1:1000	1:4000
<b>pACC</b>	CST	3661S	280	1:500	1:4000
<b>ACC</b>	CST	3662S	280	1:1000	1:4000
<b>MLYCD</b>	Abcam	ab95945	55	1:2500	1:4000
<b><math>\beta</math>-actin</b>	Santa Cruz Biotechnology	Sc-47778	54	1:500	1:4000

pAKT: phosphorylated threonine kinase B; AKT: threonine kinase B; pAMPK: phosphorylated 5'adenosine monophosphate activated protein kinase; AMPK $\alpha$ : 5'adenosine monophosphate activated protein kinase alpha; pACC: phosphorylated Acetyl CoA Carboxylase; ACC: Acetyl CoA Carboxylase; MLYCD: Malonyl CoA Decarboxylase;  $\beta$ -actin: beta actin

### **3.13. Statistical Analysis**

#### **3.13.1. Standard statistical analysis**

GraphPad Prism Software (version 6.0, La Jolla, USA) was used for one-way analysis of variance (ANOVA) and data was expressed as the means of three independent experiments, with at least three technical replicates per experiment. Error bars reflect the standard error of the mean. Significant differences between groups was assessed using one-way analysis of variance (ANOVA) test, with Tukey-Kramer multiple comparison test. Data was considered significantly different at  $p < 0.05$ . In addition, for Western blot analysis, biological fold change ( $> 1.5$ ) was additionally considered as biologically significant changes in protein expression.

#### **3.13.2. Principle Component Analysis**

To understand the possible correlation between variation in chemical constituents and biological activity, principal component analysis (PCA) was applied using standard statistical software XLStat (version 2014, Addinsoft, New York, USA) in consultation with Marieta van der Rijst, a statistician at the Agricultural Research Council (ARC). Significant differences between groups was determined using one-way standard ANOVA techniques and non-parametric tests when necessary. Statistical differences for this study was set at  $p < 0.05$ .

# CHAPTER 4

## RESULTS

### 4.1. Introduction to the results

Ethanol (80% and 60%) solvent extracts and hot water extracts were prepared from ten different plant batches of green rooibos and freeze dried. For this study the test extracts (green rooibos extracts) and reference extract (ARC 2) were supplied by Professor E. Joubert at the Agricultural Research Council (ARC), Infruitec-Nietvoorbij, Stellenbosch, South Africa. The aspalathin-enriched GRT was supplied by Afriplex, Paarl, South Africa. All extracts were characterised by the ARC (Table 6). HPLC analysis was used to chemically characterise the extracts for their phenolic composition (Figure 13 and Table 6). The 30 extracts were assessed *in vitro* for their antidiabetic bioactivity potential and statistical analysis applied to the data to find an association between the phenolic composition and bioactivity *in vitro*.

The assessment of plant extracts for their potential antidiabetic activity in the selected cell types i.e. C2C12 muscle cells, C3A liver cells and 3T3-L1 adipocytes provided an *in vitro* model for determining the theoretical glucose lowering potential of these extracts. These three cell types represented the hepatic and peripheral glucose utilizing tissues that respond to the prandial glucose fluctuations regulated by insulin. These cells *in vitro*, thus represent major target tissues of most antidiabetic therapeutics and provide a good screening model for potential antidiabetic activity of extracts.

To ensure that the results were not skewed by cytotoxic effect of the extracts, ATP assays were performed (Figure 14 a-f) in C2C12 skeletal muscle cells. No signs of cytotoxicity were demonstrated for any of the extracts at the concentrations tested (cytotoxicity > 90% cell viability). Antidiabetic potential of the extracts were assessed by glucose uptake in C2C12 muscle (Figure 15), C3A liver (Figure 16) and 3T3-L1 adipocytes (Figure 17) and the effect of the extracts on lipid accumulation was also determined in 3T3-L1 adipocytes (Figure 18). An 80% aspalathin-enriched green rooibos extract (ARC 2) with an aspalathin content of 18% (Table 6) with proven *in vitro* and *in vivo* antidiabetic activity was included as a reference extract. The green

rooibos extracts were tested at an optimum dose of 10 µg/mL for ARC 2 as previously published (Muller *et al.*, 2012; Mazibuko *et al.*, 2013). A new pharmaceutical grade 60% ethanolic green rooibos extract, GRT was also included as a likely rooibos nutraceutical. The inhibitory effects of the extracts on the insulin modulating enzyme PTP1B, were also assessed in an enzyme based assay.

To ascertain if the different chemical compositions present in the extracts related to the different extraction methods, Western blot was performed to ascertain the activation status on signalling and effector proteins related to insulin signalling, AMPK and AKT. For lipid metabolism, ACC and Malonyl-CoA decarboxylase was assessed. Two plant batches of each extract type were selected (plant batch 2 and 4, denoted as Ex 2 and Ex 4) based on dissimilar abundance of the major phenolic compounds, in particular their dihydrochalcone content and glucose uptake in C2C12 cells.

Principle component analysis was used to statistically relate bioactivity to the phenolic composition (Figure 25 a-b), in an attempt to find an association between individual and/or groups of compounds that were likely to have been responsible for the observed bioactivity. These compounds or groups of compounds could then be considered as potential bioactivity markers.

For all *in vitro* experimentation, data are expressed as the mean of three independent experiments, each done in triplicate ± the standard error of the mean. The normal controls refer to cells exposed to the vehicle solvent without extract treatments.

#### 4.1.1. HPLC-DAD identification of the major phenolic compounds in green rooibos extracts

Green rooibos extracts are a complex mixture of chemical constituents. The major phenolic compounds in these extracts were identified by HPLC-DAD analysis (Figure 13 and Table 6)

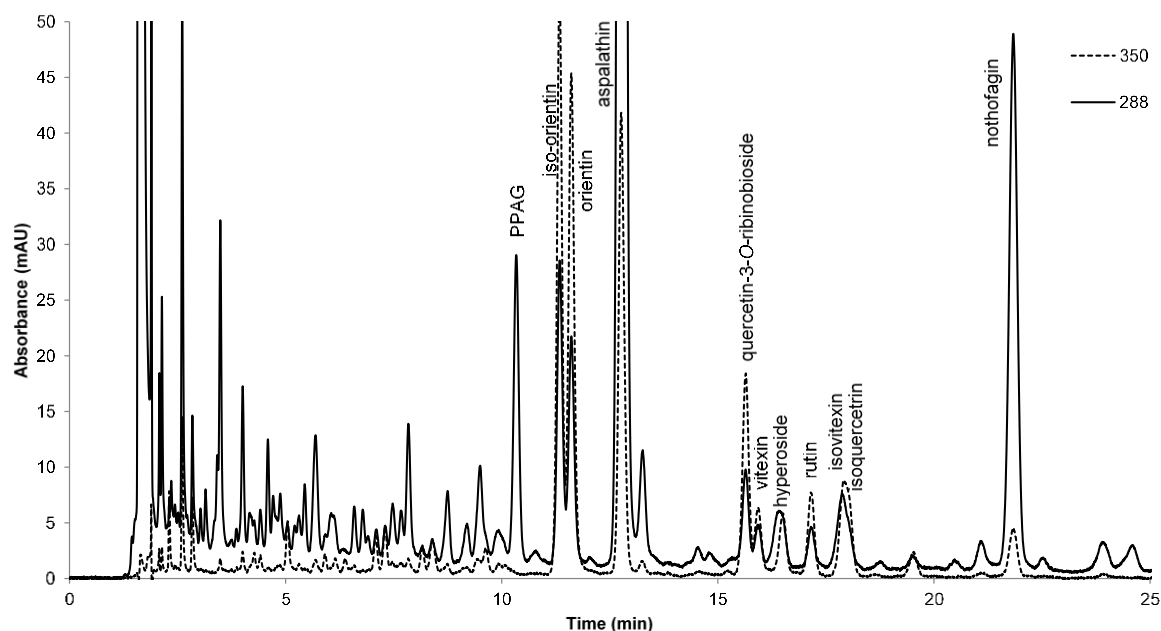


**Figure 13.** A typical HPLC chromatogram of a hot water green rooibos extract at 288 and 350 nm depicting the presence of the major phenolic compounds: Z-2-( $\beta$ -D-glucopyranosyloxy)-3-phenylpropenoic acid, iso-orientin, orientin, aspalathin, quercetin-3-O-robinobioside, vitexin, hyperoside, rutin, isoquercetrin and nothofagin at a retention time between 10 and 25 minutes.

#### 4.1.2. Aspalathin content of the of rooibos extracts

The presence of the dihydrochalcone aspalathin, as the major phenolic compound in rooibos demonstrated that the aspalathin content in the organic (80 and 60% EtOH) green rooibos extracts was much higher than the aqueous GRE's shown in Table 6. The 80% ethanol extracts had the highest aspalathin content with an average of  $17.09 \pm 2.66\%$ , comparable to the reference extract ARC 2 which was 18.44%. The 60% ethanol extract and the hot water extract had an aspalathin content of  $12.54 \pm 2.51\%$  and  $9.52 \pm 1.85\%$ , respectively.

**Table 6. Chemical characterisation of three GRE's by HPLC -DAD analysis.**

Content g/100g SS												
Sample	ASP	NOT	ISOO	ORI	Q3ROB	VIT	HYP	RUT	ISOVIT	ISOQ	LUT7GLC	PPAG
<b>ARC 2</b>	18.44	1.29	2.05	1.05	1.05	0.27	0.27	0.54	0.39	0.38	0.00	0.49
<b>GRT</b>	12.78	1.97	1.43	1.26	1.04	0.34	0.40	0.50	0.30	0.57	0.00	0.42
<b>ARC 1023 (80% EtOH)</b>												
<b>80_1</b>	16.06	1.63	1.87	1.53	1.01	0.32	0.41	0.47	0.40	0.49	0.05	0.43
<b>80_2</b>	17.54	1.82	1.46	1.21	0.98	0.25	0.39	0.40	0.28	0.49	0.07	0.57
<b>80_3</b>	15.06	1.04	1.66	1.37	0.81	0.25	0.29	0.31	0.34	0.31	0.06	0.58
<b>80_4</b>	11.55	0.82	1.39	1.27	1.01	0.22	0.35	0.38	0.31	0.39	0.07	0.52
<b>80_5</b>	17.88	2.16	1.58	1.27	0.93	0.24	0.36	0.39	0.38	0.45	0.06	0.52
<b>80_6</b>	18.76	1.97	1.55	1.28	1.02	0.26	0.40	0.39	0.36	0.53	0.07	0.47
<b>80_7</b>	15.89	1.08	1.39	1.16	1.41	0.24	0.65	0.55	0.32	0.99	0.06	0.47
<b>80_8</b>	21.38	1.50	1.56	1.24	1.19	0.24	0.46	0.49	0.38	0.63	0.08	0.50
<b>80_9</b>	19.02	1.57	1.59	1.23	1.11	0.26	0.37	0.44	0.39	0.50	0.07	0.53
<b>80_10</b>	17.78	1.39	1.59	1.31	1.20	0.26	0.40	0.48	0.39	0.51	0.07	0.52
<b>Mean</b>	<b>17.09</b>	<b>1.50</b>	<b>1.56</b>	<b>1.29</b>	<b>1.07</b>	<b>0.25</b>	<b>0.41</b>	<b>0.43</b>	<b>0.35</b>	<b>0.53</b>	<b>0.07</b>	<b>0.51</b>
<b>SD</b>	<b>2.66</b>	<b>0.43</b>	<b>0.14</b>	<b>0.10</b>	<b>0.17</b>	<b>0.03</b>	<b>0.09</b>	<b>0.07</b>	<b>0.04</b>	<b>0.18</b>	<b>0.01</b>	<b>0.05</b>
<b>ARC 1022 (60% EtOH)</b>												
<b>60_1</b>	11.78	1.15	1.79	1.33	1.10	0.26	0.42	0.48	0.36	0.54	0.06	0.39
<b>60_2</b>	13.04	1.32	1.38	1.07	0.96	0.19	0.34	0.37	0.26	0.45	0.07	0.49
<b>60_3</b>	8.58	0.56	1.00	0.81	0.56	0.14	0.17	0.20	0.21	0.17	0.05	0.39
<b>60_4</b>	8.67	0.60	1.32	1.13	1.07	0.18	0.34	0.38	0.32	0.32	0.07	0.47
<b>60_5</b>	13.88	1.66	1.44	1.10	0.88	0.19	0.33	0.36	0.34	0.41	0.06	0.47
<b>60_6</b>	12.80	1.30	1.36	1.05	0.98	0.21	0.37	0.36	0.34	0.41	0.07	0.41
<b>60_7</b>	15.32	0.90	1.43	1.11	1.54	0.23	0.68	0.59	0.31	1.02	0.06	0.48
<b>60_8</b>	16.17	1.17	1.44	1.10	1.17	0.21	0.43	0.46	0.35	0.57	0.06	0.47
<b>60_9</b>	11.50	0.90	1.18	0.91	0.90	0.18	0.31	0.36	0.29	0.39	0.05	0.40
<b>60_10</b>	13.67	1.05	1.44	1.13	1.16	0.22	0.37	0.45	0.35	0.47	0.07	0.47
<b>Mean</b>	<b>12.54</b>	<b>1.06</b>	<b>1.38</b>	<b>1.08</b>	<b>1.03</b>	<b>0.20</b>	<b>0.38</b>	<b>0.40</b>	<b>0.31</b>	<b>0.48</b>	<b>0.06</b>	<b>0.44</b>
<b>SD</b>	<b>2.51</b>	<b>0.34</b>	<b>0.20</b>	<b>0.14</b>	<b>0.25</b>	<b>0.03</b>	<b>0.13</b>	<b>0.10</b>	<b>0.05</b>	<b>0.22</b>	<b>0.01</b>	<b>0.04</b>
<b>ARC 1026 (Aq)</b>												
<b>A_1</b>	8.38	0.79	1.06	0.97	0.77	0.18	0.23	0.36	0.20	0.28	0.05	0.47
<b>A_2</b>	10.45	0.97	0.97	0.90	0.79	0.15	0.22	0.32	0.16	0.28	0.06	0.61
<b>A_3</b>	7.74	0.48	0.83	0.80	0.56	0.14	0.15	0.21	0.15	0.14	0.06	0.60
<b>A_4</b>	5.41	0.36	0.72	0.74	0.71	0.12	0.16	0.26	0.16	0.16	0.07	0.49
<b>A_5</b>	10.79	1.18	0.95	0.88	0.68	0.16	0.20	0.30	0.20	0.25	0.07	0.56
<b>A_6</b>	9.70	0.93	0.82	0.79	0.71	0.16	0.23	0.28	0.17	0.25	0.07	0.50
<b>A_7</b>	9.86	0.65	0.96	0.88	1.15	0.19	0.40	0.47	0.21	0.54	0.08	0.54
<b>A_8</b>	11.55	0.79	0.95	0.90	0.91	0.16	0.26	0.37	0.22	0.27	0.08	0.51
<b>A_9</b>	10.92	0.80	0.95	0.85	0.84	0.17	0.21	0.34	0.20	0.28	0.06	0.51
<b>A_10</b>	10.44	0.75	0.95	0.89	0.88	0.18	0.24	0.36	0.21	0.27	0.08	0.53
<b>Mean</b>	<b>9.52</b>	<b>0.77</b>	<b>0.91</b>	<b>0.86</b>	<b>0.80</b>	<b>0.16</b>	<b>0.23</b>	<b>0.33</b>	<b>0.19</b>	<b>0.27</b>	<b>0.07</b>	<b>0.53</b>
<b>SD</b>	<b>1.85</b>	<b>0.24</b>	<b>0.10</b>	<b>0.07</b>	<b>0.16</b>	<b>0.02</b>	<b>0.07</b>	<b>0.07</b>	<b>0.03</b>	<b>0.11</b>	<b>0.01</b>	<b>0.05</b>

HPLC quantification of the major phenolic compounds. Aspalathin (ASP), nothofagin (NOT), isoorientin (ISOO), orientin (ORI), quercetin-3-O-robinobioside (Q3ROB), vitexin (VIT), hyperoside (HYP), rutin (RUT), isovitexin (ISOVIT), isoquercetrin (ISOQ), luteolin-7-O-glucoside (LUT7GLC), Z-2-(β-D-glucopyranosyloxy)-3-phenylpropenoic acid (PPAG). **ARC 2** - analysed by T. Beelders (2012). **GRT** - analysed by D. de Beer using T. Beelders method (2012). Green rooibos extracts (80% and 60% EtOH and Aq) - analysed by M. Brand/Walters using Walters (2016) method. Other abbreviations include freeze dried extract (FDE), ethanol (EtOH) and soluble solids (SS).

## **4.2. *In vitro* results**

The efficacy of the different green rooibos extracts (80% and 60% ethanol and hot water GRE) from the ten plant batches were assessed in terms of any potential cytotoxic effects at the optimized concentrations of 1 and 10 µg/mL using a chemiluminescent assay. The antidiabetic potential was also evaluated by assessing the effects of the extracts on PTP1B inhibition and their ability to enhance glucose uptake in C2C12 skeletal muscle, C3A liver and 3T3-L1 adipocytes. The effect of the extracts was also assessed on lipid accumulation in 3T3-L1 cells. The *in vitro* results reflected were from three independent experiments, each with three technical repeats, sample sizes were (N = 9) and data are expressed as the mean ± the standard error of the mean. The normal control refers to cells not exposed to the extracts.

### **4.2.1. Cytotoxicity of the extracts in C2C12 cells**

Based on previous studies by Muller (2012) and Mazibuko (2013, 2014), using the aspalathin-enriched green rooibos reference extract ARC 2, the most effective concentrations for C2C12, C3A and 3T3-L1 cells in terms of glucose uptake was established to be between 1 and 10 µg/mL. For comparative purposes, the three different types of green rooibos extracts were assessed for bioactivity at these concentrations and to confirm that the extracts were non-cytotoxic to the above mentioned cells, ATP assays were performed on C2C12's at 1 and 10 µg/mL over a period of 4 hours. None of the extracts were deemed cytotoxic (cell viability > 80%) (Figure 14 a-f).

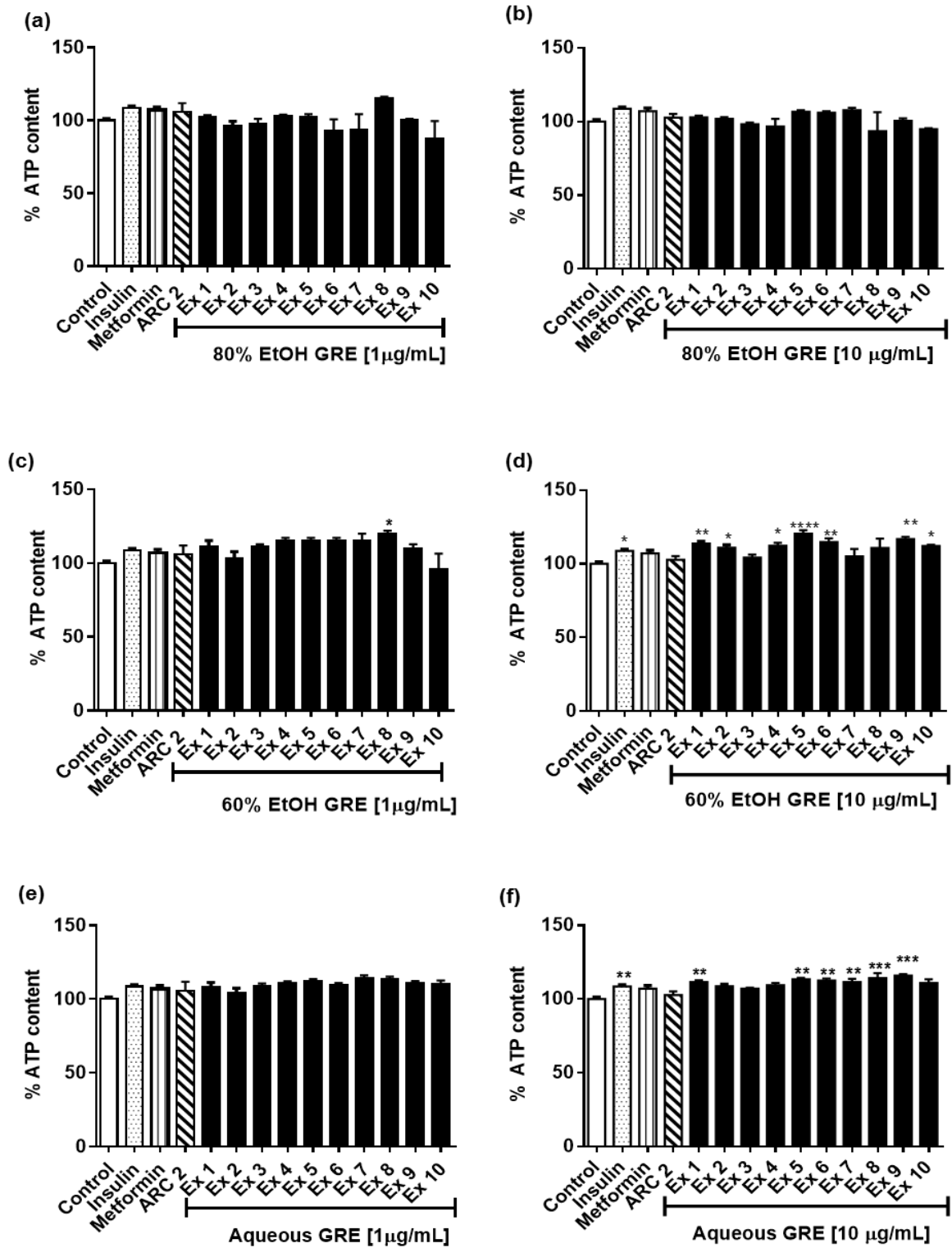


**Figure 14. Cellular ATP quantification of C2C12 cells treated with ethanol and aqueous green rooibos extracts from ten different plant batches.** Cells were exposed to the different green rooibos extracts at concentrations of 1 and 10 µg/mL for 4 hours. Ex 1 – Ex 10 represents the ten different plant batches. Data is representative of three independent experiments, each with three technical replicates (n=9). Data are presented as mean ± SEM with \* (p < 0.05); \*\* (p < 0.01) and \*\*\* (p < 0.001).

#### **4.2.2. Glucose uptake of GRE's in C2C12 myocytes**

Glucose metabolism by muscle, liver and fat cells plays an essential role in glucose homeostasis. Glucose uptake in the muscle and liver cell lines was determined by the intracellular accumulation of  $^3\text{H}$ -2-deoxy-D-glucose, which is a radiolabelled glucose analogue. Insulin and ARC 2 significantly increased glucose uptake in the C2C12 cells. Extracts 1-4 of the 80% ethanol extract (Figure 15 a) significantly increased glucose uptake (Ex 1:  $179.7 \pm 18.9\%$ ; Ex 2:  $170.0 \pm 12.2\%$ ; Ex 3:  $161.2 \pm 5.9\%$ ; Ex 4:  $182.0 \pm 16.3\%$ ) compared to the control. Extracts 1-4 were comparable to the reference extract ARC 2 ( $157.3 \pm 9.7\%$ ;  $p > 0.05$  vs. Ex 1-4). In the 60% ethanol GRE, extracts 1-5 also significantly increased glucose uptake (Ex 1:  $128.0 \pm 4.1\%$ ; Ex 2:  $134.0 \pm 4.2\%$ ; Ex 4:  $142.0 \pm 19.5\%$ ; Ex 5:  $128.3 \pm 6.5\%$ ) comparable to ARC 2 (Figure 15 b). Extracts 6-10 did not significantly increase glucose uptake. No significant differences were observed for the aqueous GRE (Figure 15 c).

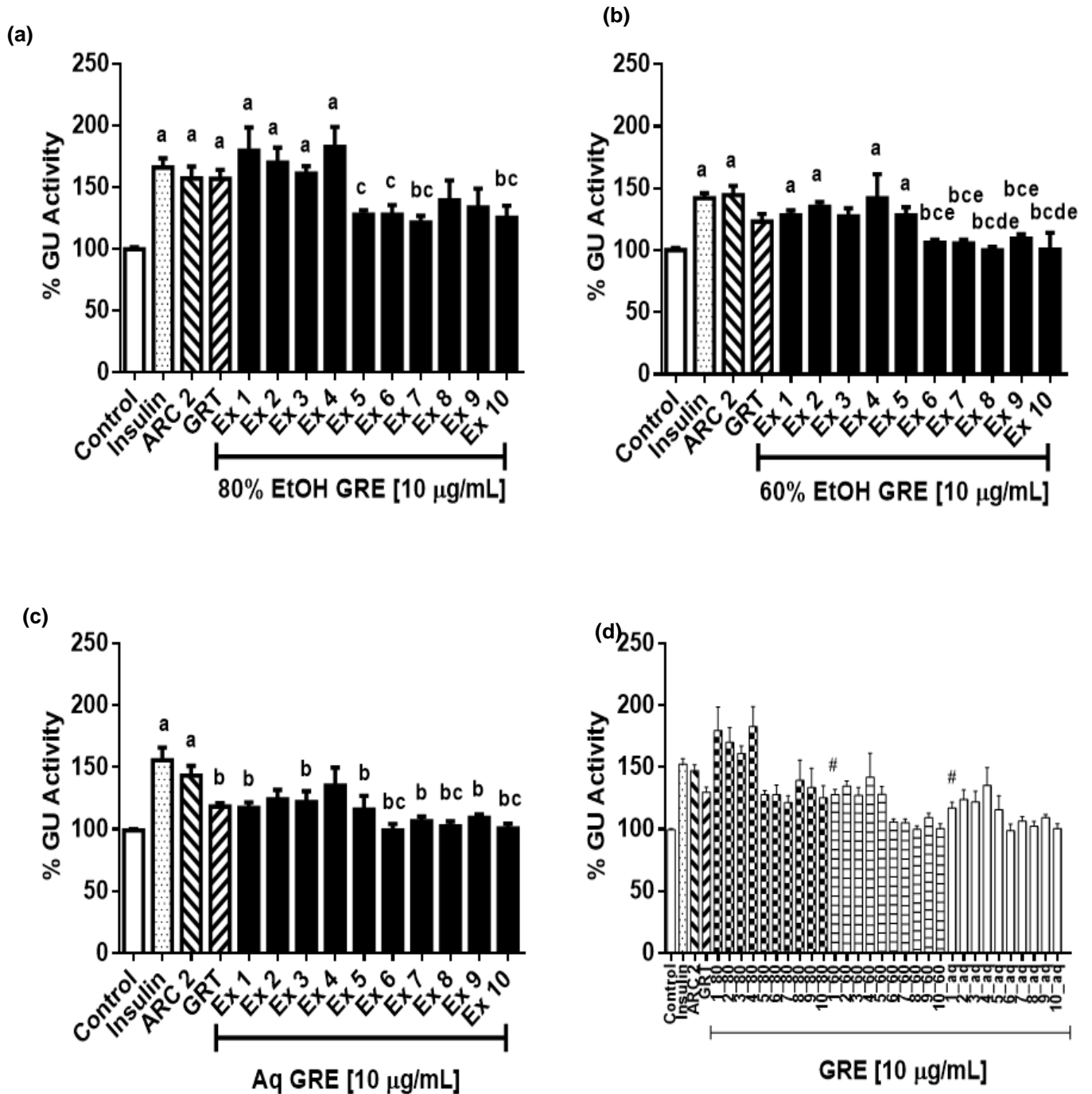


**Figure 15. Glucose uptake in differentiated C2C12 myocytes after treatment with green rooibos extracts (GRE) produced from 10 different plant batches by 80% ethanol extraction (a), 60% ethanol (b) and hot water extraction (c), (d) represents the combined glucose uptake of all three extracts.** The percentage of glucose uptake of cells treated with the extracts (10 µg/mL) or relevant controls [0.01% DMSO (Control) and 1 µM insulin (positive control)] for 4 hours in KRBH buffer containing 8 mM glucose, is presented. Data is representative of three independent experiments, each with three technical replicates (n=9). Data are presented as mean ± SEM. Bars with alphabets denote statistical significant differences between results (one-way ANOVA; p < 0.05). a - denotes significant difference to the control, b - denotes significant difference to insulin, c - denotes significant difference to ARC 2 and d- denotes significant difference to GRT. In combined data graph (d) # denotes differences to extract 1. GU Activity– Glucose uptake activity.

### 4.2.3. Glucose uptake of GRE's in C3A hepatocytes

In the C3A liver cells, the green rooibos extracts were not as effective in glucose uptake compared to the C2C12 cells. In the 80% ethanol extracts, only Ex 1 ( $162.4 \pm 18.9\%$ ) was significantly different to the control and was comparable to ARC 2, while extracts 2-5, albeit not significantly to the control, also increased glucose uptake  $\sim 140\%$ . Their activity was not significantly different to the reference extract ARC 2. As with the C2C12 cells, extracts 6-10 performed worse (Figure 16 a) with extracts 9 and 10 significantly lower than ARC 2. Only extract 8 of the 80% ethanol extract significantly increased glucose uptake. For the 60% ethanol extract, although the extracts showed some activity, none of the extracts were significantly different to the control, while extracts 9 and 10 (Figure 16 b) were significantly different to ARC 2 (Ex 9:  $108.1 \pm 7.0\%$ ; Ex 10:  $95.9 \pm 1.7\%$  vs. ARC 2  $166.2 \pm 10.1\%$ ;  $p < 0.05$ ). The aqueous GRE's, in contrast to the C2C12 cells, yielded significant increases (Figure 16 c) in glucose uptake of extracts 1, 2, 4, 7 and 8 (Ex 1:  $138.1 \pm 10.23\%$ ; Ex 2:  $134.7 \pm 11.1\%$ ; Ex 4:  $129.9 \pm 4.2\%$ ; Ex 7:  $131.7 \pm 5.0\%$ ; Ex 8:  $129.3 \pm 2.2\%$  vs. ARC 2:  $142.3 \pm 12.6\%$ ;  $p > 0.05$ ). There were no significant differences between the extracts produced from the different plant batches.

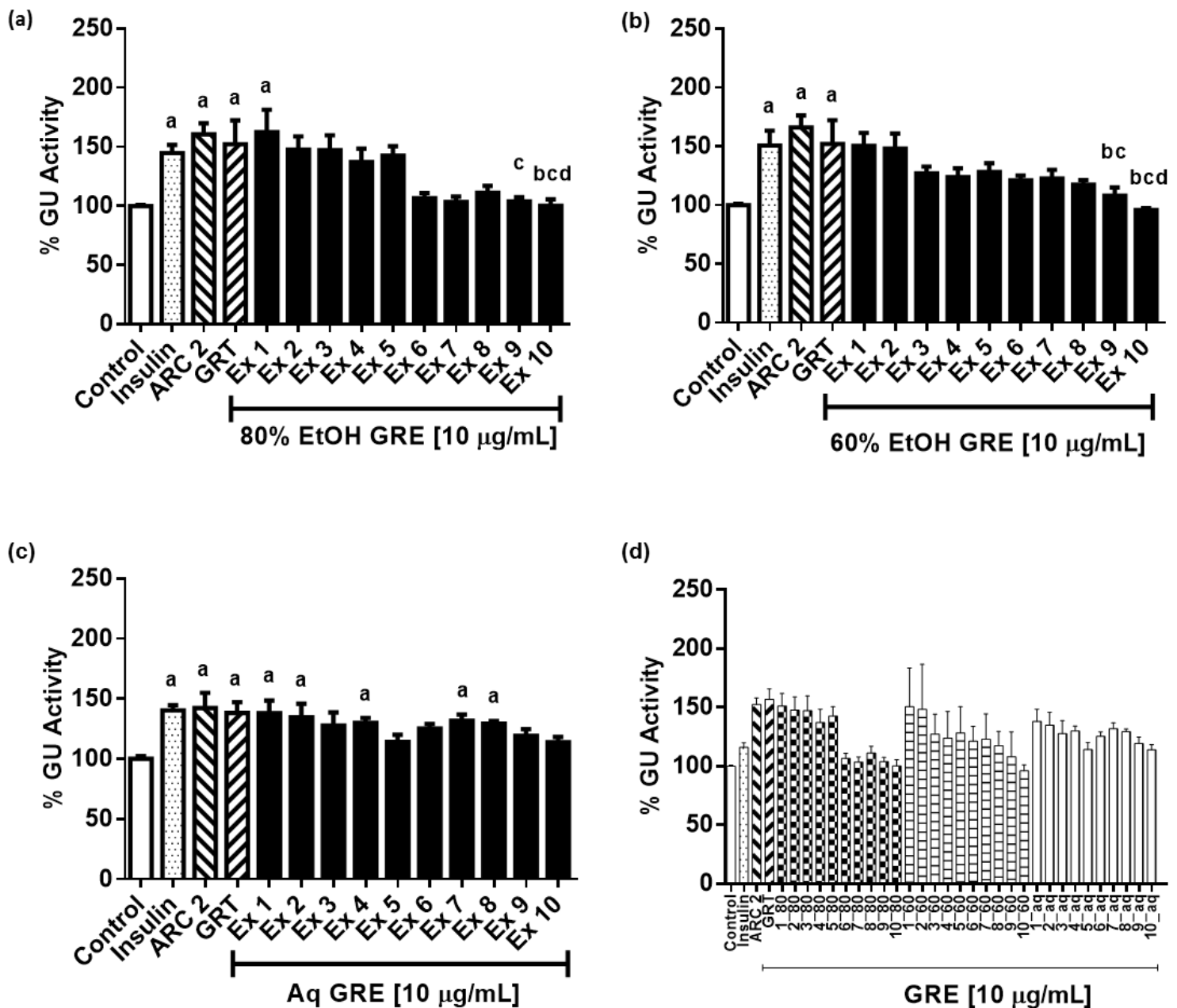


**Figure 16. Glucose uptake in C3A hepatocytes after treatment with green rooibos extracts (GRE) produced from 10 different plant batches by 80% ethanol extraction (a), 60% ethanol (b) and hot water extract (c), and combined are presented (d).** Similarly, to the C2C12 cells, the C3A cells were also treated over a period of 4 hours with 8 mM glucose in KRBH. The treated hepatocytes were then pulse labelled with 0.5 µCi/mL <sup>3</sup>H-2-deoxy- D-glucose for 15 minutes in glucose-free-KRBH. The amount of absorbed <sup>3</sup>H-2-deoxy- D-glucose was recorded as counts per minute using a liquid scintillation counter. Data is representative of three independent experiments, each with three technical replicates (n=9). Data are presented as mean ± SEM. Bars with alphabets denote statistical significant differences between results (one-way ANOVA; p < 0.05). a - denotes significant difference to the control, b - denotes significant difference to insulin, c - denotes significant difference to ARC 2 and d- denotes significant difference to GRT. GU Activity – Glucose uptake activity.

#### **4.2.4. Glucose uptake of GRE's in 3T3-L1 adipocytes**

In contrast to the C2C12 and C3A cells, for glucose uptake, a colourimetric method was used to determine the glucose usage from the media i.e. the residual glucose present in the media. This method was employed for the 3T3-L1 adipocytes, as this allows to simultaneously determine the glucose consumption as well as the lipid accumulation in the cytoplasm of these cells. Glucose uptake in this cell line was not as effective as that demonstrated by the C2C12 cells. Although the ethanol and aqueous extracts did show some increase in glucose uptake (Figure 17 a-c), none of these increases were significantly different to insulin. Glucose uptake with the 60% ethanol extracts was significantly lower than insulin (Insulin:  $148.9 \pm 3.9\%$  vs. Ex 5:  $117.0 \pm 6.8\%$ , Ex 6:  $118.9 \pm 5.3\%$ ; Ex 7:  $108.7 \pm 7.0\%$ ; Ex 8:  $116.1 \pm 7.9\%$ ; Ex 9:  $106.6 \pm 7.7\%$  and Ex 10:  $106.3 \pm 6.9\%$ ) the positive control.

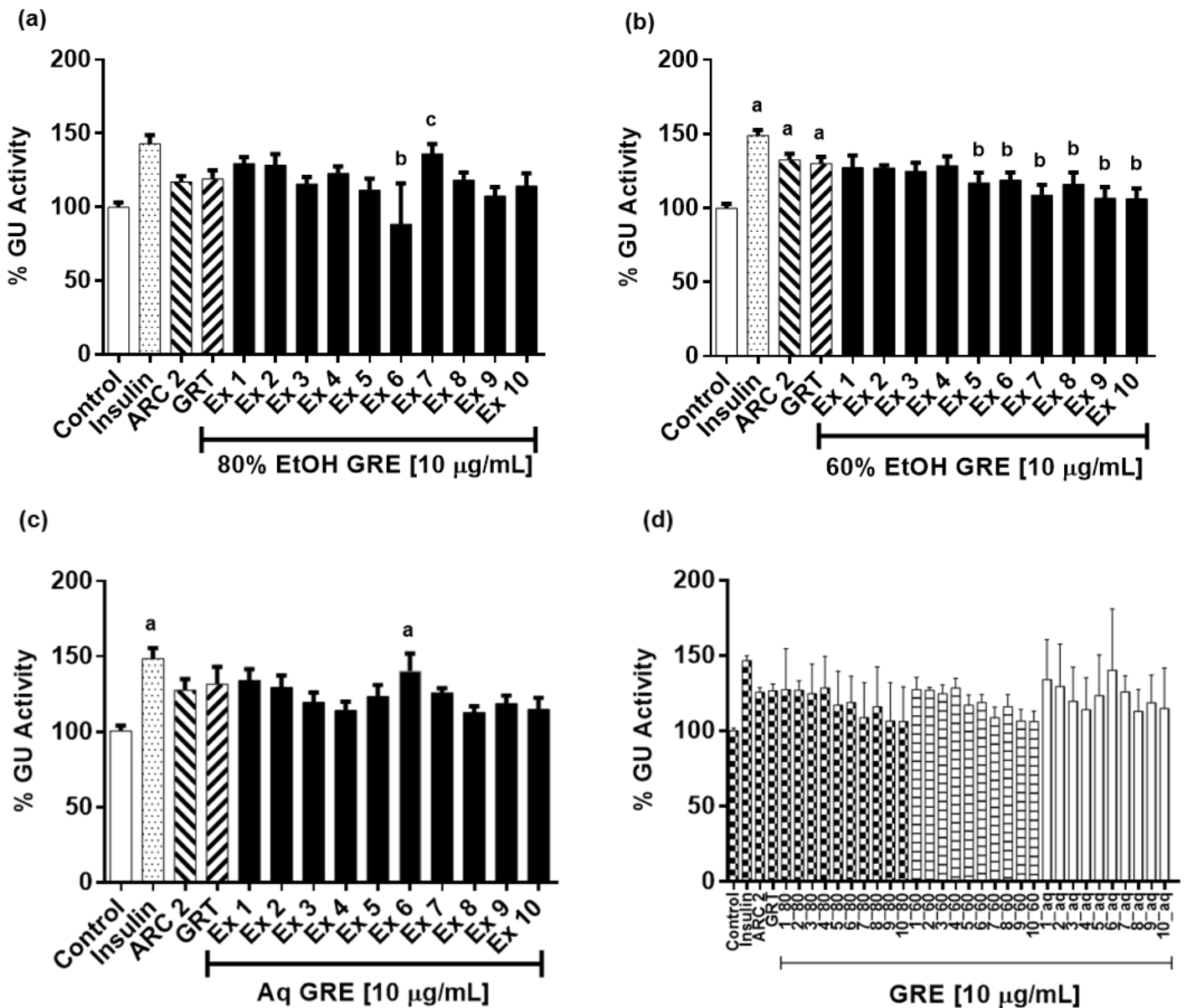


**Figure 17. Glucose uptake in 3T3-L1 adipocytes after treatment with green roibos extracts (GRE) produced from 10 different plant batches by 80% ethanol extraction (a), 60% ethanol (b) and hot water extraction (c), and combined are presented (d).** 3T3-L1 adipocytes were also treated over a period of 4 hours but with 25 mM DMEM without phenol red and pyruvate. Glucose uptake was determined by measuring residual glucose in the media after a 4 hour treatment, using a colourimetric method. Glucose usage was determined by subtracting the residual concentration of glucose present in the media from the original amount of glucose. Data is representative of three independent experiments, each with three technical replicates (n=9). Data are presented as mean  $\pm$  SEM. Bars with alphabets denote statistical significant differences between results (one-way ANOVA;  $p < 0.05$ ). a - denotes significant difference to the control, b - denotes significant difference to insulin, c - denotes significant difference to ARC 2 and d- denotes significant difference to GRT. GU Activity– Glucose uptake activity.

#### 4.2.5. Lipid accumulation in 3T3-L1 adipocytes

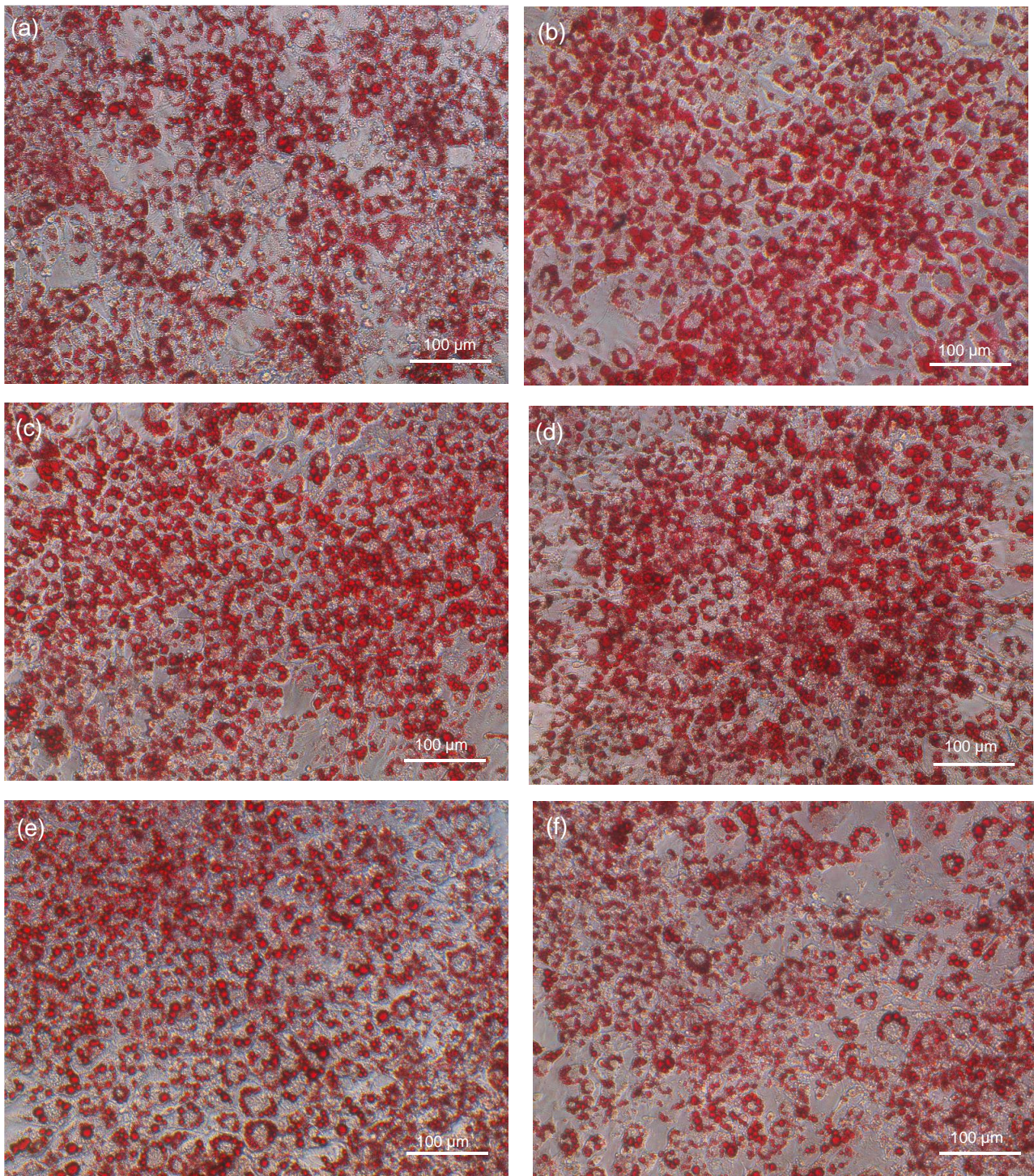


**Figure 18. Oil Red O stained 3T3-L1 adipocytes demonstrating lipid accumulation.** Lipid accumulation was determined after a 4-hour treatment period with (a) Control (0.01 % DMSO), (b) 1 µM Insulin, (c) 10 µg/mL ARC 2, and 10 µg/mL of the (d) 80% EtOH GRE (e) 60% EtOH GRE and (f) Aqueous GRE from plant batch 4 (as a representative example), respectively. Photomicrographs were taken using x400 magnification.

#### 4.2.6. Oil Red O Quantification

The amount of Oil Red O accumulated in mature adipocytes was quantified using isopropanol extraction (Figure 18 a-f). Significant increases in lipid accumulation was observed in the 80 and 60% ethanol extracts compared to that of the aqueous GRE (Figure 19 a-c). In contrast to glucose uptake, lipid accumulation was affected by the three different types of extract. For the 80% ethanol extracts, extracts 4, 5 and 6 significantly enhanced lipid accumulation to  $270.3 \pm 53.2\%$ ;  $281.6 \pm 62.7\%$ ;  $261.2 \pm 56.0\%$ , respectively. Similar effects were observed for extracts 2, 3, 4 and 7 in the 60% ethanol extracts:  $248.7 \pm 36.0\%$ ;  $350 \pm 67.1\%$ ;  $301.3 \pm 69.4\%$ ;  $245.0 \pm 27.4\%$ , respectively. In comparison, ARC 2 did not promote lipid accumulation significantly. However, GRT, the 60% ethanol commercial extract was more effective and comparable to insulin. The aqueous GRE's did not significantly increase lipid accumulation.

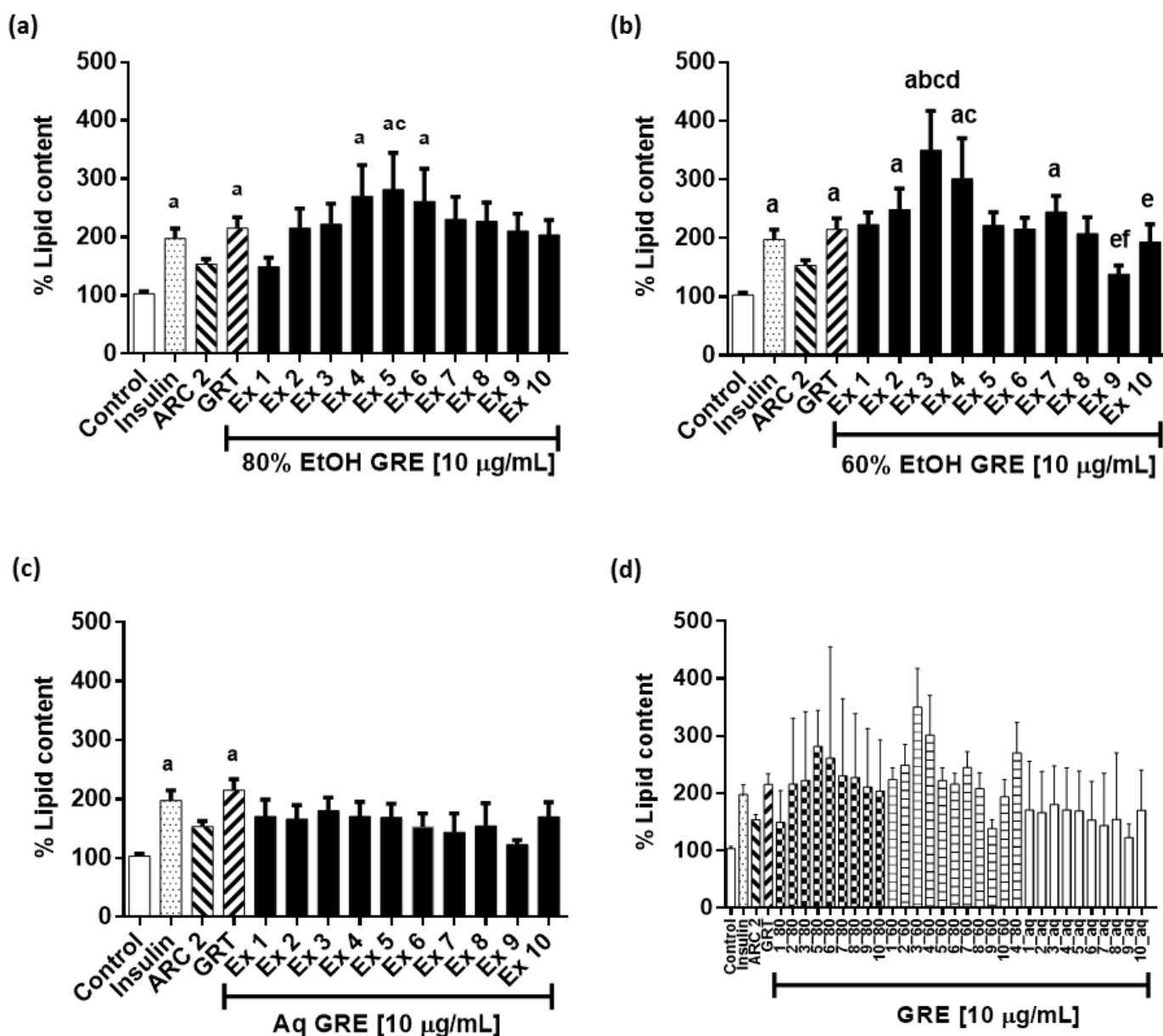


**Figure 19. Quantification of lipid accumulation in 3T3-L1 adipocytes.** (a) 80% ethanol GRE, (b) 60% ethanol GRE, (c) Aqueous GRE and (d) combined GRE. To quantify the relative total amount of Oil Red O stained cellular lipid, the stain was extracted from the cells using isopropanol and the absorbance measured at 490 nm. To compensate for cell numbers, the Oil Red O staining was normalized against crystal violet staining of nuclei. Data is representative of three independent experiments, each with three technical replicates (n=9). Data are presented as mean ± SEM. Bars with alphabets denote statistical significant differences between results (one-way ANOVA; p < 0.05). a - denotes significant difference to the control, b - denotes significant difference to insulin, c - denotes significant difference to ARC 2 and d- denotes significant difference to GRT.

### 4.3. Protein Tyrosine Phosphatase 1B (PTP1B) enzyme inhibition

Enzyme inhibition assays were conducted to assess the potential of the three types of GRE's on the inhibition of PTP1B enzyme, known to modulate insulin signalling.

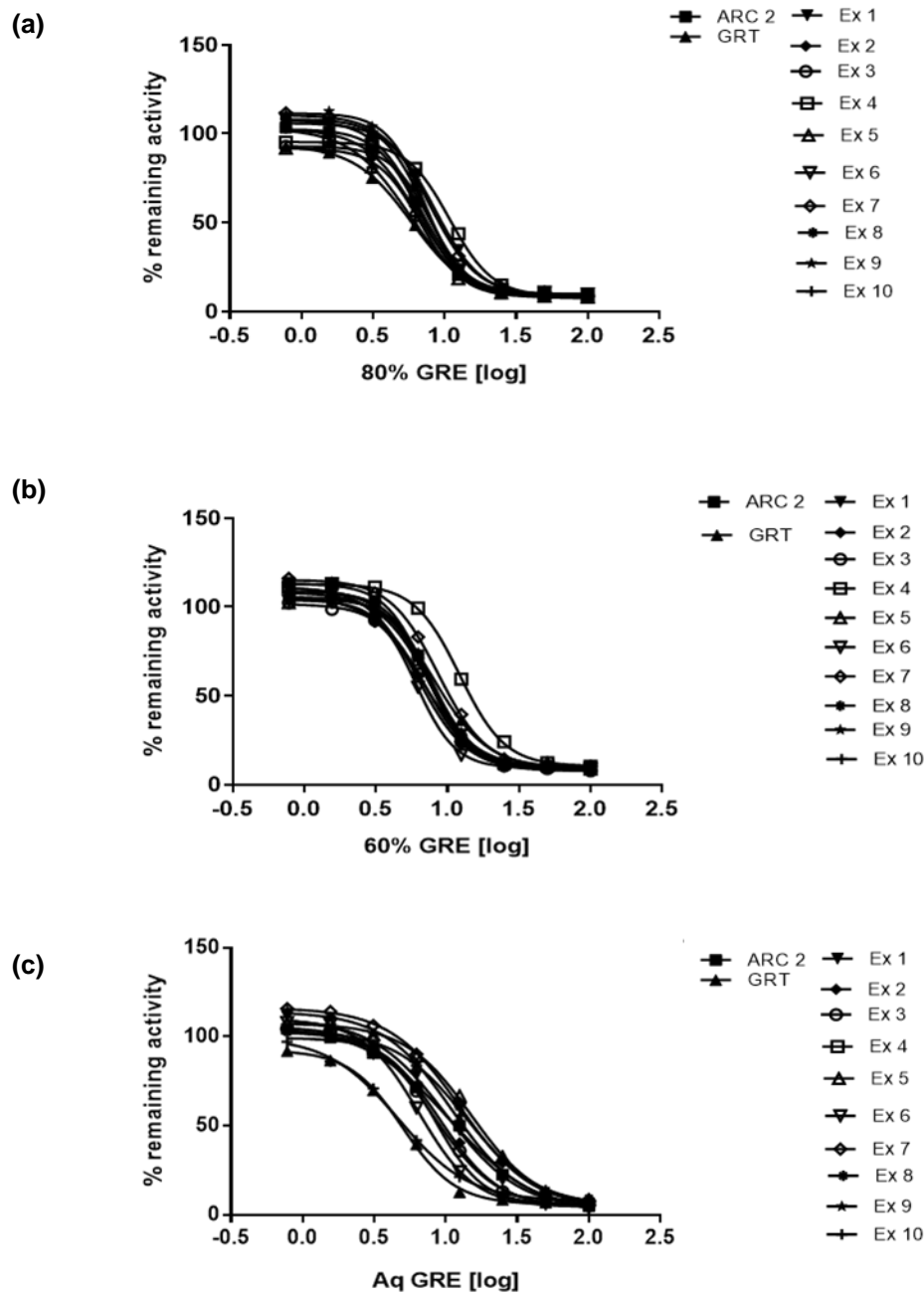


**Figure 20.** *In vitro* PTP1B enzyme inhibition studies with 80% and a 60% ethanol extract, and aqueous extracts of ten different plant batches. Data is representative of three independent experiments done in duplicate. Data are presented as mean  $\pm$  SEM of the three types of GRE were done in triplicates independent experiments. IC<sub>50</sub> values obtained were all below 20 µg/mL.

**Table 7. IC<sub>50</sub> values of enzyme inhibition against the PTP1B enzyme using three different types of GRE's.**

IC <sub>50</sub> Values (µg/mL)			
Extracts	80% EtOH	60% EtOH	Aq
ARC 2	7.2 ± 1.63		
GRT		7.95 ± 2.04	
Extract 1	8.60 ± 1.99	7.44 ± 1.73	10.03 ± 2.13
Extract 2	6.40 ± 1.50	6.22 ± 1.45	9.14 ± 1.95
Extract 3	7.98 ± 1.86	7.11 ± 1.69	8.31 ± 1.77
Extract 4	10.88 ± 2.54	12.21 ± 2.82	8.51 ± 1.86
Extract 5	6.80 ± 1.62	7.50 ± 1.78	15.12 ± 3.28
Extract 6	6.66 ± 1.53	6.04 ± 1.42	6.52 ± 1.42
Extract 7	7.93 ± 1.80	8.61 ± 2.01	12.76 ± 2.86
Extract 8	7.23 ± 1.63	7.84 ± 1.86	13.91 ± 3.12
Extract 9	7.27 ± 1.73	7.62 ± 1.86	11.06 ± 2.60
Extract 10	5.58 ± 1.50	6.73 ± 1.70	4.68 ± 1.21

All extracts showed potent inhibitory effects with IC<sub>50</sub> values below 20 µg/mL. Average IC<sub>50</sub> values of 7.5 ± 0.5; 7.7 ± 0.6; 10.0 ± 1.0. for the 80 and 60% ethanol and aqueous GRE's, respectively. The inhibitory effects between the different extracts was not significantly different. Of interest was extract 10, which produced the lowest IC<sub>50</sub> values for all three extracts, with the aqueous extract as the most potent 4.68 ± 1.21 (Table 7). ARC 2: reference aspalathin-enriched green rooibos extract. GRT: aspalathin-enriched pharmaceutical grade 60% ethanol green rooibos extract. Extracts 1-10: green rooibos extracts produced from 10 different plant batches by 80% ethanol (EtOH), 60% ethanol (EtOH) and Aqueous (Aq) extraction.

#### **4.4. Western blot analysis**

Extract 2 (Ex 2) was selected based on comparable bioactivity but higher aspalathin content and extract 4 (Ex 4) was selected based on its relatively low aspalathin content for protein expression studies. Western blot analysis was performed in the C2C12 skeletal muscle cells, as this cell model displayed the most bioactivity *in vitro*, using selected effector proteins. To assess the effect of the extracts on insulin signalling, AKT was selected as the effector protein. The effects on AMPK, a master regulator of cellular energy and a major drug target for T2D, was also assessed. Acetyl-CoA carboxylase (ACC) and Malonyl-CoA decarboxylase (MLYCD) were used to assess the effect of the extracts on acetyl-CoA conversion in lipid metabolism.

#### 4.4.1. Effect of aspalathin-enriched green rooibos extract (GRE) on AMPK expression and activation in C2C12 muscle cells

The extracts from the two plant batches showed similar effects. Although not statistically significant, both total and activated AMPK in the 80% extracts as well as the reference extracts increased phosphorylated AMPK activation. Extract 4 was comparable to ARC 2, increasing the activation of AMPK by > 1.5 fold. The aqueous extracts did not appear to affect AMPK expression.

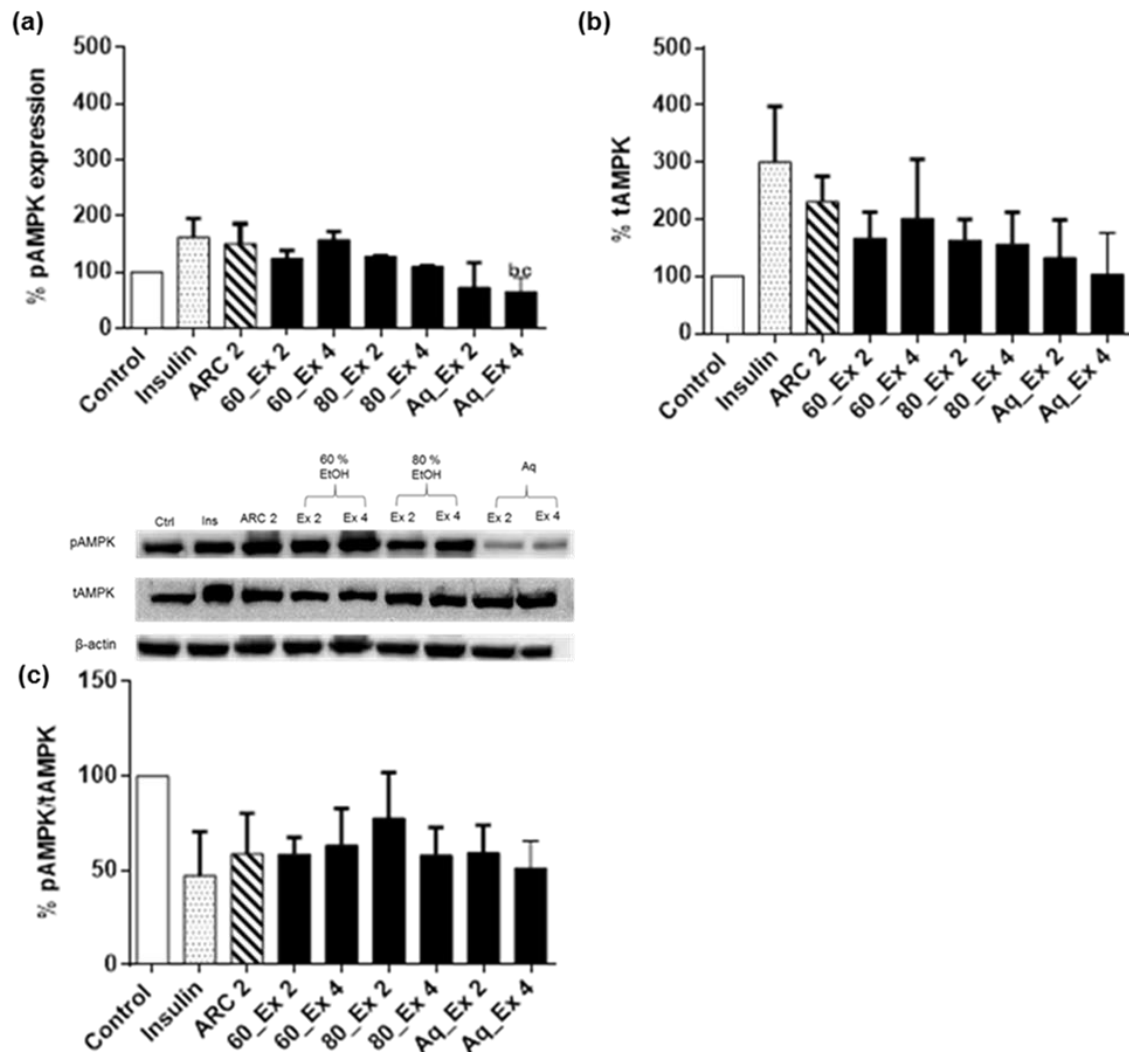


**Figure 21. Effect of green rooibos extract on AMPK activation.** C2C12 muscle cells, grown in 8 mM glucose DMEM were treated with 10  $\mu$ g/mL GRE for 4 hours. Insulin at a concentration of 1  $\mu$ M was included as a positive control. Cells were lysed and subjected to Western blot analyses. The % of pAMPK/tAMPK was used to estimate the level of AMPK activation. Results are expressed as the mean of three independent experiments relative to control at 100%  $\pm$  SEM. Bars with alphabets indicate statistical differences at  $p \leq 0.05$ . b - denotes significant difference to insulin and c - denotes significant difference to ARC 2.

#### 4.4.2. AKT expression and activation in C2C12 muscle cells

Insulin was shown to enhance the phosphorylation of AKT ( $p = 0.02$ ; t-test to control) with a concomitant decrease in total AKT. ARC 2 did not affect AKT activation. Both the 60% ethanol and aqueous extract of plant batch 4 increased total AKT by  $> 1.5$  fold, however this was not significantly different to the control.

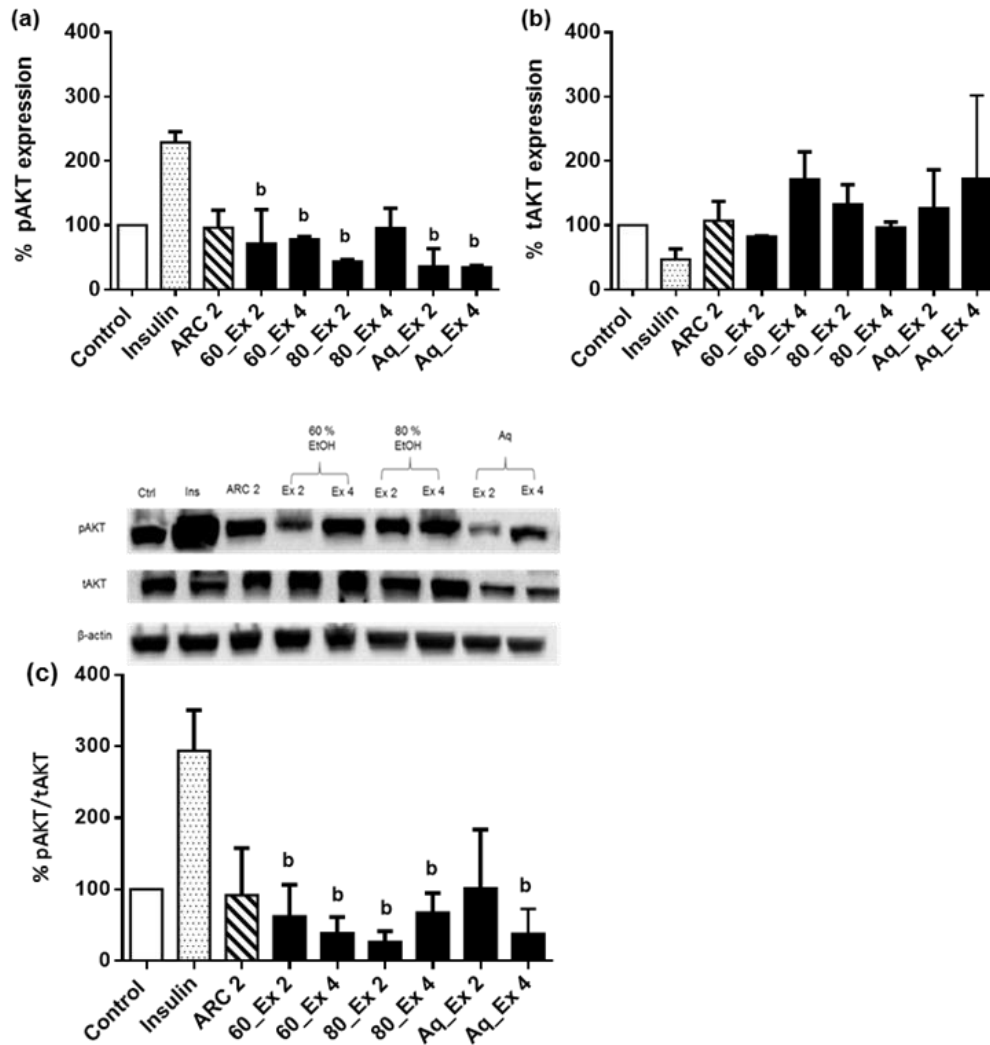


**Figure 22. Effect of green rooibos extract on AKT activation.** C2C12 muscle cells, grown in DMEM supplemented with 8 mM glucose were treated with 10  $\mu$ g/mL GRE for 4 hours. Insulin at a concentration of 1  $\mu$ M was included as a positive control. Cells were lysed and subjected to Western blot analyses. The % of pAKT/tAKT was used to estimate the level of AKT activation. Results are expressed as the mean of three independent experiments relative to control at 100%  $\pm$  SEM. Bars with alphabets indicate statistical differences at  $p \leq 0.05$ . b - denotes significant difference to insulin.

#### 4.4.3. Acetyl CoA Carboxylase (ACC) expression and activation in C2C12 muscle cells

Insulin and ARC 2 increased ACC activation by ~ 1.5 fold, however this was not significant.

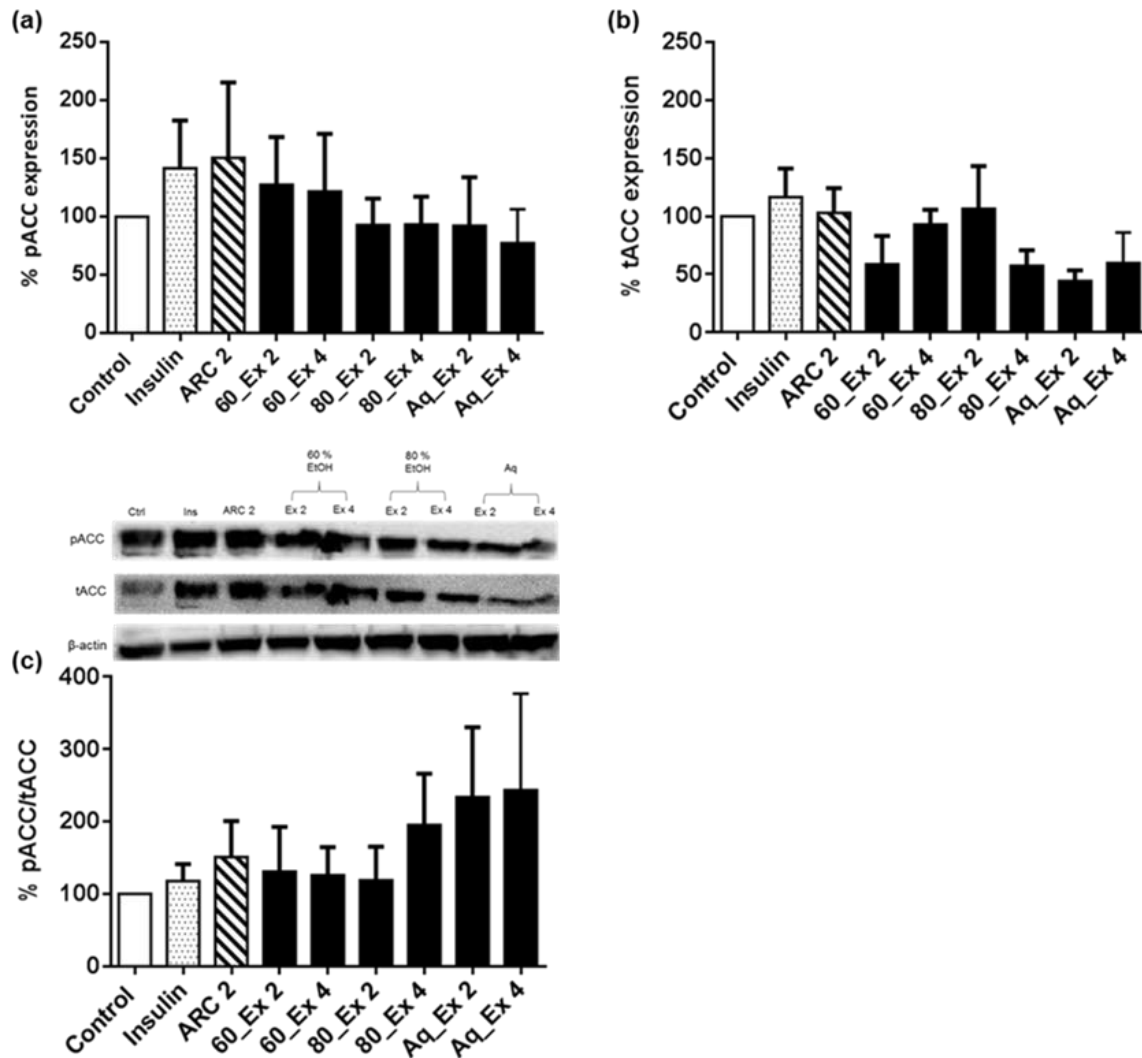


**Figure 23. Effect of green roibos extract on ACC activation.** C2C12 muscle cells, grown in DMEM supplemented with 8 mM glucose were treated with 10  $\mu$ g/mL GRE for 4 hours. Insulin at a concentration of 1  $\mu$ M was included as a positive control. Cells were lysed and subjected to Western blot analyses. The % of pACC/tACC was used to estimate the level of ACC activation. Results are expressed as the mean of three independent experiments relative to control at 100%  $\pm$  SEM.

#### 4.4.4. Expression and activation of Malonyl-CoA decarboxylase (MLYCD) in C2C12 muscle cells.

Insulin and ARC 2 were not able to significantly promote the expression of MLYCD in C2C12 cells. However, extract 2 of the 80% ethanol GRE (1023) did promote the expression of MLYCD.

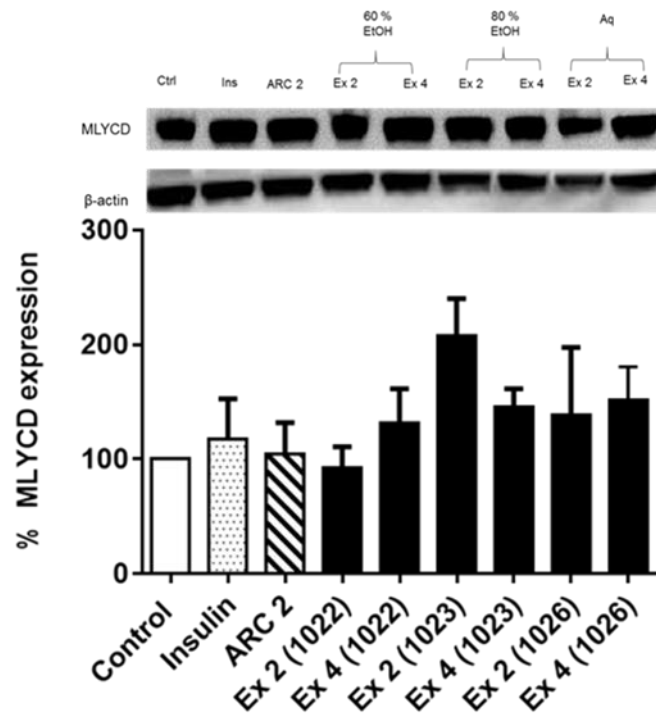


**Figure 24. Effect of green rooibos extract on MLYCD activation.** C2C12 muscle cells, grown in DMEM supplemented with 8 mM glucose were treated with 10  $\mu$ g/mL GRE for 4 hours. Insulin at a concentration of 1  $\mu$ M was included as a positive control. Cells were lysed and subjected to Western blot analyses. Results are expressed as the mean of three independent experiments relative to control at 100%  $\pm$  SEM. No statistical differences were observed.

#### 4.5. Statistical analysis

**Table 8. Comparative table of bioactivity and chemical composition.**

Sample	Bioactivity			(Content g/100g SS)											
	C2C12 GU	3T3-L1 LA	PTP1B	PPAG	ASP	NOT	ISOO	ORI	Q3ROB	VIT	HYP	RUT	ISOVIT	ISOQ	LUT7GLC
ARC 2	157.28	148.75	7.84	0.49	18.44	1.29	2.05	1.05	1.05	0.27	0.27	0.54	0.39	0.38	0.00
GRT	157.03	226.87	6.92	0.42	12.78	1.97	1.43	1.26	1.04	0.34	0.40	0.50	0.30	0.57	0.00
80_1	179.66	149.04	9.52	0.43	16.06	1.63	1.87	1.53	1.01	0.32	0.41	0.47	0.40	0.49	0.05
80_2	170.02	215.61	7.24	0.57	17.54	1.82	1.46	1.21	0.98	0.25	0.39	0.40	0.28	0.49	0.07
80_3	161.22	222.44	9.08	0.58	15.06	1.04	1.66	1.37	0.81	0.25	0.29	0.31	0.34	0.31	0.06
80_4	182.74	270.29	12.39	0.52	11.55	0.82	1.39	1.27	1.01	0.22	0.35	0.38	0.31	0.39	0.07
80_5	127.94	281.56	7.03	0.52	17.88	2.16	1.58	1.27	0.93	0.24	0.36	0.39	0.38	0.45	0.06
80_6	127.92	261.22	7.28	0.47	18.76	1.97	1.55	1.28	1.02	0.26	0.40	0.39	0.36	0.53	0.07
80_7	121.60	230.14	7.55	0.47	15.89	1.08	1.39	1.16	1.41	0.24	0.65	0.55	0.32	0.99	0.06
80_8	139.58	227.09	7.74	0.50	21.38	1.50	1.56	1.24	1.19	0.24	0.46	0.49	0.38	0.63	0.08
80_9	133.49	210.81	7.22	0.53	19.02	1.57	1.59	1.23	1.11	0.26	0.37	0.44	0.39	0.50	0.07
80_10	125.20	203.71	6.40	0.52	17.78	1.39	1.59	1.31	1.20	0.26	0.40	0.48	0.39	0.51	0.07
60_1	128.04	223.36	9.09	0.39	11.78	1.15	1.79	1.33	1.10	0.26	0.42	0.48	0.36	0.54	0.06
60_2	134.77	248.73	7.74	0.49	13.04	1.32	1.38	1.07	0.96	0.19	0.34	0.37	0.26	0.45	0.07
60_3	127.28	350.02	9.13	0.39	8.58	0.56	1.00	0.81	0.56	0.14	0.17	0.20	0.21	0.17	0.05
60_4	142.05	301.30	15.54	0.47	8.67	0.60	1.32	1.13	1.07	0.18	0.34	0.38	0.32	0.32	0.07
60_5	128.33	221.96	9.51	0.47	13.88	1.66	1.44	1.10	0.88	0.19	0.33	0.36	0.34	0.41	0.06
60_6	105.75	215.66	6.64	0.41	12.80	1.30	1.36	1.05	0.98	0.21	0.37	0.36	0.34	0.41	0.07
60_7	105.27	244.96	10.62	0.48	15.32	0.90	1.43	1.11	1.54	0.23	0.68	0.59	0.31	1.02	0.06
60_8	99.80	207.72	9.64	0.47	16.17	1.17	1.44	1.10	1.17	0.21	0.43	0.46	0.35	0.57	0.06
60_9	109.33	138.47	9.43	0.40	11.50	0.90	1.18	0.91	0.90	0.18	0.31	0.36	0.29	0.39	0.05
60_10	96.81	193.49	8.98	0.47	13.67	1.05	1.44	1.13	1.16	0.22	0.37	0.45	0.35	0.47	0.07
Aq_1	117.15	170.58	8.49	0.47	8.38	0.79	1.06	0.97	0.77	0.18	0.23	0.36	0.20	0.28	0.05
Aq_2	124.23	165.92	8.40	0.61	10.45	0.97	0.97	0.90	0.79	0.15	0.22	0.32	0.16	0.28	0.06
Aq_3	121.75	180.34	8.11	0.60	7.74	0.48	0.83	0.80	0.56	0.14	0.15	0.21	0.15	0.14	0.06
Aq_4	135.26	170.64	11.11	0.49	5.41	0.36	0.72	0.74	0.71	0.12	0.16	0.26	0.16	0.16	0.07
Aq_5	115.60	169.13	12.21	0.56	10.79	1.18	0.95	0.88	0.68	0.16	0.20	0.30	0.20	0.25	0.07
Aq_6	98.68	153.19	5.78	0.50	9.70	0.93	0.82	0.79	0.71	0.16	0.23	0.28	0.17	0.25	0.07
Aq_7	106.75	143.37	10.83	0.54	9.86	0.65	0.96	0.88	1.15	0.19	0.40	0.47	0.21	0.54	0.08
Aq_8	102.17	154.47	11.39	0.51	11.55	0.79	0.95	0.90	0.91	0.16	0.26	0.37	0.22	0.27	0.08
Aq_9	109.37	122.69	8.55	0.51	10.92	0.80	0.95	0.85	0.84	0.17	0.21	0.34	0.20	0.28	0.06
Aq_10	100.68	170.04	7.23	0.53	10.44	0.75	0.95	0.89	0.88	0.18	0.24	0.36	0.21	0.27	0.08

C2C12 GU – C2C12 Glucose Uptake, 3T3-L1 LA – 3T3-L1 Lipid Accumulation, PTP1B – Protein tyrosine phosphatase 1B IC<sub>50</sub> values, PPAG – enolic phenylpropanoic acid glucoside, ASP – Aspalathin, NOT – Nothofagin, ISOO – Isoorientin, ORI – Orientin, Q3ROB - quercetin-3-O-robinobioside, VIT – Vitexin, HYP – Hyperoside, RUT – Rutin, ISOVIT – Isovitexin, ISOQ – Isoquercetrin, LUT7GLC – Luteolin-7-O-glucoside.

#### 4.6. Principle Component Analysis of all three GRE's compared to bioactivity

(a)

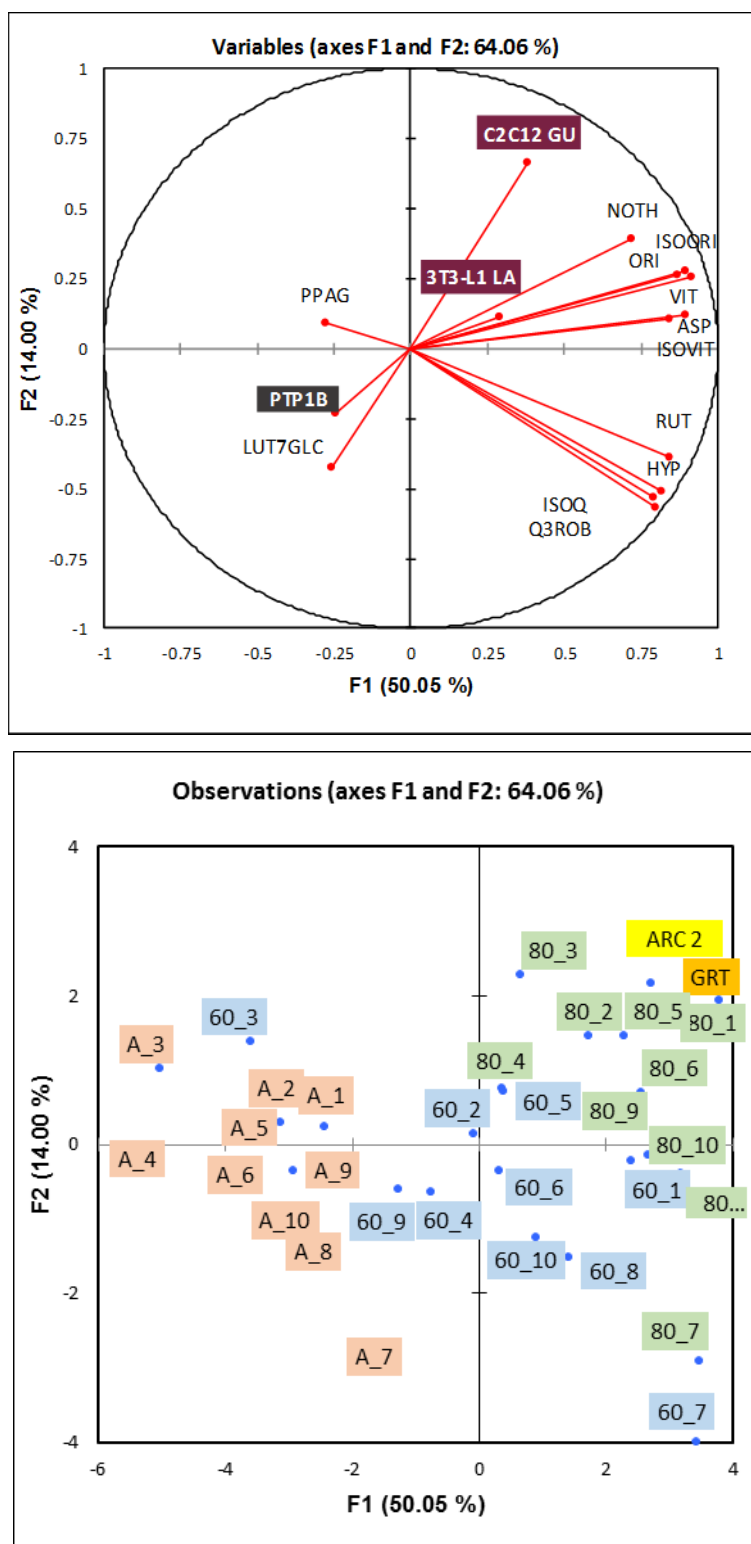


**Figure 25. Principal component analysis loadings (a) and scores (b) plots showing association between bioactivity, phenolic composition and extract samples.** The individual 80% ethanol-water, 60% ethanol water and hot water extracts are labelled as 80\_1 to 80\_10, 60\_1 to 60\_10 and A\_1 to A\_10, respectively. The compound labels are indicated in Table 8.

The multivariate statistical analysis used in this study was Principle Component Analysis (PCA) which is a pattern-recognition method, commonly used in chemometric analysis to visualize grouping trends and outliers. The first two principle components (PCs) are expressed in a PCA plot which demonstrates the variation between each extract and biological activity. The closer the PCs are, the higher the similarity between the samples (Lv *et al.*, 2015). The PCA loadings plot (Figure 25 a) shows that the phenolic composition, and in particular the dihydrochalcones (aspalathin and nothofagin) and their flavone derivatives (orientin and iso-orientin, vitexin and isovitexin, respectively), associated with the ability of the extracts to enhance glucose uptake in C2C12 muscle cells (C2C12 GU) and lipid accumulation in 3T3-L1 cells (3T3-L1 LA). A clear separation between the hot water extracts and the 80% ethanol-water extracts is evident in the PCA scores plot (Figure 25 b). ARC 2 and GRT are also grouped with the 80% ethanol-water extracts (Figure 25 b), having a dihydrochalcone and flavone (DHC + FLV) content of 23.49% and 18.08%, respectively. By comparison the 80% ethanol-water, 60% ethanol-water and hot water extracts had a mean DHC+ FLV content of 22.05%, 16.67% and 12.42%, respectively.

# CHAPTER 5

## DISCUSSION AND CONCLUSION

In recent years, there has been great interest in the health-promoting properties of *Aspalathus linearis* (rooibos), particularly its beneficial role in glucose and lipid metabolism (Kamakura *et al.*, 2015; Kawano *et al.*, 2009; Mazibuko *et al.*, 2013; Mazibuko *et al.*, 2015; Muller *et al.*, 2012; Muller *et al.*, 2016), with specific reference to its potential as a nutraceutical in the field of metabolic diseases (Canda *et al.*, 2014; Patel *et al.*, 2016). Its beneficial effects on glycaemia, lipidaemia, insulin resistance and chronic inflammation have received much scientific and commercial interest (Beltrán-Debón *et al.*, 2011; Joubert and de Beer 2011; Mazibuko *et al.*, 2013; Muller *et al.*, 2012). Nutraceuticals, food and cosmetic products derived from rooibos are already available in the market (de Beer *et al.*, 2016; Joubert and de Beer, 2011), however, most of these products lack scientific proof for their efficacy and safety. If available, scientific evidence for efficacy of these health products is based on proof of concept studies *in vitro* and in animal studies. Thus, there is a paucity of human studies confirming the efficacy of these products. Furthermore, there are no standards set for dosage and other quality parameters. Potential side effects and possible interaction with other chronic medication is largely unknown or undisclosed (Wachtel-Galor and Benzie, 2011; Shaw *et al.*, 2012; Tamargo *et al.*, 2015).

### 5.1. Rooibos as a health product

In terms of rooibos, focus is drawn to the abundance and uniqueness of the dihydrochalcone, aspalathin, to which many of the beneficial metabolic effects have been attributed (Canda *et al.*, 2014; Hong *et al.*, 2014; Mazibuko *et al.*, 2013; Muller *et al.*, 2012). *In vitro*, aspalathin has been demonstrated to contribute to glucose-uptake in C2C12, C3A and 3T3-L1 cells (Chen *et al.*, 2013; Kamakura *et al.*, 2015; Kawano *et al.*, 2009; Kreuz *et al.*, 2008; Mazibuko *et al.*, 2013). Other phenolic compounds such as orientin, isoorientin, nothofagin and Z-2-( $\beta$ -D-glucopyranosyloxy)-3-phenylpropenoic acid (PPAG), have also been shown to have positive metabolic effects (Kamakura *et al.*, 2015; Muller *et al.*, 2013; Patel *et al.*, 2016). In unfermented (green) rooibos, these phenolic compounds are present in higher concentrations (Beelders *et al.*, 2012; Joubert and de Beer 2011) which makes it the likely choice for producing nutraceuticals, such as the aspalathin-enriched green rooibos extract, GRT. Producing a standardised health product from rooibos presents a number of challenges. These include a great variation in the chemical make-up of the plant material (de Beer *et al.* 2016) and lack of human trials (Shan *et al.*, 2007; Zhang *et al.*, 2012). In addition, agroprocessing and extraction methods greatly influence the composition of the final product (Astill *et al.*, 2001; Ghanbari *et al.*, 2012).

*In vitro* and *in vivo* studies by (Muller *et al.*, 2012) showed that the reference aspalathin-enriched green rooibos extract ARC 2 was able to enhance glucose uptake in C2C12 myotubules and improve glucose tolerance in streptozotocin-induced diabetic rats. Furthermore, research demonstrated the restoration of glucose uptake and insulin responsiveness by ARC 2 and aspalathin in palmitate-induced insulin resistant C2C12, C3A and 3T3-L1 adipocytes (Mazibuko *et al.*, 2013; Mazibuko 2014; Mazibuko *et al.*, 2015). Although these *in vitro* studies confirm the antidiabetic potential of this 80% ethanol aspalathin-enriched green rooibos extract (ARC 2), no studies have been conducted that compare the effects of extract type and the impact of plant material variation with *in vitro* bioactivity. These are crucial aspects for the nutraceutical industry to produce optimized extracts with predictable bioactivity that are cost-effective (Apak *et al.*, 2016; Walters *et al.*, 2016). The extraction solvent has a great impact on the chemical composition and quality of the phenolic content. Solvents such as ethanol and acetonitrile may be employed to enhance the extraction of phenolic compounds (Walters *et al.*, 2016). This was evident in our study, whereby

plant material extracted with ethanol (80 and 60% EtOH) contained much higher aspalathin and total phenolic content than those extracted with hot-water (shown in Table 6).

## 5.2. Phenolic composition of three different types of GRE

Chemical characterisation of the phenolic compounds in the three different types of extracts investigated in this study revealed, as expected, a large variation in phenolic content, not only with extract type but also related to the different plant batches. The 80% ethanol extract produced the highest average aspalathin content ( $17.09 \pm 2.66$  g/100 g SS; range 20.38 – 11.55). The 60% ethanol extract yielded an average of  $12.54 \pm 2.51$  g/100g SS with a range of 16.17 - 8.58, while the aqueous extract yielded an aspalathin content of  $9.52 \pm 1.85$  g/100g SS with a range from 11.55 - 5.41. The plant batches yielding the highest aspalathin content also had the highest total phenolic content and *vice versa*. The implication thereof, for this study, is that standardising by the aspalathin content infers standardising to other phenolic compound content. For comparative purposes an ARC 2, aspalathin-enriched green rooibos extract (GRE), with a phenolic composition similar to that of the test 80% ethanol extracts, proven to have significant antidiabetic bioactivity, was included as a reference extract. In addition, a commercially produced pharmaceutical grade, aspalathin-enriched green rooibos extract (GRT) was included for comparison of efficacy to the commercial product.

## 5.3. Bioactivity of GRE

This study evaluated the relationship between the chemical composition of different extract types as well as variation of plant batches with *in vitro* bioactivity. To achieve this, three different types of green rooibos extracts (80 and 60% ethanol and a hot water extract) were produced from ten randomly selected plant batches within the same rooibos plantation by the ARC (Walters *et al.*, 2016). All extracts were tested at the optimized concentration of 10 µg/mL, previously shown to be the most effective concentration for increasing glucose uptake and shown to be non-toxic in C2C12 muscle cells and Chang liver cells (Muller *et al.*, 2012).

The extracts were then evaluated for their antidiabetic activities *in vitro*. This included the effect of the extracts on glucose uptake in C2C12 muscle, C3A liver and 3T3-L1 adipocyte cells. These cells represent the major tissues involved in maintaining glucose homeostasis (Herman and Kahn 2006; Olson 2012). In addition, lipid accumulation in adipocytes, under hyperglycaemic conditions of 25 mM glucose, was also assessed in 3T3-L1 adipocytes. At a functional level, the inhibitory effects of the extracts on PTP1B, the insulin signal-modulating enzyme and potential antidiabetic drug target, was assessed enzymatically *in vitro*. To further understand the molecular mechanisms of action that the extracts have on effector signalling proteins, relevant to insulin signalling, AMPK and lipid metabolism, extracts from two different plant batches (denoted as Ex 2 and Ex 4) were selected for Western blot analyses. These extracts were selected based on their dissimilar chemical composition and bioactivity. To establish whether chemical entities within the different extracts could predict bioactivity. PCA statistical analysis was applied to evaluate clustering relationships between the phenolic compounds analysed and selected bioactivity parameters.

### **5.3.1. Glucose uptake in C2C12 muscle cells**

In C2C12 cells, the ethanol extracts produced the highest increase in glucose uptake, particularly extracts 1, 2 and 4 in the 80 and 60 % ethanol extracts. These three extracts were as effective as insulin (positive control), ARC 2 (80% ethanol-enriched GRE) and GRT (the 60% ethanol GRE). These findings are supported by Muller *et al.*, (2012) that demonstrated enhanced glucose uptake for C2C12 cells over a broad concentration range (0.05–5 µg/mL) for ARC 2 (also known as SB1) (Muller *et al.*, 2012). Similar results were also shown by Kamakura *et al.*, (2015) for ARC 2 (SB1) in L6 myotubules and Son *et al.* 2012, from the same laboratory in Tokyo, reported that aspalathin, isolated from rooibos, increased glucose uptake in L6 myotubes. Therefore, in this study the observed effect in skeletal muscle cells is likely to be attributed, at least in part, to the effect of aspalathin. A previous study by Mazibuko (2014) confirmed similar bioactivity for aspalathin and its flavone derivatives orientin and isoorientin in palmitate-induced insulin resistant C2C12 cells. The effect of nothofagin, vitexin and isovitexin have not been compared to date. The higher content of aspalathin, orientin and isoorientin in the extracts prepared using 80% ethanol (Table 6) are thus likely contributors to the increase in glucose uptake. Variation was

also demonstrated between plant batches, with batches 5 - 10 and 6 - 10, respectively for the 80 and 60% EtOH extracts, being less effective in comparison to ARC 2. For the aqueous GRE, none of the extracts were as effective as the reference extract, ARC 2. The observed variation in glucose uptake activity was not strictly related to aspalathin content as plant batch 8 of both the ethanol (80 and 60% ETOH) extracts had the highest aspalathin content (21.3 and 16.2 g/100g SS, respectively), but produced significantly lower glucose uptake activity compared to ARC 2. While ethanol extracts produced from plant batch 4, with the lowest aspalathin content (11.6 and 8.7 g/100 g SS, respectively for the 80 and 60% ETOH extracts), were demonstrated to be the most active extracts with comparable glucose uptake effects to that of ARC 2. The unexpected discrepancy in bioactivity for extracts 8 and 4 confirms that aspalathin, the most abundant phenolic compound known to increase glucose uptake in skeletal muscle, was not the sole contributor to the observed effect. The role of other phenolic compounds, such as the inositol derivative, pinitol, known to have insulin-mimic activities or non-phenolic compounds within the polysaccharidic and lipidic fractions, may have additively or synergistically contributed to the overall bioefficacy of the 80% ethanol extracts. Muller *et al.*, 2012 showed an additive hypoglycaemic effect for aspalathin and rutin, administered in a 1:1 ratio to streptozotocin-induced diabetic rats. Thus, the ratio of the different bioactive phenolic compounds, not considered in this study, rather than the concentration of single bioactive constituents such as aspalathin, could be important considerations for further study.

### **5.3.2. Glucose uptake in C3A liver cells**

In the C3A cells, only extract 1 of the 80% ethanol extract significantly increased glucose uptake. Additionally, extracts 9 and 10 were significantly less effective than ARC 2 for both the 80 and 60% ethanol extracts. In contrast to the C2C12 cells, the aqueous extracts appeared to be more effective with extracts 1, 2, 4, 7 and 8 demonstrating significant increases in glucose uptake. These increases were comparable to the reference extracts ARC 2 and GRT. These findings are particularly interesting as the extracts from these plant batches had dissimilar aspalathin content. This supports the bioactive role of other compounds present in the aqueous extract, not identified by HPLC-DAD, which could have enhanced the glucose uptake either by additive or synergistic effects. C3A cells express typical liver characteristics with GLUT

2 being the predominant glucose transporter (Karim *et al.*, 2012; Zhao and Keating 2007). GLUT 2 is a low affinity high capacity bidirectional glucose transporter responsible for both glucose uptake and glucose release from the liver (Fehr *et al.*, 2005). In contrast to muscle, where insulin action induces rapid translocation of GLUT 4 and resultant glucose influx into the cell, in the liver, glucose uptake rate is proportional to blood glucose levels. Under high glucose conditions, insulin internalizes GLUT2, stops glucose release by inhibiting gluconeogenic enzymes and enhances the intracellular utilisation and storage of glucose downstream to glucokinase, which is responsible for the phosphorylation of glucose to glucose-6-phosphate, an essential step for glycolysis and glycogen synthesis (Guo *et al.*, 2012; Leturque *et al.*, 2009; Rui 2014).

### **5.3.3. Glucose uptake and lipid accumulation in 3T3-L1 adipocyte cells**

The three different types of GRE's increased glucose uptake in the 3T3-L1 adipocytes however, as was the case for the reference extracts ARC 2 and GRT, this effect was not significantly enhanced compared to insulin. The lack of significant glucose uptake results from the 3T3-L1 adipocytes could have been due to the design of this experiment. In contrast to the C2C12 and C3A cells, where glucose uptake was estimated by <sup>3</sup>H-2-deoxy-D-glucose uptake over a 15 minute period, the 3T3-L1 adipocyte glucose uptake was calculated from the remaining glucose left in the media after 4 hours culture. These methods thus give different answers as the <sup>3</sup>H-2-deoxy-D-glucose gave insight into glucose uptake rate rather than the total glucose uptake, as was the case for the 3T3-L1 cells. The motivation for conducting total glucose uptake, using a colourimetric method in the 3T3-L1 cells, was that the method allowed for the simultaneous quantification of lipid accumulation which was an additional metabolic parameter of the study. However, as the glucose uptake dynamics especially between treatments change over time, this method is inherently less sensitive which could have accounted for the tepid glucose uptake results. However, lipid accumulation results were more conclusive with the ethanolic extracts inducing a significant increase over the 4 hour period. This effect was comparable to that of insulin and ARC 2. The enhanced uptake of glucose and conversion to fat, under hyperglycaemic conditions, is regulated by insulin and plays an essential role in the maintenance of normoglycaemia. Under conditions of fast, the stored fat is released

back into the circulation as fatty acids and glycerol (Dimitriadis *et al.*, 2011). These effects are similar to that of thiazolidinediones or glitazones which are specifically effective in the treatment of insulin resistance. Glitazones act as agonists of peroxisome proliferator-activated receptor- $\gamma$  (PPAR- $\gamma$ ) nuclear receptors and increase triglyceride synthesis, thereby improving free fatty acid (FFA) metabolism in adipose tissues (Kendall 2006; Miyazaki *et al.*, 2001).

#### **5.4. PTP1B inhibition studies**

In literature it is known that compounds exhibiting strong inhibition against different enzymes have  $IC_{50}$  values below 10  $\mu$ M (Dierks *et al.*, 2001). A study conducted by Kong *et al.*, 2011 investigated the inhibitory effects of *M. speciosa* alkaloid extract (MSE) on human recombinant cytochrome P450, revealed potent inhibitory effects for this extract on CYP3A4 and CYP2D6. Inhibitory concentrations for these two enzymes were 0.78  $\mu$ g/mL and 0.636  $\mu$ g/mL, respectively. As demonstrated by Kong *et al.*, 2011, compounds with  $IC_{50}$  values  $\leq$  20  $\mu$ g/mL (or  $\leq$  10  $\mu$ M) were considered potent,  $IC_{50}$  values from 20 - 100  $\mu$ g/mL moderate and compounds with  $IC_{50}$  values  $\geq$  50  $\mu$ g/mL as weak. The same standards were applied to assess the inhibitory potential of the green rooibos extracts. In this study, green rooibos extracts were tested for their inhibitory potential on the enzyme PTP1B. Interestingly, all extracts displayed potent inhibitory effects on this enzyme with  $IC_{50}$  values below 20  $\mu$ g/mL. This suggests that the extracts could potentially have antidiabetic effects due to the suppression of PTP1B. Although it appeared that PTP1B inhibition was related to extracts with higher aspalathin concentration, the PCA analysis did not support such a relationship and in fact the loadings plot presented a negative relationship to the dihydrochalcones (aspalathin and nothofagin) and their flavone derivatives (isoorientin and orientin, isovitexin and vitexin). Luteolin-7-O-glucoside was demonstrated to weakly correlate with the inhibition of PTP1B (Figure 25 a). This finding however, is supported by a previous study that demonstrated the inhibitory effect of luteolin on PTP1B,  $IC_{50}$  of  $6.70 \pm 0.03$   $\mu$ M (Choi *et al.*, 2014).

#### **5.5. Molecular effects of selected GRE in C2C12 muscle cells**

The mechanism of glucose uptake by GRE on insulin signalling and AMPK activation, both shown to be effectors of GLUT 4 translocation, was not as effective as that

demonstrated by Kamakura *et al.*, 2015 and Mazibuko *et al.*, 2013. For this study, we could not demonstrate significant activity for either AMPK activation or AKT activation, neither was ACC nor MLYCD activity significantly affected after 4 hours of treatment with the selected GRE. This discrepancy could be related to the longer exposure time used in this study and the different cell lines used, compared to that of Kamakura *et al.* (2015). A study conducted by Mazibuko (2013) used C2C12 cells, however these cells were pre-treated with palmitate over a period of 16 hours to induce insulin resistance prior to treatment with GRE.

### **5.6. Multivariate statistical analysis**

In this study, despite large plant batch variation in phenolic composition, the PCA analysis showed that the 80% ethanol extracts clustered with both the reference (ARC 2) and the pharmaceutical extract (GRT). Aspalathin and the 3-deoxy-dihydrochalcone, nothofagin and their flavone derivatives (isoorientin and orientin, isovitexin and vitexin, respectively) clustered with C2C12 glucose uptake as well as the 3T3-L1 lipid accumulation (Figure 25 a). As demonstrated in Figure 25 b, the PCA scores plot distinguishes between bioactivity phenolic composition of the different extracts. The ethanol (80 and 60%) and aqueous GRE clustered apart from each other, with the two reference extracts, ARC 2 and GRT clustering with the 80% ethanol GRE. As mentioned previously, in contrast to glucose uptake and lipid accumulation, PTP1B was negatively associated with the dihydrochalcones and flavones. Interestingly, several compounds previously shown to have antidiabetic activity were not identified as major contributors to bioactivity by PCA analysis. These include the flavonol glycoside, rutin (quercetin-3-O-robinobioside) (Kappel *et al.*, 2013; Stanely Mainzen Prince and Kannan 2006), flavanones such as hesperidin (Mahmoud *et al.*, 2012) and phenyl pyruvic acid-2-O-b-glucoside (PPAG) (Muller *et al.*, 2013). These findings suggest that for these extracts, the complex chemical make-up does affect various metabolic and cell signalling targets, some of which are complimentary. As such, contribution of individual compounds to the potency of the extract may not be easily quantifiable.

## 5.7. Summary

In summary, this study revealed the underlying complexities between phenolic composition and biological function within complex mixtures of the assessed GRE. In general, the 80% ethanol extracts that contained higher phenolic content were more effective in enhancing glucose uptake, lipid accumulation and were more potent PTP1B inhibitors. However, within the different extract plant batches, the extracts with the highest aspalathin content did not necessarily perform the best, suggesting that the ratio of bioactive phenolic compounds, rather than the concentration of individual phenolic compounds, had a meaningful impact on overall bioactivity. The additive effect of different phenolic compounds was previously demonstrated by Muller *et al.*, 2012, in which the hypoglycaemic effect of aspalathin and rutin in a 1:1 m/m ratio was enhanced to a similar level demonstrated by the aspalathin-enriched reference extract ARC 2. Hence, in this study, identifying single chemical entities (API's) as surrogate markers for the prediction of bioactivity, in terms of these enriched-green rooibos extracts, has not been conclusively demonstrated. Phenolic composition in these extracts are highly complex and variable, requiring advanced mathematical modelling to relate chemical composition with bioactivity. The search for bioactive API's as surrogate markers is further complicated by the fact that we have only characterised the major phenolic compounds that account for ~ 26% of the extracts chemical make-up. The remaining 74% includes a magnitude of other chemical compounds, including other bioactive compounds such as pinitol that could be present in concentrations as high as 2-3% (Bates *et al.*, 2000; Davis *et al.*, 2000). Pinitol has been shown to increase glucose uptake in L6 muscle cells and improve glycaemia in streptozotocin diabetic mice (Bates *et al.*, 2000; Bailey 2007). Also included in the non-characterised portion of the extract could be compounds such as eriodictyol-glucoopyranosides (Zhang *et al.*, 2012), the breakdown products of aspalathin, which could still have significant bioactivity (Walters *et al.*, 2016). The role of other non-phenolic compounds, such as polysaccharides, on the bioactivity of the different extracts is unknown. However, based on our results, the more polar compounds present in the aqueous green rooibos extracts did not appear to enhance glucose uptake. In this study PCA analysis was able to correlate glucose uptake and lipid accumulation activity with the dihydrochalcones and their flavone derivatives. However, further statistical analysis will be required to take into account other variables, such as the ratio of specific chemical entities and relate this to their predicted bioactivity.

## 5.8. Conclusion

Plant selection and extract preparation greatly impact the bioactivity of green rooibos extracts and this is related to their chemical composition. *In vitro* assessment of glucose uptake, lipid accumulation and PTP1B enzyme inhibition showed that the 80% ethanol extract, with its higher phenolic content, was more effective at increasing glucose uptake, lipid accumulation and PTP1B inhibition. PCA analysis further demonstrated that glucose uptake activity in C2C12 cells and lipid accumulation in 3T3-L1 adipocytes, but not PTP1B, were associated with the dihydrochalcones, aspalathin and nothofagin and their flavone derivatives isoorientin and orientin, as well as isovitexin and vitexin, respectively. This finding therefore suggests that this group of related phenolic compounds could potentially act as surrogate markers for quality assurance and efficacy prediction of rooibos extracts. This study provides a proof of concept method which can be used to identify bioactive, chemical constituents from API's. These API's can be identified from complex mixtures as marker surrogates for standardising the quality and activity of extracts as nutraceuticals.

## 5.9. Limitations of this study

The complexity of unravelling the contribution of individual chemical entities within a group of compounds from the extracts used in this study presented a major challenge. Our approach was to test the respective extracts at the same concentration and apply advanced statistical analysis to identify markers or API's. Although this approach did provide positive results, further verification will still be needed. One approach that could strengthen our results would be to normalise the extracts concentrations to their phenolic content. Using a single concentration could have masked the contribution of minor compounds contributing to the observed bioactivity. Thus, by standardizing the extract concentration to the aspalathin content, more comparative results could have been achieved as differences observed could have been contributed to compounds other than aspalathin.

Western blot analysis of the selected effector proteins related to insulin signalling, AMPK activation and lipid metabolism did not realise the expected results. Based on previous studies using ARC 2 in C2C12 and L6 muscle cells, strong activation for AKT

and AMPK was demonstrated (Kamakura *et al.*, 2015; Mazibuko *et al.*, 2013). Reasons for the differences in the observed activation and expression of these effector proteins could be related to the longer exposure time (4 hours) of the cells to the extracts in this study, compared to 2 and 3 hours, respectively for Kamakura (2015) and Mazibuko (2013).

### **5.10. Future work**

The rooibos extracts produced by different extraction solvents from ten plant batches showed large variation, particularly for their phenolic composition. Although bioactivity correlated with the dihydrochalcones and their flavone derivatives, the contribution of single, chemical entities within this group could not be assessed. The addition of single compounds to this study would further substantiate their contribution to the observed bioactivity. The inhibitory effect of aspalathin and other major phenolic compounds could be useful in assessing the inhibition PTP1B at a cellular level. It would be of great interest to investigate the relative contribution to the observed bioactivity of these phenolic compounds as single compounds and in specific combinations. To further strengthen the findings, apart from using pure extracts, it would be interesting to fractionise the extracts and see to which extract fraction bioactivity can be attributed. This approach would dissect the extract into less complex and more manageable chemical mixtures.

Another approach would be to use specific inhibitors to suppress specific biological signalling pathways such as insulin signalling (PI3K inhibitor wortmannin), AMPK activation (compound C) and PTP1B (vanadate). By selective inhibition of the different effector mechanisms, more specific associations could be made by in terms of mechanism of action related to specific compounds.

## BIBLIOGRAPHY

- Abdi, H. and Williams, L.J., 2010. Principal component analysis. *Wiley Interdisciplinary Reviews: Computational Statistics*, 2(4), pp.433–459.
- Aden, D.P. *et al.*, 1979. Controlled synthesis of HBsAg in a differentiated human liver carcinoma-derived cell line. *Nature*, 282(5739), pp.615–616.
- Agbaire, P.O., 2011. Nutritional and anti-nutritional levels of some local vegetables (*Vernonia anydalira*, *Manihot esculenta*, *Teifera occidentalis*, *Talinum triangulare*, *Amaranthus spinosus*) from Delta State, Nigeria. *Journal of Applied Sciences and Environmental Management*, 15(4), pp.625–628.
- Ahmed, S. *et al.*, 2014. Effects of extreme climate events on tea (*Camellia sinensis*) functional quality validate indigenous farmer knowledge and sensory preferences in tropical China. *PLOS One*, 9(10), pp. e109126.
- Ajuwon, O.R. *et al.*, 2013. Protective Effects of Rooibos (*Aspalathus linearis*) and/or red palm oil (*Elaeis guineensis*) Supplementation on tert-butyl hydroperoxide-induced oxidative hepatotoxicity in Wistar rats. *Evidence-Based Complementary and Alternative Medicine*, pp.984273.
- Al-Arouj, M. *et al.*, 2010. Recommendations for management of diabetes during Ramadan. *Diabetes Care*, pp. 1895-1902.
- Ali, O., 2013. Genetics of type 2 diabetes. *World Journal of Diabetes*, 4(4), pp.114–123.
- Ambriz-Pérez, D.L. *et al.*, 2016. Phenolic compounds: Natural alternative in inflammation treatment. A Review. *Cogent Food and Agriculture*, 2(1), p.1131412.
- American Diabetes Association, 2014. Diagnosis and classification of diabetes mellitus. *Diabetes Care*, 37 (Supplement 1), pp. S81-90.
- American Diabetes Association. (2008). Diagnosis and Classification of Diabetes Mellitus. *Diabetes Care*, 31 (Supplement 1), pp. S62–S67.

- Anhê, F.F. *et al.*, 2013. Polyphenols and type 2 diabetes: A prospective review. *PharmaNutrition*, 1(4), pp.105–114.
- Apak, R. *et al.*, 2016. Antioxidant Activity/Capacity Measurement. 3. Reactive Oxygen and Nitrogen Species (ROS/RNS) Scavenging Assays, Oxidative Stress Biomarkers, and Chromatographic/Chemometric Assays. *Journal of Agricultural and Food Chemistry*, 64(5), pp.1046–1070.
- Ariga, M. *et al.*, 2008. Functional role of sortilin in myogenesis and development of insulin-responsive glucose transport system in C2C12 myocytes. *The Journal of Biological Chemistry*, 283(15), pp.10208–10220.
- Aryal, S., 2015. Glycolysis- 10 steps explained steps by steps with diagram. *Online Microbiology Notes*. Available at: <http://www.microbiologyinfo.com/glycolysis-10-steps-explained-steps-by-steps-with-diagram>. [Accessed December 03, 2016].
- Asante-Appiah, E. and Kennedy, B.P., 2003. Protein tyrosine phosphatases: the quest for negative regulators of insulin action. *American Journal of Physiology. Endocrinology and Metabolism*, 284(4), pp.E663-670.
- Astill, C. *et al.*, 2001. Factors Affecting the Caffeine and Polyphenol Contents of Black and Green Tea Infusions. *Journal of Agricultural and Food Chemistry*, 49(11), pp.5340–5347.
- Azevedo, M. and Alla, S., 2008. Diabetes in Sub-Saharan Africa: Kenya, Mali, Mozambique, Nigeria, South Africa and Zambia. *International Journal of Diabetes in Developing Countries*, 28(4), pp.101–108.
- Babu, P.V.A., Liu, D. and Gilbert, E.R., 2013. Recent advances in understanding the anti-diabetic actions of dietary flavonoids. *The Journal of Nutritional Biochemistry*, 24(11), pp.1777–1789.
- Bahadoran, Z., *et al.*, 2013. Dietary polyphenols as potential nutraceuticals in management of diabetes: a review. *Journal of Diabetes and Metabolic Disorders*, 12(1), pp.43.

- Bailey, C.J., 2007. Treating insulin resistance: future prospects. *Diabetes and Vascular Disease Research*, 4(1), pp.20–31.
- Balasaheb Nimse, S. and Pal, D., 2015. Free radicals, natural antioxidants, and their reaction mechanisms. *RSC Advances*, 5(35), pp.27986–28006.
- Barnes, J., 2003. Quality, efficacy and safety of complementary medicines: fashions, facts and the future. Part I. Regulation and quality. *British Journal of Clinical Pharmacology*, 55(3), pp.226–233.
- Baskin, D.G. *et al.*, 1999. Insulin and leptin: dual adiposity signals to the brain for the regulation of food intake and body weight. *Brain Research*, 848(1–2), pp.114–123.
- Bates, S.H. *et al.*, 2000. Insulin-like effect of pinitol. *British Journal of Pharmacology*, 130(8), pp.1944–1948.
- Baudoin, R. *et al.*, 2011. Behaviour of HepG2/C3A cell cultures in a microfluidic bioreactor. *Biochemical Engineering Journal*, 53(2), pp.172–181.
- Beelders, T. *et al.*, 2012. Comprehensive two-dimensional liquid chromatographic analysis of rooibos (*Aspalathus linearis*) phenolics. *Journal of Separation Science*, 35(14), pp.1808–1820.
- de Beer, D. *et al.*, 2015. Isolation of aspalathin and nothofagin from rooibos (*Aspalathus linearis*) using high-performance counter current chromatography: sample loading and compound stability considerations. *Journal of Chromatography. A*, 1381, pp.29–36.
- de Beer, D., Miller, N. and Joubert, E., 2016. Production of dihydrochalcone-rich green rooibos (*Aspalathus linearis*) extract taking into account seasonal and batch-to-batch variation in phenolic composition of plant material. *South African Journal of Botany*. Available at: <http://dx.doi.org/10.1016/j.sajb.2016.02.198>.
- Beltrán-Debón, R. *et al.*, 2011. Continuous administration of polyphenols from aqueous rooibos (*Aspalathus linearis*) extract ameliorates dietary-induced

metabolic disturbances in hyperlipidaemic mice. *Phytomedicine: International Journal of Phytotherapy and Phytopharmacology*, 18(5), pp.414–424.

Bennett, W.L. *et al.*, 2011. Comparative effectiveness and safety of medications for type 2 diabetes: an update including new drugs and 2-drug combinations. *Annals of Internal Medicine*, 154(9), pp.602–613.

Berg, J.M., *et al.*, 2002. The Citric Acid Cycle Oxidizes Two-Carbon Units. Available at: <https://www.ncbi.nlm.nih.gov/books/NBK22427/> [Accessed November 30, 2016].

Bitá, C.E. and Gerats, T., 2013. Plant tolerance to high temperature in a changing environment: scientific fundamentals and production of heat stress-tolerant crops. *Frontiers in Plant Science*, 4, pp.273.

Blau, H.M., *et al.*, 1983. Cytoplasmic activation of human nuclear genes in stable heterocaryons. *Cell*, 32(4), pp.1171–1180.

Bodmer, M. *et al.*, 2008. Metformin, sulfonylureas, or other antidiabetes drugs and the risk of lactic acidosis or hypoglycaemia: a nested case-control analysis. *Diabetes Care*, 31(11), pp.2086–2091.

Boundless, 2016 a. The Energy-Releasing Steps of Glycolysis. *Boundless*. Available at: </biology/textbooks/boundless-biology-textbook/cellular-respiration-7/glycolysis-74/the-energy-releasing-steps-of-glycolysis-357-11583/> [Accessed November 30, 2016].

Boundless, 2016 b. The role of energy and metabolism. *Boundless*. Available at: </biology/textbooks/boundless-biology-textbook/metabolism-6/energy-and-metabolism-68/the-role-of-energy-and-metabolism-341-11478/> [Accessed December 3, 2016].

Bravo, L., 1998. Polyphenols: chemistry, dietary sources, metabolism, and nutritional significance. *Nutrition Reviews*, 56(11), pp.317–333.

- Breiter, T. *et al.*, 2011. Bioavailability and antioxidant potential of rooibos flavonoids in humans following the consumption of different rooibos formulations. *Food Chemistry*, 128(2), pp.338–347.
- Brin, M.F., *et al.*, 2014. Botulinum toxin type A products are not interchangeable: a review of the evidence. *Biologics: Targets and Therapy*, 8, pp.227–241.
- Browne, S.M. and Al-Rubeai, M., 2011. Defining viability in mammalian cell cultures. *Biotechnology Letters*, 33(9), pp.1745–1749.
- Brownlee, M., 2001. Biochemistry and molecular cell biology of diabetic complications. *Nature*, 414(6865), pp.813–820.
- Bryant, N.J., *et al.*, 2002. Regulated transport of the glucose transporter GLUT4. *Nature Reviews. Molecular Cell Biology*, 3(4), pp.267–277.
- Burattini, S. *et al.*, 2004. C2C12 murine myoblasts as a model of skeletal muscle development: morpho-functional characterization. *European journal of histochemistry: EJH*, 48(3), pp.223–233.
- Burks, D.J. and White, M.F., 2001. IRS proteins and  $\beta$ -cell function. *Diabetes*, 50(Supplement 1), pp.S140.
- Campbell, W.W. *et al.*, 2004. Pinitol Supplementation Does Not Affect Insulin-Mediated Glucose Metabolism and Muscle Insulin Receptor Content and Phosphorylation in Older Humans. *The Journal of Nutrition*, 134(11), pp.2998–3003.
- Canda, B.D., Oguntibeju, O.O. and Marnewick, J.L., 2014. Effects of consumption of rooibos (*Aspalathus linearis*) and a rooibos-derived commercial supplement on hepatic tissue injury by tert-butyl hydroperoxide in Wistar rats. *Oxidative Medicine and Cellular Longevity*, 2014, pp.716832.
- Cardona, F. *et al.*, 2013. Benefits of polyphenols on gut microbiota and implications in human health. *The Journal of Nutritional Biochemistry*, 24(8), pp.1415–1422.

- Carruthers, A. *et al.*, 2009. Will the original glucose transporter isoform please stand up! *American Journal of Physiology. Endocrinology and Metabolism*, 297(4), pp.E836-848.
- Chang, L., *et al.*, 2004. Insulin Signalling and the Regulation of Glucose Transport. *Molecular Medicine*, 10(7–12), pp.65–71.
- Chen, W. *et al.*, 2013. Ameliorative effect of aspalathin from rooibos (*Aspalathus linearis*) on acute oxidative stress in *Caenorhabditis elegans*. *Phytomedicine: International Journal of Phytotherapy and Phytopharmacology*, 20(3–4), pp.380–386.
- Cheng, J.-F. *et al.*, 2006. Synthesis and Structure - Activity relationship of small-molecule malonyl Coenzyme A decarboxylase inhibitors. *Journal of Medicinal Chemistry*, 49(5), pp.1517–1525.
- Choi, J.S. *et al.*, 2014. The effects of C-glycosylation of luteolin on its antioxidant, anti-Alzheimer's disease, anti-diabetic, and anti-inflammatory activities. *Archives of Pharmacal Research*, 37(10), pp.1354–1363.
- Cohen, P., 1999. The Croonian Lecture 1998. Identification of a protein kinase cascade of major importance in insulin signal transduction. *Philosophical Transactions of the Royal Society of London. Series B, Biological Sciences*, 354(1382), pp.485–495.
- Conejo, R. and Lorenzo, M., 2001. Insulin signalling leading to proliferation, survival, and membrane ruffling in C2C12 myoblasts. *Journal of Cellular Physiology*, 187(1), pp.96–108.
- Cook, W.S. and Unger, R.H., 2002. Protein tyrosine phosphatase 1B: a potential leptin resistance factor of obesity. *Developmental Cell*, 2(4), pp.385–387.
- Cooper, R.N. *et al.*, 1999. *In vivo* satellite cell activation via Myf5 and MyoD in regenerating mouse skeletal muscle. *Journal of Cell Science*, 112 (Pt 17), pp.2895–2901.

- Croteau, R., Kutchan, T.M. and Lewis, N.G., 2000. Natural Products Natural products (secondary metabolites). *Biochemistry and molecular biology of plants*, 24, pp.1250-1319.
- Daneman, D., 2006. Type 1 diabetes. *The Lancet*, 367(9513), pp.847–858.
- Das, L. *et al.*, 2012. Role of nutraceuticals in human health. *Journal of Food Science and Technology*, 49(2), pp.173–183.
- Davis, A. *et al.*, 2000. Effect of pinitol treatment on insulin action in subjects with insulin resistance. *Diabetes Care*, 23(7), pp.1000–1005.
- DeFronzo, R.A., 2004. Pathogenesis of type 2 diabetes mellitus. *The Medical Clinics of North America*, 88(4), pp.787–835, ix.
- DeFronzo, R.A. and Tripathy, D., 2009. Skeletal Muscle Insulin Resistance Is the Primary Defect in Type 2 Diabetes. *Diabetes Care*, 32(Supplement 2), pp.S157–S163.
- Del Rio, D. *et al.*, 2013. Dietary (poly)phenolics in human health: structures, bioavailability, and evidence of protective effects against chronic diseases. *Antioxidants and Redox Signalling*, 18(14), pp.1818–1892.
- Dierks, E.A. *et al.*, 2001. A method for the simultaneous evaluation of the activities of seven major human drug-metabolizing cytochrome P450s using an *in vitro* cocktail of probe substrates and fast gradient liquid chromatography tandem mass spectrometry. *Drug Metabolism and Disposition: The Biological Fate of Chemicals*, 29(1), pp.23–29.
- Dimitriadis, G. *et al.*, 2011. Insulin effects in muscle and adipose tissue. *Diabetes Research and Clinical Practice*, 93 (Supplement 1), pp.S52-59.
- Do, M.T. *et al.*, 2013. Phillyrin attenuates high glucose-induced lipid accumulation in human HepG2 hepatocytes through the activation of LKB1/AMP-activated protein kinase-dependent signalling. *Food Chemistry*, 136(2), pp.415–425.

- Dyck, J.R. *et al.*, 1998. Characterization of cardiac malonyl-CoA decarboxylase and its putative role in regulating fatty acid oxidation. *The American Journal of Physiology*, 275(6 Pt 2), pp.H2122-2129.
- El-Abhar, H.S. and Schaalan, M.F., 2014. Phytotherapy in diabetes: Review on potential mechanistic perspectives. *World Journal of Diabetes*, 5(2), pp.176–197.
- Erickson, 2003. Rooibos Tea: Research into Antioxidant and Antimutagenic Properties. *The Journal of the American Botanical Council*, (59), pp.34–45.
- Etcheverry, P. *et al.*, 2012. Application of *in vitro* bioaccessibility and bioavailability methods for calcium, carotenoids, folate, iron, magnesium, polyphenols, zinc, and vitamins B6, B12, D, and E. *Frontiers in Physiology*, 3. Available at: <http://www.ncbi.nlm.nih.gov/pmc/articles/PMC3429087/> [Accessed November 27, 2016].
- Eyre, H. *et al.*, 2004. Preventing cancer, cardiovascular disease, and diabetes: a common agenda for the American Cancer Society, the American Diabetes Association, and the American Heart Association. *Stroke*, 35(8), pp.1999–2010.
- Fehr, M. *et al.*, 2005. Evidence for high-capacity bidirectional glucose transport across the endoplasmic reticulum membrane by genetically encoded fluorescence resonance energy transfer nanosensors. *Molecular and Cellular Biology*, 25(24), pp.11102-11112.
- Ferrándiz, M.L. and Alcaraz, M.J., 1991. Anti-inflammatory activity and inhibition of arachidonic acid metabolism by flavonoids. *Agents and Actions*, 32(3–4), pp.283–288.
- Filippi, C. *et al.*, 2004. Improvement of C3A cell metabolism for usage in bioartificial liver support systems. *Journal of Hepatology*, 41(4), pp.599–605.
- von Gadow, A., Joubert, E. and Hansmann, C.F., 1997. Comparison of the antioxidant activity of aspalathin with that of other plant phenols of rooibos tea (*Aspalathus*

- linearis*),  $\alpha$ -tocopherol, BHT, and BHA. *Journal of Agricultural and Food Chemistry*, 45(3), pp.632–638.
- Ghanbari, R. *et al.*, 2012. Valuable nutrients and functional bioactives in different parts of olive (*Olea europaea L.*)—A Review. *International Journal of Molecular Sciences*, 13(3), pp.3291–3340.
- Gill, G.V. *et al.*, 2009. A sub-Saharan African perspective of diabetes. *Diabetologia*, 52 (1), pp.8-16.
- Giri, L., *et al.*, 2004. A steady state analysis indicates that negative feedback regulation of PTP1B by Akt elicits bistability in insulin-stimulated GLUT4 translocation. *Theoretical Biology and Medical Modelling*, 1(2), pp.1-16.
- Goldstein, B.J., 2001. Protein-tyrosine phosphatase 1B (PTP1B): a novel therapeutic target for type 2 diabetes mellitus, obesity and related states of insulin resistance. *Current Drug Targets. Immune, Endocrine and Metabolic Disorders*, 1(3), pp.265–275.
- Gorovits, N. and Charron, M.J., 2003. What we know about facilitative glucose transporters: Lessons from cultured cells, animal models, and human studies. *Biochemistry and Molecular Biology Education*, 31(3), pp.163–172.
- Green, H. and Kehinde, O., 1974. Sublines of mouse 3T3 cells that accumulate lipid. *Cell*, pp.1-4.
- Gruzman, A. *et al.*, 2009. Adenosine monophosphate-activated protein kinase (AMPK) as a new target for antidiabetic drugs: A Review on Metabolic, Pharmacological and Chemical Considerations. *The review of diabetic studies*, 6(1), pp.13–36.
- Guilherme, A. *et al.*, 2008. Adipocyte dysfunctions linking obesity to insulin resistance and type 2 diabetes. *Nature reviews. Molecular cell biology*, 9(5), pp.367–377.
- Guo, X. *et al.*, 2012. Glycolysis in the control of blood glucose homeostasis. *Acta Pharmaceutica Sinica B*, 2(4), pp.358–367.
- Gwinn, D.M. *et al.*, 2008. AMPK phosphorylation of raptor mediates a metabolic checkpoint. *Molecular Cell*, 30(2), pp.214–226.

- Han, X., Shen, T. and Lou, H., 2007. Dietary polyphenols and their biological significance. *International Journal of Molecular Sciences*, 8(9), pp.950-988.
- Harada, N. *et al.*, 2016. Mogrol Derived from *Siraitia grosvenorii* mogrosides suppresses 3T3-L1 adipocyte differentiation by reducing cAMP-response element-binding protein phosphorylation and increasing AMP-activated protein kinase phosphorylation. *PLOS One*, 11(9), pp. 1-13.
- Hardie, D.G. *et al.*, 2012. AMPK: a nutrient and energy sensor that maintains energy homeostasis. *Nature Reviews. Molecular Cell Biology*, 13(4), pp.251–262.
- Hardie, D.G., Schaffer, B.E. and Brunet, A., 2016. AMPK: An Energy-Sensing Pathway with Multiple Inputs and Outputs. *Trends in Cell Biology*, 26(3), pp.190–201.
- Hasani-Ranjbar, S. *et al.*, 2010. The efficacy and safety of herbal medicines used in the treatment of hyperlipidaemia; a systematic review. *Current Pharmaceutical Design*, 16(26), pp.2935–2947.
- Havel, P.J., 2000. Role of adipose tissue in body-weight regulation: mechanisms regulating leptin production and energy balance. *The Proceedings of the Nutrition Society*, 59(3), pp.359–371.
- Hawley, S.A. *et al.*, 2010. Use of cells expressing gamma subunit variants to identify diverse mechanisms of AMPK activation. *Cell Metabolism*, 11(6), pp.554–565.
- He, X.X. *et al.*, 2011. Thiazolidinediones and metformin associated with improved survival of diabetic prostate cancer patients. *Annals of Oncology: Official Journal of the European Society for Medical Oncology*, 22(12), pp.2640–2645.
- Heilig, C. *et al.*, 2003. Implications of Glucose Transporter Protein Type 1 (GLUT1)-Haplodeficiency in Embryonic Stem Cells for Their Survival in Response to Hypoxic Stress. *The American Journal of Pathology*, 163(5), pp.1873–1885.
- Hemmingsen, B. *et al.*, 2012. Comparison of metformin and insulin versus insulin alone for type 2 diabetes: systematic review of randomised clinical trials with meta-analyses and trial sequential analyses. *BMJ (Clinical research ed.)*, 344, p. e1771.

- Herman, M.A. and Kahn, B.B., 2006. Glucose transport and sensing in the maintenance of glucose homeostasis and metabolic harmony. *The Journal of Clinical Investigation*, 116(7), pp.1767–1775.
- Hers, I., *et al.*, 2011. Akt signalling in health and disease. *Cellular Signalling*, 23(10), pp.1515–1527.
- Hill, J. and Olson, E., 2012. *Muscle 2-Volume Set: Fundamental Biology and Mechanisms of Disease*, Academic Press.
- Hong, I.S., *et al.*, 2014. Anti-Oxidative Effects of Rooibos Tea (*Aspalathus linearis*) on Immobilization-Induced Oxidative Stress in Rat Brain. *PLOS ONE*, 9(1). Available at: <http://www.ncbi.nlm.nih.gov/pmc/articles/PMC3897768/> [Accessed December 1, 2016].
- Hotelling, H., 1933. Analysis of a Complex of Statistical Variables into Principal Components. *Journal of Educational Psychology*, 24(6 and 7), pp.417–441 and 498–520.
- Huang, S. and Czech, M.P., 2007. The GLUT4 glucose transporter. *Cell Metabolism*, 5(4), pp.237–252.
- Hurt, R.T. *et al.*, 2010. The obesity epidemic: challenges, health initiatives, and implications for gastroenterologists. *Gastroenterology and Hepatology*, 6(12), pp.780–792.
- Hussain, M.S. *et al.*, 2012. Current approaches toward production of secondary plant metabolites. *Journal of Pharmacy and Bioallied Sciences*, 4(1), pp.10–20.
- International Diabetes Federation. IDF Diabetes Atlas 7<sup>th</sup> edition, 2015. Brussels, Belgium. <http://www.idf.org/sites/default/files/Atlas7e-poster.pdf>
- Inzucchi, S.E. *et al.*, 2015. Management of hyperglycemia in type 2 diabetes, 2015: a patient-centered approach: update to a position statement of the American Diabetes Association and the European Association for the Study of Diabetes. *Diabetes Care*, 38(1), pp.140–149.

- Iyer, V.V. *et al.*, 2010. Effects of glucose and insulin on HepG2-C3A cell metabolism. *Biotechnology and Bioengineering*, 107(2), pp.347–356.
- Jassey, V.E.J. *et al.*, 2011. Experimental climate effect on seasonal variability of polyphenol/phenoloxidase interplay along a narrow fen–bog ecological gradient in *Sphagnum fallax*. *Global Change Biology*, 17(9), pp.2945–2957.
- Jensen, J. *et al.*, 2011. The Role of skeletal muscle glycogen breakdown for regulation of insulin sensitivity by exercise. *Frontiers in Physiology*, 2. Available at: <http://www.ncbi.nlm.nih.gov/pmc/articles/PMC3248697/> [Accessed November 25, 2016].
- Jia, L. and Liu, X., 2007. The conduct of drug metabolism studies considered good practice (II): *in vitro* experiments. *Current Drug Metabolism*, 8(8), pp.822–829.
- Johnson, T.O. *et al.*, 2002. Protein tyrosine phosphatase1B inhibitors for diabetes. *Nature Reviews. Drug Discovery*, 1, pp.696-709.
- Johnson, R. *et al.*, 2016. Aspalathin, a dihydrochalcone C-glucoside, protects H9c2 cardiomyocytes against high glucose induced shifts in substrate preference and apoptosis. *Molecular Nutrition and Food Research*, 60(4), pp.922–934.
- Jolliffe, I.T., 2002. Principal Component Analysis. In Aberdeen, UK: Springer Series in Statistics. Available at: [http://cda.psych.uiuc.edu/statistical\\_learning\\_course/Jolliffe%20I.%20Principal%20Component%20Analysis%20\(2ed.,%20Springer,%202002\)\(518s\)\\_MVsa\\_.pdf](http://cda.psych.uiuc.edu/statistical_learning_course/Jolliffe%20I.%20Principal%20Component%20Analysis%20(2ed.,%20Springer,%202002)(518s)_MVsa_.pdf).
- Joly, E. *et al.*, 2005. Malonyl-CoA decarboxylase is present in the cytosolic, mitochondrial and peroxisomal compartments of rat hepatocytes. *FEBS Letters*, 579(29), pp.6581–6586.
- Jørgensen, S.B. *et al.*, 2004. Knockout of the  $\alpha 2$  but not  $\alpha 1$  5'-AMP-activated protein kinase isoform abolishes 5-aminoimidazole-4-carboxamide-1- $\beta$ -D-ribofuranoside but not contraction-induced glucose uptake in skeletal muscle. *The Journal of Biological Chemistry*, 279(2), pp.1070–1079.

- Joubert, E., 1996. HPLC quantification of the dihydrochalcones, aspalathin and nothofagin in rooibos tea (*Aspalathus linearis*) as affected by processing. *Food Chemistry*, 55(4), pp.403–411.
- Joubert, E. *et al.*, 2008. South African herbal teas: *Aspalathus linearis*, *Cyclopia* spp. and *Athrixia phylicoides*--a review. *Journal of Ethnopharmacology*, 119(3), pp.376–412.
- Joubert, E. *et al.*, 2012. Variation in phenolic content and antioxidant activity of fermented rooibos herbal tea infusions: role of production season and quality grade. *Journal of Agricultural and Food Chemistry*, 60(36), pp.9171–9179.
- Joubert, E. and de Beer, D., 2011. Rooibos (*Aspalathus linearis*) beyond the farm gate: From herbal tea to potential phytopharmaceutical. *South African Journal of Botany*, 77(4), pp.869–886.
- Kamakura, R. *et al.*, 2015. Antidiabetic effect of green rooibos (*Aspalathus linearis*) extract in cultured cells and type 2 diabetic model KK-A(y) mice. *Cytotechnology*, 67(4), pp.699–710.
- Kang, C. *et al.*, 2015. Steroidal alkaloids from *Veratrum nigrum* enhance glucose uptake in skeletal muscle cells. *Journal of Natural Products*, 78(4), pp.803–810.
- Kanherkar, R.R. *et al.*, 2014. Epigenetics across the human lifespan. *Frontiers in Cell and Developmental Biology*, 2. Available at: <http://journal.frontiersin.org/article/10.3389/fcell.2014.00049/abstract> [Accessed November 23, 2016].
- Kappel, V.D. *et al.*, 2013. Involvement of GLUT-4 in the stimulatory effect of rutin on glucose uptake in rat soleus muscle. *The Journal of Pharmacy and Pharmacology*, 65(8), pp.1179–1186.
- Karim, S., *et al.*, 2012. Hepatic expression and cellular distribution of the glucose transporter family. *World Journal of Gastroenterology: WJG*, 18(46), pp.6771–6781.

- Kasuga, M., 2006. Insulin resistance and pancreatic  $\beta$  cell failure. *Journal of Clinical Investigation*, 116(7), pp. 1756–1760.
- Kawano, A. *et al.*, 2009. Hypoglycemic effect of aspalathin, a rooibos tea component from *Aspalathus linearis*, in type 2 diabetic model db/db mice. *Phytomedicine: International Journal of Phytotherapy and Phytopharmacology*, 16(5), pp.437–443.
- Kahn, S.E. *et al.*, 2006. Mechanisms linking obesity to insulin resistance and type 2 diabetes. *Nature*, 444(7121), pp.840-846.
- Kelly, J.H., 1994. Permanent human hepatocyte cell line and its use in use in a liver assist device (LAD). United states patent 5,290,684.
- Kelly, J.H. and Darlington, G.J., 1989. Modulation of the liver specific phenotype in the human hepatoblastoma line Hep G2. *In vitro Cellular and Developmental Biology: Journal of the Tissue Culture Association*, 25(2), pp.217–222.
- Kendall, D.M., 2006. Thiazolidinediones. *Diabetes Care*, 29(1), pp.154–157.
- Kennedy, D.O. and Wightman, E.L., 2011. Herbal extracts and phytochemicals: plant secondary metabolites and the enhancement of human brain function. *Advances in Nutrition (Bethesda, Md.)*, 2(1), pp.32–50.
- Kong, W.M. *et al.*, 2011. Evaluation of the effects of *Mitragyna speciosa* alkaloid extract on cytochrome P450 enzymes using a high throughput assay. *Molecules (Basel, Switzerland)*, 16(9), pp.7344–7356.
- Korkina, L.G., 2007. Phenylpropanoids as naturally occurring antioxidants: from plant defense to human health. *Cellular and Molecular Biology (Noisy-Le-Grand, France)*, 53(1), pp.15–25.
- Kreuz, S. *et al.*, 2008. Aspalathin, a flavonoid in *Aspalathus linearis* (rooibos), is absorbed by pig intestine as a C-glycoside. *Nutrition Research (New York, N.Y.)*, 28(10), pp.690–701.
- Kunle, O.F. *et al.*, 2012. Standardization of herbal medicines - A review. *International Journal of Biodiversity and Conservation*, 4(3), pp.101–112.

- Lauritzen, H.P.M.M., 2013. Insulin- and contraction-induced glucose transporter 4 traffic in muscle: insights from a novel imaging approach. *Exercise and Sport Sciences Reviews*, 41(2), pp.77–86.
- Leclercq, I.A. *et al.*, 2007. Insulin resistance in hepatocytes and sinusoidal liver cells: mechanisms and consequences. *Journal of Hepatology*, 47(1), pp.142–156.
- Lee, J. *et al.*, 2014. Insulin Receptor Activation with Transmembrane Domain Ligands. *The Journal of Biological Chemistry*, 289(28), pp.19769–19777.
- Lee, L.T. *et al.*, 2002. Blockade of the epidermal growth factor receptor tyrosine kinase activity by quercetin and luteolin leads to growth inhibition and apoptosis of pancreatic tumour cells. *Anticancer Research*, 22(3), pp.1615–1627.
- Leturque, A., Brot-Laroche, E. and Le Gall, M., 2009. GLUT2 mutations, translocation, and receptor function in diet sugar managing. *American Journal of Physiology. Endocrinology and Metabolism*, 296(5), pp.E985-992.
- Levitt, N.S., 2008. Diabetes in Africa: epidemiology, management and healthcare challenges. *Heart (British Cardiac Society)*, 94(11), pp.1376–1382.
- Li, S. *et al.*, 2008. Chemical markers for the quality control of herbal medicines: an overview. *Chinese Medicine*, 3, pp.7.
- Li, N. *et al.*, 2015. Two new diphenyl ethers from *Acanthopanax senticosus* (Rupr. and Maxim.) Harms with PTP1B inhibitory activity. *Phytochemistry Letters* 13: pp.286-289.
- Lin, Y. *et al.*, 2008. Luteolin, a flavonoid with potential for cancer prevention and therapy. *Current Cancer Drug Targets*, 8(7), pp.634–646.
- Lodish, H. *et al.*, 2000. Oxidation of Glucose and Fatty Acids to CO<sub>2</sub>. Available at: <https://www.ncbi.nlm.nih.gov/books/NBK21624/> [Accessed November 25, 2016].
- Luna, B. and Feinglos, M.N., 2001. Oral agents in the management of type 2 diabetes mellitus. *American Family Physician*, 63(9), pp.1747–1756.

- Lv, M. et al., 2015. Plant metabolomics driven chemical and biological comparison of the root bark of *Dictamnus dasycarpus* and *Dictamnus angustifolius*. *Royal Society of Chemical Advances*, 5(10), pp.15700-15708.
- MacDougald, O.A. and Lane, M.D., 1995. Transcriptional regulation of gene expression during adipocyte differentiation. *Annual Review of Biochemistry*, 64, pp.345–373.
- Mahmoud, A.M. et al., 2012. Hesperidin and naringin attenuate hyperglycemia-mediated oxidative stress and pro-inflammatory cytokine production in high fat fed/streptozotocin-induced type 2 diabetic rats. *Journal of Diabetes and Its Complications*, 26(6), pp.483–490.
- Manach, C. et al., 2004. Polyphenols: food sources and bioavailability. *The American Journal of Clinical Nutrition*, 79(5), pp.727–747.
- Martin, K.R. and Appel, C.L., 2010. Polyphenols as dietary supplements: A double-edged sword. Available at: <https://www.scienceopen.com/document?vid=ede47a40-5a0e-47c5-bf4e-1d72a5fd30fe> [Accessed November 27, 2016].
- Maruyama, I.N., 2014. Mechanisms of Activation of Receptor Tyrosine Kinases: Monomers or Dimers. *Cells*, 3(2), pp.304–330.
- Massimo D'Archivio et al., 2007. Polyphenols, dietary sources and bioavailability. *Annali dell'Istituto Superiore di Sanità*, 43(4), pp.348–361.
- Mavri-Damelin, D. et al., 2008. Cells for bioartificial liver devices: the human hepatoma-derived cell line C3A produces urea but does not detoxify ammonia. *Biotechnology and Bioengineering*, 99(3), pp.644–651.
- Mazibuko, S.E. et al., 2013. Amelioration of palmitate-induced insulin resistance in C2C12 muscle cells by rooibos (*Aspalathus linearis*). *Phytomedicine: International Journal of Phytotherapy and Phytopharmacology*, 20(10), pp.813–819.

- Mazibuko, S.E 2014. *In vitro* and *in vivo* effect of *Aspalathus linearis* and its major polyphenols on carbohydrate and lipid metabolism in insulin resistant models. Kwa-Dlangezwa, Kwa-Zulu Natal, South Africa: University of Zululand.
- Mazibuko, S.E. *et al.*, 2015. Aspalathin improves glucose and lipid metabolism in 3T3-L1 adipocytes exposed to palmitate. *Molecular Nutrition and Food Research*, 59(11), pp.2199–2208.
- Mergenthaler, P. *et al.*, 2013. Sugar for the brain: the role of glucose in physiological and pathological brain function. *Trends in neurosciences*, 36(10), pp.587-597.
- Miwa, I. *et al.*, 1972. Mutarotase effect on colorimetric determination of blood glucose with -D-glucose oxidase. *Clinica Chimica Acta; International Journal of Clinical Chemistry* 37, pp.538-540.
- Miyazaki, Y. *et al.*, 2001. Improved glycaemic control and enhanced insulin sensitivity in type 2 diabetic subjects treated with pioglitazone. *Diabetes Care*, 24(4), pp.710–719.
- Morton, J.F., 1983. Rooibos Tea, *Aspalathus linearis*, a Caffeineless, Low-Tannin Beverage. *Economic Botany*, 37(2), pp.164–173.
- Mouria, M. *et al.*, 2002. Food-derived polyphenols inhibit pancreatic cancer growth through mitochondrial cytochrome C release and apoptosis. *International Journal of Cancer*, 98(5), pp.761–769.
- Mueckler, M. *et al.*, 1985. Sequence and structure of a human glucose transporter. *Science (New York)*, 229(4717), pp.941–945.
- Mueckler, M. and Thorens, B., 2013. The SLC2 (GLUT) family of membrane transporters. *Molecular Aspects of Medicine*, 34(2–3), pp.121–138.
- Muller, C.J.F. *et al.*, 2012. Acute assessment of an aspalathin-enriched green rooibos (*Aspalathus linearis*) extract with hypoglycemic potential. *Phytomedicine: International Journal of Phytotherapy and Phytopharmacology*, 20(1), pp.32–39.

- Muller, C.J.F. *et al.*, 2016. Potential of rooibos, its major c-glucosyl flavonoids and z-2-( $\beta$ -d-glucopyranoloxo)-3-phenylpropenoic acid in prevention of metabolic syndrome. *Critical Reviews in Food Science and Nutrition*, (just accepted) pp.00-00.
- Muller, C.J.F. *et al.*, 2013. Z-2-( $\beta$ -D-glucopyranosyloxy)-3-phenylpropenoic acid, an  $\alpha$ -hydroxy acid from rooibos (*Aspalathus linearis*) with hypoglycemic activity. *Molecular Nutrition and Food Research*, 57(12), pp.2216–2222.
- National Diabetes Data Group., 1979. National Institute of Health Bethesda, Maryland. *Diabetes*, 28, pp.1039-1057. <http://dx.doi.org/10.2337/diab.28.12.1039>
- Nedachi, T. and Kanzaki, M., 2006. Regulation of glucose transporters by insulin and extracellular glucose in C2C12 myotubes. *American Journal of Physiology. Endocrinology and Metabolism*, 291(4), pp.E817-828.
- Oh, Y.S. and Jun, H.S., 2014. Role of bioactive food components in diabetes prevention: effects on  $\beta$ -cell function and preservation. *Nutrition and Metabolic Insights*, 7, pp.51–59.
- Oliveira, L. *et al.*, 2014. Health promoting and sensory properties of phenolic compounds in food. *Revista Ceres*, 61, pp.764–779.
- Olson, A.L., 2012. Regulation of GLUT4 and Insulin-Dependent Glucose Flux. *International Scholarly Research Notices*, 2012, pp. e856987.
- Pandey, K.B. and Rizvi, S.I., 2009. Plant polyphenols as dietary antioxidants in human health and disease. *Oxidative Medicine and Cellular Longevity*, 2(5), pp.270–278.
- Patel, O. *et al.*, 2016. Inhibitory Interactions of *Aspalathus linearis* (Rooibos) Extracts and Compounds, Aspalathin and Z-2-( $\beta$ -d-Glucopyranosyloxy)-3-phenylpropenoic Acid, on Cytochromes Metabolizing Hypoglycemic and Hypolipidemic Drugs. *Molecules (Basel, Switzerland)*, 21(11), pp.1515.
- Pietrocola, F. *et al.*, 2015. Acetyl Coenzyme A: A central metabolite and second messenger. *Cell Metabolism*, 21(6), pp.805–821.

- Plant, N., 2004. Strategies for using *in vitro* screens in drug metabolism. *Drug Discovery Today*, 9(7), pp.328–336.
- Poian, A.T.D. and Castanho, M., 2015. *Integrative Human Biochemistry: A Textbook for Medical Biochemistry*, Springer New York.
- Preethi MP *et al.*, 2014. Principal component analysis and HPTLC fingerprint of *in vitro* and field grown root extracts of *Withania coagulans*. 6(5), pp.480–488.
- Qiu, J. *et al.*, 2014. Stimulation of glucose uptake by theasinensins through the AMP-activated protein kinase pathway in rat skeletal muscle cells. *Biochemical Pharmacology*, 87(2), pp.344–351.
- Ramakrishna, A. and Ravishankar, G.A., 2011. Influence of abiotic stress signals on secondary metabolites in plants. *Plant Signaling and Behaviour*, 6(11), pp.1720–1731.
- Reed, B.C. *et al.*, 1977. Alterations in insulin binding accompanying differentiation of 3T3-L1 preadipocytes. *Proceedings of the National Academy of Sciences of the United States of America*, 74(11), pp.4876–4880.
- Rein, M.J. *et al.*, 2013. Bioavailability of bioactive food compounds: a challenging journey to bioefficacy. *British Journal of Clinical Pharmacology*, 75(3), pp.588–602.
- Richter, E.A., *et al.*, 2001. Glucose, exercise and insulin: emerging concepts. *The Journal of Physiology*, 535(Pt 2), pp.313–322.
- Riss, T.L. *et al.*, 2004. Cell Viability Assays. *Assay Guidance Manual*. Bethesda (MD): Eli Lilly and Company and the National Center for Advancing Translational Sciences. Available at: <http://www.ncbi.nlm.nih.gov/books/NBK144065/> [Accessed November 25, 2016].
- Roberts, C.K. *et al.*, 2013. Metabolic syndrome and insulin resistance: underlying causes and modification by exercise training. *Comprehensive Physiology*, 3(1), pp.1–58.

- Rodney Croteau, Toni M. Kutchan and Norman G. Lewis, 2000. Natural Products (Secondary Metabolites). In *Biochemistry and Molecular Biology of Plants*. pp. 1250–1318. Available at: <http://www.science.lecture.ub.ac.id/files/2012/04/plant-biosynthesis1.pdf>.
- Rodriguez, S. *et al.*, 2014. Chemical-genetic induction of Malonyl-CoA decarboxylase in skeletal muscle. *BMC Biochemistry*, 15(20), pp.1-14.
- Ronnett, G.V. *et al.*, 2006. Fatty Acid Metabolism, the Central Nervous System, and Feeding. *Obesity*, 14(S8), pp.201S–207S.
- Rui, L., 2014. Energy Metabolism in the Liver. *Comprehensive Physiology*, 4(1), pp.177–197.
- Sahoo, N. and Manchikanti, P., 2013. Herbal drug regulation and commercialization: an Indian industry perspective. *Journal of Alternative and Complementary Medicine (New York, N.Y.)*, 19(12), pp.957–963.
- Saltiel, A.R. and Kahn, C.R., 2001. Insulin signalling and the regulation of glucose and lipid metabolism. *Nature*, 414(6865), pp.799–806.
- Santangelo, C. *et al.*, 2007. Polyphenols, intracellular signalling and inflammation. *Annali dell'Istituto Superiore Di Sanità*, 43(4), pp.394–405.
- Schulze, M.B. and Hu, F.B., 2005. Primary prevention of diabetes: what can be done and how much can be prevented? *Annual Review of Public Health*, 26, pp.445–467.
- Shan, J.J. *et al.*, 2007. Challenges in natural health product research: The importance of standardization. *Proceedings of the Western Pharmacology Society*, 50, pp.24–30.
- Shaw, D. *et al.*, 2012. Pharmacovigilance of herbal medicine. *Journal of Ethnopharmacology*, 140(3), pp.513–518.
- Skorve, J. *et al.*, 1990. Regulation of fatty acid oxidation and triglyceride and phospholipid metabolism by hypolipidemic sulfur-substituted fatty acid analogues. *Journal of Lipid Research*, 31(9), pp.1627–1635.

- Son, M.J. *et al.*, 2013. Aspalathin improves hyperglycemia and glucose intolerance in obese diabetic ob/ob mice. *European Journal of Nutrition*, 52(6), pp.1607–1619.
- Sousa, A.G. *et al.*, 2011. Association between genetics of diabetes, coronary artery disease, and macrovascular complications: exploring a common ground hypothesis. *The review of diabetic studies*, 8(2), pp.230–244.
- Spiegelman, B.M. and Flier, J.S., 2001. Obesity and the regulation of energy balance. *Cell*, 104(4), pp.531–543.
- Srivastava, R.K. *et al.*, 2014. Sulforaphane synergizes with quercetin to inhibit self-renewal capacity of pancreatic cancer stem cells. *Frontiers in Bioscience (Elite Edition)*, 3, pp.515-528.
- Standley, L. *et al.*, 2001. Influence of processing stages on antimutagenic and antioxidant potentials of rooibos tea. *Journal of Agricultural and Food Chemistry*, 49(1), pp.114–117.
- Stanely Mainzen Prince, P. and Kannan, N.K., 2006. Protective effect of rutin on lipids, lipoproteins, lipid metabolizing enzymes and glycoproteins in streptozotocin-induced diabetic rats. *The Journal of Pharmacy and Pharmacology*, 58(10), pp.1373–1383.
- Su, X. and Abumrad, N.A., 2009. Cellular fatty acid uptake: a pathway under construction. *Trends in endocrinology and metabolism: TEM*, 20(2), pp.72–77.
- Tahrani, A.A. *et al.*, 2011. Management of type 2 diabetes: new and future developments in treatment. *Lancet (London, England)*, 378(9786), pp.182–197.
- Tamargo, J., *et al.*, 2015. Narrow therapeutic index drugs: a clinical pharmacological consideration to flecainide. *European Journal of Clinical Pharmacology*, 71(5), pp.549–567.
- Tapas, A.R. *et al.*, R.B., 2008. Flavonoids as Nutraceuticals: A Review. *Tropical Journal of Pharmaceutical Research*, 7(3), pp.1089–1099.

- Tiganis, T. and Bennett, A.M., 2007. Protein tyrosine phosphatase function: the substrate perspective. *The Biochemical Journal*, 402(1), pp.1–15.
- Tong, L. and Harwood, H.J., 2006. Acetyl-coenzyme A carboxylases: versatile targets for drug discovery. *Journal of Cellular Biochemistry*, 99(6), pp.1476–1488.
- Tuomilehto, J. *et al.*, 2001. Prevention of type 2 diabetes mellitus by changes in lifestyle among subjects with impaired glucose tolerance. *New England Journal of Medicine*, 344(18), pp.1343–1350.
- Veronin, M.A., *et al.*, 2014. Quantification of active pharmaceutical ingredient and impurities in sildenafil citrate obtained from the Internet. *Therapeutic Advances in Drug Safety*, 5(5), pp.180–189.
- Vinayagam, R. and Xu, B., 2015. Antidiabetic properties of dietary flavonoids: a cellular mechanism review. *Nutrition and Metabolism*, 12, pp.60.
- Wachtel-Galor, S. and Benzie, I.F.F., 2011. Herbal Medicine: An introduction to its history, usage, regulation, current trends, and research needs. *Herbal Medicine: Biomolecular and Clinical Aspects*. Boca Raton (FL): CRC Press/Taylor and Francis. Available at: <http://www.ncbi.nlm.nih.gov/books/NBK92773/> [Accessed December 1, 2016].
- Wakil, S.J. and Abu-Elheiga, L.A., 2009. Fatty acid metabolism: target for metabolic syndrome. *Journal of Lipid Research*, 50 (Supplement), pp.S138-143.
- Walters, N.A. *et al.*, 2016. Improved HPLC method for rooibos phenolics targeting changes due to fermentation. *Journal of Food Composition and Analysis*. Available at: <http://www.sciencedirect.com/science/article/pii/S0889157516301934> [Accessed November 23, 2016].
- Wang, N. *et al.*, 2013. Impairment of pancreatic  $\beta$ -cell function by chronic intermittent hypoxia. *Experimental Physiology*, 98(9), pp.1376–1385.
- Wilcox, G., 2005. Insulin and insulin resistance. *The Clinical Biochemist. Reviews*, 26(2), pp.19–39.

- Wilgen, B.W. van *et al.*, 2016. Ecological research and conservation management in the Cape Floristic Region between 1945 and 2015: History, current understanding and future challenges. *Research Gate*, pp.1–97.
- Woods, S.C. *et al.*, 1998. Signals that regulate food intake and energy homeostasis. *Science (New York, N.Y.)*, 280(5368), pp.1378–1383.
- Yaffe, D. and Saxel, O., 1977. Serial passaging and differentiation of myogenic cells isolated from dystrophic mouse muscle. *Nature*, 270(5639), pp.725–727.
- Yokoyama, W.M. *et al.*, 2012. Cryopreservation and thawing of cells. *Current Protocols in Immunology*, Appendix 3, pp.3G.
- Young, M.E. *et al.*, 2001. Regulation of cardiac and skeletal muscle malonyl-CoA decarboxylase by fatty acids. *American Journal of Physiology - Endocrinology and Metabolism*, 280(3), pp.E471–E479.
- Zammit, V.A., 1999. The malonyl-CoA-long-chain acyl-CoA axis in the maintenance of mammalian cell function. *Biochemical Journal*, 343(Pt 3), pp.505–515.
- Zebisch, K. *et al.*, 2012. Protocol for effective differentiation of 3T3-L1 cells to adipocytes. *Analytical Biochemistry*, 425(1), pp.88–90.
- Zhang, J. *et al.*, 2012. Quality of herbal medicines: Challenges and solutions. *Complementary Therapies in Medicine*, 20(1–2), pp.100–106.
- Zhang, W.-Y. *et al.*, 2012. Effect of eriodictyol on glucose uptake and insulin resistance *in vitro*. *Journal of Agricultural and Food Chemistry*, 60(31), pp.7652–7658.
- Zhang, H. *et al.*, 2015. The Role of Hormones in Glucose Homeostasis and Diabetes Treatment. *Recent Advances in Diabetes Treatment*, Chapter 3, pp. 2-80.
- Zhao, F.-Q. and Keating, A.F., 2007. Functional Properties and Genomics of Glucose Transporters. *Current Genomics*, 8(2), pp.113–128.
- Zimmet, P. *et al.*, 2003. Preventing type 2 diabetes and the dysmetabolic syndrome in the real world: a realistic view. *Diabetic Medicine: A Journal of the British Diabetic Association*, 20(9), pp.693–702.

Zonszein, J. and Groop, P.H., 2016. Strategies for diabetes management: using newer oral combination therapies early in the disease. *Diabetes therapy: Research, treatment and education of diabetes and related disorders*, 7(4), pp.621–639.

# APPENDIX 1

## Chemicals and reagents used in this study

Product	Supplier/Company	Catalogue number
1,1-Dimethylbiguanide hydrochloride (Metformin)	Sigma-Aldrich, Saint Louis, USA	D150959-5g
1.5 mL centrifuge tubes	Sigma-Aldrich, St Louis, MO, USA	0030123.344
10% Mini-PROTEAN® TGX™ Precast Protein Gels	Bio-Rad, Berkeley, California, USA	4561033
10x Tris/Glycine/SDS	Bio-Rad, Berkeley, California, USA	1610772
12% Mini-PROTEAN® TGX™ Precast Protein Gels	Bio-Rad, Berkeley, California, USA	4561044
15 mL Centrifuge tubes	NEST Biotechnology Co. LTD, Jiangsu, China	601001
1M HEPES	Lonza, Walkersville, MD, USA	CC-5022
1M HEPES buffer	Lonza, Walkersville, MD, USA	BE17-737E
2 mL Cryo-vials	Corning, MA, USA	430659
2 mL Safe-lock tubes	Eppendorf, Hamburg, Germany	F164928G
2-deoxy-[3H]-D-glucose	American Radiolabeled Chemicals, Inc	ART 0200C
3-isobutyl -1-methyl-xanthine (IBMX)	Sigma-Aldrich, Saint Louis, USA	I5879
3T3-L1 preadipocytes	American Type Culture Collection, Manassas, USA	CL-173
50 mL Centrifuge tubes	NEST Biotechnology Co. LTD, Jiangsu, China	602072
5x TransBlot® Turbo Transfer Buffer, RTA Transfer Kit, LF PVDF	Bio-Rad, Berkeley, California, USA	170-42474
ATP assay kit	ViaLight, Lonza, Basel, Switzerland	LT27-008
Bio-Rad Protein DC assay kit	Bio-Rad, Berkeley, California, USA	500-0201

Bovine serum albumin (BSA) – fatty-acid free	Capricorn scientific	BSA-FAF-1U
C2C12 murine skeletal muscle cells	European Collection of Authenticated Cell Cultures, Salisbury, UK	91031101
C3A human liver cells	American Type Culture Collection, Manassas, USA	CRL-10741
Calcium chloride (CaCl <sub>2</sub> )	Sigma-Aldrich, Saint Louis, USA	10043-52-4
Carbon dioxide (CO <sub>2</sub> )	Air Products, Centurion, SA	K239C
Cell counting chamber slides	Life Technologies Corporation, Carlsbad, CA, USA	C10228
CELLBIND -24 well plates	Corning, MA, USA	3337
CELLBIND -96 well plates	Corning, MA, USA	3300
Citric acid monohydrate	Sigma-Aldrich, St Louis, MO, USA	5949-29-1
Clarity™ Western C ECL Substrate	Bio-Rad, Berkeley, California, USA	170-5061
Corning® 500mL Bottle Top Vacuum Filter	Corning Inc, New York, USA	430513
Crystal violet	Merck, Whitehouse Station, NJ, USA	115940
Dexamethasone	Sigma-Aldrich, Saint Louis, USA	D4902
D-Glucose powder	Sigma-Aldrich, Saint Louis, USA	D5030
Dimethyl Sulfoxide (DMSO)	Sigma-Aldrich, Saint Louis, USA	276855
Dithiothreitol	Sigma-Aldrich, St Louis, MO, USA	3483-12-3
Donkey anti-rabbit (IgG-HRP)	Santa Cruz Biotechnology, Santa Cruz, CA, USA	sc-2317
Dulbecco`s modified Eagle`s medium (DMEM without phenol red)	Sigma-Aldrich, Saint Louis, USA	D5030

Dulbecco's Modified Eagle's Medium (DMEM)	Lonza, Walkersville, MD, USA	BE12-604F
Dulbecco's phosphate saline buffer (DPBS)	Lonza, Walkersville, MD, USA	BE17-513F
Eagle's Minimum Essential Medium (EMEM)	Lonza, Walkersville, MD, USA	BE12-662F
Ethyl alcohol	Sigma-Aldrich, Saint Louis, USA	64-17-5
Ethylenediaminetetraacetic acid disodium salt dihydrate (EDTA)	Sigma-Aldrich, Saint Louis, USA	6381-92-6
Foetal bovine serum (FBS)	Lonza, Walkersville, MD, USA	BC/S0615
Glass Pasteur Pipettes	Lasec, Marienfeld, Germany	600333
Glucose Standard 1	Wako Chemicals, Osaka, Japan	299-65731
Glucose Standard 2	Wako Chemicals, Osaka, Japan	296-65741
Horse-serum	Highveld biological, SA	308
Insulin	Sigma-Aldrich, Saint Louis, USA	11061-68-0
Isopropanol	Sigma-Aldrich, Saint Louis, USA	I9516
LabAssay Glucose Chromogen Reagent	Wako Chemicals, Osaka, Japan	295-65711
L-Glutamine	Lonza, Walkersville, MD, USA	17-605E
L-Glutamine	Lonza, Walkersville, MD, USA	BE17-605E
Low fat free milk powder	Clover, JHB, SA	2082054
Magnesium chloride (MgCl <sub>2</sub> )	Sigma-Aldrich, Saint Louis, USA	7786-30-3
Methanol	VWR Chemicals, Fontenay-sous-Bois, France	67-56-1
Millex-GP syringe filter unit	Millipore PES membrane, Merck	SLGP033RS
New born calf serum (NCS)	The Scientific Group, JHB, SA	BC/S0125-HI
Oil O Red	Sigma-Aldrich, Saint Louis, USA	1320-06-5

p-Nitrophenyl phosphate disodium salt hexahydrate	Sigma-Aldrich, St Louis, MO, USA	SRE0026
Ponceau S Stain	Sigma-Aldrich, Saint Louis, USA	6226-79-5
Potassium Chloride (KCl)	Sigma-Aldrich, Saint Louis, USA	7447-40-7
Precision Protein™ StrepTactin-HRP Conjugate	Bio-Rad, Berkeley, California, USA	1610381
Protease Inhibitors	Roche, Basel, Switzerland	11206893001
Protein Assay Reagent B	Bio-Rad, Berkeley, California, USA	500-0114
Quantity One Software	Bio-Rad, Berkeley, California, USA	170-9600
Quickstart™ Bradford 1x Dye Reagent	Bio-Rad, Berkeley, California, USA	500-0205
Ready gel Ultima Gold	Merck, Whitehouse Station, NJ, USA	6013329
Recombinant human PTP1B Protein	Abcam, Cambridge, United Kingdom	ab51277
Scintillation vials	CJ Labs, JHB, SA	80-370-02
Serological pipettes -2mL	Corning, MA, USA	4501
Serological pipettes-10mL	Corning, MA, USA	4101
Serological pipettes-25mL	Corning, MA, USA	4251
Serological pipettes-50mL	Corning, MA, USA	4490
Sodium bicarbonate (NaHCO <sub>3</sub> )	Sigma-Aldrich, Saint Louis, USA	144-55-8
Sodium chloride (NaCl)	Sigma-Aldrich, Saint Louis, USA	7647-14-5
Sodium citrate tribasic dihydrate	Sigma-Aldrich, St Louis, MO, USA	6132-04-3
Sodium dodecyl sulphate (SDS)	Sigma-Aldrich, Saint Louis, USA	151-21-3
Sodium hydroxide (NaOH)	Sigma-Aldrich, Saint Louis, USA	1310-73-2

Stainless steel beads	Qiagen, Hilden, Germany	69989
Sterile TC water	Lonza, Walkersville, MD, USA	59900C
T75 Flasks	Greiner bio-one, Frickenhausen, Germany	658975
Tissue lyser	Qiagen, Hilden, Germany	85600
Trizma® base	Sigma-Aldrich, Saint Louis, USA	77-86-1
Trypan blue	Invitrogen, Carlsbad, CA, USA	15050-065
Trypsin-versene	Lonza, Walkersville, MD, USA	17-161F
Tween-20	Sigma-Aldrich, Saint Louis, USA	58980C
β-Actin Antibody	Santa Cruz Biotechnology, Santa Cruz, CA, USA	sc-47778
β-mercaptoethanol	Sigma-Aldrich, St Louis, MO, USA	60-24-2

## APPENDIX 2

### Krebs Ringer Bicarbonate HEPES (KRBH) buffer

To make 500 mL KRBH the following ingredients were weighed in 50 mL tubes:

Reagent	Weight (g)	[Final]
NaCl	3.36	115 mM
NaHCO <sub>3</sub>	1.008	24 mM
KCl	0.186	5 mM
MgCl <sub>2</sub>	0.048	1 mM
CaCl <sub>2</sub>	0.139	2.5 mM
BSA	0.5	0.1 % (w/v)
1M HEPES	5 mL	10 mM

Each reagent was dissolved in sterile Tissue Culture (TC) water and the tube of each reagent was rinsed out with TC water five times into a clean, autoclaved 500 mL measuring cylinder. 5 mL HEPES buffer was added to the buffer and the buffer was filter sterilized.

To make up 8 mM glucose containing KRBH buffer, 720.64 mg D-Glucose was added with the above listed reagents and dissolved in 500 mL sterile TC water. The buffer was then filtered using a filtration unit (0.22 µm filter size).

### Sorenson's buffer

Reagent	Weight (g)	[Final]
Glycine	0.751	0.1 M
NaCl	0.584	0.1 M

The above reagents were dissolved in 100 mL TC water and the pH set to 10.5 using 1 M NaOH ( $M_w$  40.00 g/mol).

### **Protein Tyrosine Phosphatase 1B (PTP1B)**

PTP1B enzyme (1 mg/mL) was sourced from Abcam (United Kingdom) and received as a recombinant human protein (catalogue number: ab51277). Enzyme stock solutions were prepared by diluting 100  $\mu$ L of the 1mg/mL enzyme with 400  $\mu$ L of 50 mL citrate buffer (pH 6.0), yielding a final concentration of 200  $\mu$ g/mL. Thereafter, a concentration of 0.05  $\mu$ g/mL of the PTP1B enzyme was prepared by diluting the 200  $\mu$ g/mL stock to 4  $\mu$ g/mL working solution in 2 mL Eppendorf tubes. The working solutions were aliquoted and stored at -20°C.

### **50 mM citric acid**

A 50 mM citric acid solution was prepared by dissolving 2.63 g of citric acid ( $M_w$  210.14 g/mol) in 250 mL in miliQ-tested water in a volumetric flask.

### **50 mM citrate buffer:**

7.35 g trisodium citrate ( $M_w$  294.10 g/mol) was weighed into a 50 mL tube and transferred into a 500 mL volumetric flask and filled to the mark using miliQ- water. The pH was adjusted to 6.0 by adding 50 mM citric acid. Thereafter, 2.9 g NaCl ( $M_w$  58.44 g/mol) and 186.12 mg EDTA ( $M_w$  372.24 g/mol) was added to the trisodium citrate buffer, yielding a final concentration of 0.1 M NaCl and 1 mM EDTA. The pH was re-checked and set to pH 6.0.

### **1 M NaOH**

To make up a 1 M NaOH solution, 1.8 g of NaOH ( $M_w$  40.00 g/mol) was dissolved in 45 mL sterile TC water.

### Plate layout for PTP1B enzyme assay

	1	2	3	4	5	6	7	8	9	10	11	12
<b>A</b>	DMSO (+) PTP1B	ARC 2 [100 µg/mL]	GRT [100 µg/mL]	GRT [100 µg/mL]	GRT [100 µg/mL]	GRT [100 µg/mL]	Extract 1 [100 µg/mL]	Extract 1 [100 µg/mL]				
<b>B</b>	DMSO (+) PTP1B	10	10	10	10	10	10	10	10	10	10	
<b>C</b>	DMSO (-) PTP1B	1	1	1	1	1	1	1	1	1	1	
<b>D</b>	DMSO (-) PTP1B	0.1	0.1	0.1	0.1	0.1	0.1	0.1	0.1	0.1	0.1	
<b>E</b>		0.01	0.01	0.01	0.01	0.01	0.01	0.01	0.01	0.01	0.01	
<b>F</b>		0.001	0.001	0.001	0.001	0.001	0.001	0.001	0.001	0.001	0.001	
<b>G</b>		0.0001	0.0001	0.0001	0.0001	0.0001	0.0001	0.0001	0.0001	0.0001	0.0001	
<b>H</b>		0.00001	0.00001	0.00001	0.00001	0.00001	0.00001	0.00001	0.00001	0.00001	0.00001	

DMSO control + PTP1B enzyme

DMSO

DMSO control + 50 mM citrate buffer (no enzyme)

DMSO

Extract concentrations ranged between 0.00001 – 100 µg/mL.

All green roibos extracts (80% and 60% ethanol and aqueous) and reference extracts were tested in duplicate using the above plate layout as an example.

The shaded columns represent those with the PTP1B enzyme (0.05 µg) and those that are unshaded contain 50 mM citrate buffer instead of enzyme.

**<sup>3</sup>H-2-deoxy-D-glucose uptake 24-well plate layout (For C2C12 and C3A cells)**

	1	2	3	4	5	6
A	Control	Insulin	ARC 2	Extract 1	Extract 2	Extract 3
B	Control	Insulin	ARC 2	Extract 1	Extract 2	Extract 3
C	Control	Insulin	ARC 2	Extract 1	Extract 2	Extract 3
D	Extract 4	Extract 4	Extract 4	Extract 5	Extract 5	Extract 5

	1	2	3	4	5	6
A	Control	Insulin	GRT	Extract 6	Extract 7	Extract 8
B	Control	Insulin	GRT	Extract 6	Extract 7	Extract 8
C	Control	Insulin	GRT	Extract 6	Extract 7	Extract 8
D	Extract 9	Extract 9	Extract 9	Extract 10	Extract 10	Extract 10

### **3T3-L1 adipocyte differentiation medium**

#### **Adipocyte differentiation medium (ADM)**

4.5 µL of 10 mM Dex

450 µL of 0.5 mM IBMX

4.5 µL of 1 µg/mL insulin

44.5 mL 10% FBS in DMEM

All the above listed reagents were aseptically dissolved in a 50 mL centrifuge tube and 200 µL was used in each well for the induction of adipocyte differentiation

A **10 mM dexamethasone** (dex) was prepared by dissolving 7.85 mg dexamethasone ( $M_w$  392.46 g/mol) in 2 mL absolute (100%) ethyl alcohol ( $M_w$  46.07 g/mol) and stored at 4°C.

A **0.5 mM 3-isobutyl-1-methylxanthine** (IBMX) was prepared by solubilizing 22.2 mg IBMX ( $M_w$  222.24 g/mol) in 2 mL 50% ethanol (EtOH).

50 % EtOH was prepared by dissolving 22.5 mL absolute (100%) ethyl alcohol with 22.5 mL sterile TC water.

#### **Adipocyte maintenance medium (AMM)**

To prepare AMM, 10% foetal bovine serum (FBS) was dissolve in 90% DMEM.

#### **Phenol red free DMEM buffer**

8.3 g of DMEM

0.5 g1.0 g of BSA

1.85 g3.7 g of NaHCO<sub>3</sub>

The above listed reagents were dissolved in 1000 mL sterile TC water and 500 mL of the buffer was filter sterilised using a 500 mL filtration unit system (0.22 µm filter size).

The remaining 500 mL was mixed with 2.25 g D-glucose and then filter sterilised into a new 500 mL filtration unit, yielding a 25 mM glucose in phenol red free DMEM buffer.

### **Oil Red O (ORO) solution**

A 1% (w/v) ORO (Sigma-Aldrich, Saint Louis, USA) stock solution was prepared by dissolving 1 g ORO powder with 100 mL isopropanol using a magnetic stirrer. On the day of the assay, a 70% (v/v) ORO working solution was prepared from the 1% ORO stock solution, by mixing 7 mL ORO stock solution with 3 mL distilled water. The working solution was prepared fresh on the day of the assay and filtered using filter paper.

### **Crystal Violet solution**

A 2% (w/v) crystal violet stock solution was prepared by dissolving 2 g of crystal violet powder with 100 mL sterile TC water. Thereafter, a 0.5% (v/v) working solution was prepared by mixing 250  $\mu$ L of the stock solution (2%) with 50 mL distilled water.

### **1x Transfer buffer for Semi-dry Western blot**

A 1x transfer buffer was prepared by mixing 200 mL of a 5x transfer buffer with 600 mL distilled water and 200 mL ethanol (reagent grade ~ 39.9% purity).

### **10x Tris-buffered saline (TBS) pH 7.6**

To make 2 L of a 10x TBS buffer, 48.44 g of 2-Amino-2-(hydroxymethyl)-1,3-propanediol (Trizma<sup>®</sup> base) ( $M_w$  121.14 g/mol) and 160.12 g of NaCl ( $M_w$  58.44 g/mol) were dissolved in 2000 mL distilled water. The pH was set to 7.6 using concentrated hydrochloric acid. The buffer was kept at 4°C.

### **1x Tris-buffered saline Tween-20 (TBST)**

A 1 L solution of TBST was prepared by dissolving 100 mL of 10x TBS with 900 mL distilled water and 1 mL Tween-20. The buffer was kept at 4°C.

### **0.1 M NaOH and 1% SDS buffer**

To yield a final concentration of 0.1 M NaOH ( $M_w$  40.00 g/mol) and 1% SDS ( $M_w$  288.38 g/mol), 2 g NaOH and 5 g SDS were dissolved in 500 mL distilled water.



## ETHICAL CLEARANCE CERTIFICATE

<b>Certificate Number</b>	UZREC 171110-030 PGM 2015/203					
<b>Project Title</b>	Assessment of chemical markers as surrogates for safety and efficacy of Rooibos extract					
<b>Principal Researcher/ Investigator</b>	A Viraragavan					
<b>Supervisor and Co-supervisor</b>	Prof AK Basson			Dr CJF Muller & Dr. S Riedel-van Heerden		
<b>Department</b>	Biochemistry & Microbiology					
<b>Nature of Project</b>	Honours/4 <sup>th</sup> Year		Master's	x	Doctoral	Departmental

The University of Zululand's Research Ethics Committee (UZREC) hereby gives ethical approval in respect of the undertakings contained in the above-mentioned project proposal and the documents listed on page 2 of this Certificate.

- Special conditions:**
- (1) The Principal Researcher must report to the UZREC in the prescribed format, where applicable, annually and at the end of the project, in respect of ethical compliance.
  - (2) Documents marked "To be submitted" (see page 2) must be presented for ethical clearance before any data collection can commence.

The Researcher may therefore commence with the research as from the date of this Certificate, using the reference number indicated above, but may not conduct any data collection using research instruments that are yet to be approved.

Please note that the UZREC must be informed immediately of

- Any material change in the conditions or undertakings mentioned in the documents that were presented to the UZREC
- Any material breaches of ethical undertakings or events that impact upon the ethical conduct of the research

**UNIVERSITY OF ZULULAND  
HIGHER DEGREES COMMITTEE**



**RESEARCH & INNOVATION**

Website: <http://www.unizulu.ac.za>

Private Bag X1001

KwaDlangezwa 3886

Tel: 035 902 6826

Fax: 035 902 6635

Email: BappooR@unizulu.ac.za

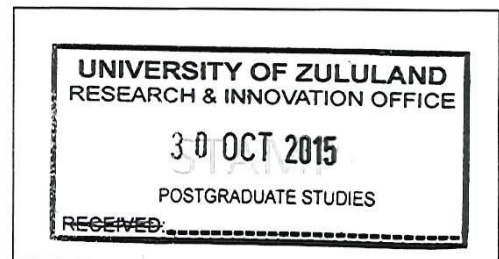
**Confirmation of Project Registration**

<b>Registration Number</b>	S1109/15	
<b>Project Title</b>	<i>Assessment of chemical markers as surrogates for safety and efficacy of Rooibos extract</i>	
<b>Principal Researcher/ Investigator</b>	Amsha Viraragavan	
<b>Student number</b>	201160287	
<b>Supervisor and Co-supervisor</b>	Dr Christo Muller (SAMRC) Prof A K Basson	Dr S Riedel van Heerden (SAMRC)
<b>Department</b>	Biochemistry	
<b>Nature of Project</b>	MSc	
<b>HDC Meeting held</b>	5 October 2015	

**Please note:** Your proposal can now be considered for ethical clearance and research funding. Kindly provide this letter with your ethical clearance certificate when submitting your final thesis for external examination.

**Ravi Bappoo (Mr)**  
**Senior Administrator: Postgraduate Studies**

**Dated: 30 October 2015**



# Amsha

*by* Amsha Viraragavan

---

FILE	AMSHA.DOCX (315.09K)	WORD COUNT	17713
TIME SUBMITTED	01-DEC-2016 02:29PM	CHARACTER COUNT	
SUBMISSION ID	745553119	99157	

# CHAPTER 1

## INTRODUCTION TO THIS STUDY

Diabetes mellitus is defined as a metabolic disease which is caused by derangements in the metabolism of carbohydrate, fat and protein resulting from defective insulin secretion, insulin action or both, with hyperglycaemia as a common feature (ADA, 2008; Wagman and Nuss, 2001; WHO, 1999). With a global increase in diabetes, the International Diabetes Federation (IDF) estimated 415 million people were diabetic in 2015 and this figure is predicted to escalate to 642 million in 2040 (<http://www.idf.org/sites/default/files/Atlas7e-poster.pdf>). Three quarters of diabetics that are affected live in low and middle-income countries (Levitt, 2008). In South Africa, the IDF estimated 3.85 million South Africans between the ages of 21 and 79 were likely to have diabetes in 2015 (IDF 2015; Statistics South Africa 2015).

In the African continent, migration from rural to urban environments leads to lifestyle modifications. These modifications include changes in diet, in particular high calorific diets rich in carbohydrates and sugar, lack of physical activity, smoking and an increased alcohol intake (Gill *et al.*, 2009). Currently an estimated 14.2 million Africans are living with diabetes, which is predicted to rise to 34.2 million by 2040. In sub-Saharan Africa, over 90% of diabetics are diagnosed with type 2 diabetes (T2D), owing to the changes in lifestyle (Levitt, 2008). South Africa is estimated to have the highest prevalence of type 2 diabetes with 2.28 million recorded in 2015 (IDF Africa)

Apart from healthy lifestyle interventions, majority of diabetic patients require pharmacological intervention which consists of one or more oral antidiabetic drugs. Of these drugs, metformin, sulfonylureas or thiazolidinediones (TZD's) are most commonly prescribed (Bodmer *et al.*, 2008; Luna and Feinglos, 2001). Current therapeutics in the treatment of diabetes is aimed at maintaining normoglycaemia and median HbA1c levels at  $\leq 7\%$  (Bennett *et al.*, 2011; He *et al.*, 2011; Inzucchi *et al.*, 2015). In most cases, despite the medication, the diabetic condition worsens over time, necessitating combination therapies including the use of insulin to control

## ORIGINALITY REPORT

---

%**20** %**10**

SIMILARITY INDEX

INTERNET SOURCES

%**14**

PUBLICATIONS

%**6**

STUDENT PAPERS

---

## PRIMARY SOURCES

---

**1**

Submitted to University of Stellenbosch,

South Africa

Student Paper

%**1**

---

**2**

196.21.83.35

Internet Source

%**1**

---

**3**

Systems Biology of Free Radicals and

Antioxidants, 2014.

Publication

%**1**

---

**4**

[www.jlr.org](http://www.jlr.org)

Internet Source

%**1**

---

**5**

[www.nature.com](http://www.nature.com)

Internet Source

%**1**

---

---

6

Submitted to University of Zululand

Student Paper

% 1

---